$\mathcal{L}_1$ ADAPTIVE CONTROLLER FOR UNDERWATER VEHICLE-MANIPULATOR SYSTEM

BY

AHMED ELTAYEB AHMED TAHA

A Thesis Presented to the
DEANSHIP OF GRADUATE STUDIES

KING FAHD UNIVERSITY OF PETROLEUM & MINERALS

DHAHRAN, SAUDI ARABIA

In Partial Fulfillment of the
Requirements for the Degree of

MASTER OF SCIENCE

In

SYSTEMS ENGINEERING

MAY 2013

$\mathcal{L}_1$ ADAPTIVE CONTROL FOR UNDERWATER VEHICLE-MANIPULATOR SYSTEM

by

AHMED ELTAYEB AHMED TAHA

A Thesis Presented to the
DEANSHIP OF GRADUATE STUDIES

In Partial Fulfillment of the Requirements
for the degree

MASTER OF SCIENCE

IN

SYSTEMS ENGINEERING

KING FAHD UNIVERSITY
OF PETROLEUM & MINERALS

Dhahran, Saudi Arabia

MAY 2013

KING FAHD UNIVERSITY OF PETROLEUM & MINERALS
DHAHRAN 31261, SAUDI ARABIA

DEANSHIP OF GRADUATE STUDIES

This thesis, written by **AHMED ELTAYEB AHMED TAHA** under the direction of his thesis adviser and approved by his thesis committee, has been presented to and accepted by the Dean of Graduate Studies, in partial fulfillment of the requirements for the degree of **MASTER OF SCIENCE IN SYSTEMS ENGINEERING**.

Thesis Committee

Dr. Sami El Ferik (Adviser)

Dr. Lahouari Cheded (Member)

Dr. M. Faizan Mysorewala (Member)

Dr. Fouad Al-Sunni
Department Chairman

Dr. Salam A. Zummo
Dean of Graduate Studies

4/6/13
Date

To
My Father and Mother, My beloved wife, Um Eltayeb, My beloved son, Eltayeb, and My Brothers and Sisters

ACKNOWLEDGMENTS

This work is the outcome of my thesis for Master's degree at KFUPM, from February 2010 to April 2013. It has taken place at System Engineering department under the supervision of my supervisor Assc. Prof. Dr. Sami El Ferik. First of all, I would like to thank my supervisor and mentor Assc. Prof. Dr. Sami El Ferik for his continuously motivation advices which helped and guided me to the right direction to finish my master's degree. I would like to thank also Dr. Lahouari Cheded, and Dr. M. Faizan Mysorewala, for being my thesis committee members. I would like to thank my all friends in systems engineering department, especially, Arief Barkah Koesdwiady, Muhammad Fuady Emzir, Ahmed Adeniran and Ahmed Gafran, for their helpful technical discussions.

TABLE OF CONTENTS

LIST OF TABLES vii

LIST OF FIGURES viii

ABSTRACT (ENGLISH) xiii

CHAPTER 1 INTRODUCTION 1

1.1 Motivation 2

1.2 Thesis Objectives 4

1.3 Thesis Organization 5

CHAPTER 2 LITERATURE REVIEW 6

2.1 Modeling of UVMS 6

2.2 Controlling of UVMS 7

CHAPTER 3 KANE'S EQUATION 11

3.1 Advantages of Kane's Method 11

3.2 Kane's Equation 12

CHAPTER 4 MODELING OF UNDERWATER VEHICLE 15

4.1 Underwater Vehicle Kinematics Equation 15

4.2 Underwater Vehicle Dynamics Equation 17

CHAPTER 5 DYNAMIC MODEL FOR THE UVMS 21

5.1 Coordinate Systems 21

5.1.1 Homogeneous Coordinates 22
5.1.2 Generalized Coordinates and Speeds 25
5.2 Kinematic Analysis 27
5.2.1 Position Vector to a Link's C.M 28
5.2.2 Angular Velocity 30
5.2.3 Linear Velocity 31
5.2.4 Angular Acceleration 32
5.2.5 Linear Acceleration 33
5.3 Inertia Forces 33
5.4 Gravity Forces 35
5.5 Hydrodynamic Forces 37
5.5.1 Added Mass 37
5.5.2 Buoyancy 40
5.5.3 Fluid Acceleration 41
5.5.4 Drag Force 42
5.6 Dynamic model 44
5.7 Properties of Equation of Motion 45
5.8 Example: 3 links Manipulator attached to the Underwater Vehicle 46
5.8.1 Coordinate Systems for the UVMS 47
5.8.2 Kinematic Analysis of the UVMS 48
5.8.3 Masses and Inertias for the UVMS model 52
5.8.4 Gravity Force 54
5.8.5 Hydrodynamic Forces 56
5.8.6 Buoyancy Force 59
5.8.7 Profile Drag Force 61

CHAPTER 6 CONTROLLER DESIGN FOR THE UNDERWATER VEHICLE 62

6.1 Feedback Linearization for the Underwater Vehicle 62
6.1.1 Simulation Results for the Underwater Vehicle 64

6.2 Sliding Mode Control for the Underwater Vehicle 72
6.2.1 Sliding Model Controller Design for AUV 73
6.3 Simulation Results 77
6.4 $\mathcal{L}_1$ Adaptive Control for the Underwater Vehicle 86
6.4.1 Preliminaries 87
6.4.2 $\mathcal{L}_1$ Adaptive Controller Formulation 88
6.4.3 Simulation Results 96
6.4.4 Discussion and Comparison 115

CHAPTER 7 CONTROLLER DESIGN FOR THE UVMS 116

7.1 Feedback Linearization Controller for the UVMS 117
7.1.1 Simulation Results 117
7.2 Sliding Mode Controller for the UVMS 123
7.2.1 Simulation Results 123
7.3 $\mathcal{L}_1$ Adaptive controller 127
7.3.1 Simulation Results 127

CHAPTER 8 CONCLUSION AND FUTURE WORK 136

8.1 Future work 137

REFERENCES 138

VITAE 143

LIST OF TABLES

5.1 Dimension of Jason Underwater Vehicle [1] 49

5.2 D-H Parameters for the three links Puma 560 49

5.3 Mass and Inertia Properties of the UVMS 53

6.1 MARES General Characteristic 96

6.2 MARES Location of center of gravity and buoyancy 96

6.3 MARES Moment Inertia 97

6.4 MARES Added Masses 97

7.1 Dimension of Jason URV [1] 117

7.2 Mass and Inertia Properties of the UVMS 118

LIST OF FIGURES

1.1 Sub-Atlantic ROV [2]. 2
1.2 Underwater Vehicle Manipulator System. 3

5.1 Representation of Homogeneous Coordinate Transformations. . . . 23
5.2 Ellipsoid Model for Vehicle Hydrodynamic Added Mass. 56

6.1 Simulink Block Diagram for the Underwater Vehicle. 64
6.2 3D tracking of the MARES AUV without uncertainty. 65
6.3 X-Y Semi Circle trajectory tracking of the MARES AUV without uncertainty. 66
6.4 Orientation of the MARES AUV without uncertainty. 67
6.5 Control Signals of the MARES AUV without uncertainty. 68
6.6 3D tracking of the MARES AUV with uncertainty in parameters. 69
6.7 X-Y Semi Circle of the MARES AUV with uncertainty in parameters. 70
6.8 Orientation of the MARES AUV with uncertainty in parameters. 71
6.9 Control Signals of the MARES AUV with uncertainty in parameters. 72
6.10 Simulink Block Diagram for the Underwater Vehicle. 78
6.11 3D trajectory tracking of the MARES AUV without uncertainty. . 79
6.12 X-Y Semi Circle trajectory tracking of the MARES AUV without uncertainty. 80
6.13 Orientation of the MARES AUV without uncertainty. 81
6.14 Control Signals of the MARES AUV without uncertainty. 82
6.15 3D tracking of the MARES AUV with uncertainty in parameters. 83

6.16 X-Y Semi Circle trajectory tracking of the MARES AUV with uncertainty in parameters. 84
6.17 Orientation of the MARES AUV with uncertainty in parameters. 85
6.18 Control Signals of the MARES AUV with uncertainty in parameters. 86
6.19 Block Diagram of the closed-loop $\mathcal{L}_1$ adaptive controller [3]. . . . 88
6.20 3D trajectory tracking of the MARES AUV without uncertainty. . 98
6.21 Orientation of the MARES AUV without uncertainty. 99
6.22 Control Signals of the MARES AUV without uncertainty. 100
6.23 Estimated Parameter ($\hat{w}$) without uncertainty. 101
6.24 Estimated Parameter ($\hat{\theta}$) without uncertainty. 102
6.25 Estimated Parameter ($\hat{\sigma}$) without uncertainty. 103
6.26 3D trajectory tracking of the MARES AUV with uncertainty in parameters. 104
6.27 Orientation of the MARES AUV with uncertainty in parameters. 105
6.28 Control Signals of the MARES AUV with uncertainty in parameters.106
6.29 Estimated Parameter ($\hat{w}$) with uncertainty in parameters. 107
6.30 Estimated Parameter ($\hat{\theta}$) with uncertainty in parameters. 108
6.31 Estimated Parameter ($\hat{\sigma}$) with uncertainty in parameters. 109
6.32 3D trajectory tracking of the MARES AUV with uncertainty and disturbance. 110
6.33 Orientation of the MARES AUV with uncertainty and disturbance. 111
6.34 Control Signals of the MARES AUV with uncertainty and disturbance. 112
6.35 Estimated Parameter ($\hat{w}$) with uncertainty and disturbance. . . . 113
6.36 Estimated Parameter ($\hat{\theta}$) with uncertainty and disturbance. 114
6.37 Estimated Parameter ($\hat{\sigma}$) with uncertainty and disturbance. . . . 115

7.1 Simulink Block Diagram for the UVMS. 117
7.2 3D trajectory tracking of the vehicle without uncertainty. 118
7.3 Orientation trajectory tracking of the vehicle without uncertainty. 119

7.4 The manipulator angles trajectory tracking without uncertainty. . 120
7.5 The Control Signals for the vehicle without uncertainty. 121
7.6 The Control Signals for the Manipulator without uncertainty. . . 122
7.7 3D trajectory tracking of the vehicle without uncertainty. 123
7.8 Orientation trajectory tracking of the vehicle without uncertainty. 124
7.9 The manipulator angles trajectory tracking without uncertainty. . 125
7.10 The Control Signals for the vehicle without uncertainty. 126
7.11 The Control Signals for the Manipulator without uncertainty. . . 127
7.12 3D trajectory tracking of the UVMS with uncertainty and disturbance. 128
7.13 Orientation trajectory tracking of the UVMS with uncertainty and disturbance. 129
7.14 The manipulator angles trajectory tracking with uncertainty and disturbance. 130
7.15 Estimated Parameter ($\hat{w}$) with uncertainty and disturbance. . . . 131
7.16 Estimated Parameter ($\hat{\theta}$) with uncertainty and disturbance. 132
7.17 Estimated Parameter ($\hat{\sigma}$) with uncertainty and disturbance. . . . 133
7.18 The Control Signals for the vehicle with uncertainty and disturbance. 134
7.19 The Control Signals for the Manipulator with uncertainty and disturbance. 135

LIST OF ABBREVIATIONS

η	Inertial Position of Vehicle
$\mathcal{L}_1$	One norm
ν	Linear velocity in Body Fixed Frame
ω	Angular velocity in Body Fixed Frame
τ	Input Torques and Moments
AUV	Autonomous Underwater Vehicle
C	Coriolis and Centripetal Matrix
D	Drag Matrix
DOF	Degree of Freedom
g	Gravity and Buoyancy Forces Vector
M	Inertia matrix including Rigid Body and Added Mass
$MARES$	Modular Autonomous Robot for Environment Sampling
$R_B^I(\eta)$	Rotation Matrix
$UVMS$	Underwater Vehicle-Manipulator System

x	State of general dynamics
y	Output of general dynamics

THESIS ABSTRACT

NAME:	Ahmed Eltayeb Ahmed Taha
TITLE OF STUDY:	$\mathcal{L}_1$ Adaptive Control For Underwater Vehicle-Manipulator System
MAJOR FIELD:	Systems Engineering
DATE OF DEGREE:	May 2013

In this thesis, general equations of motion of the Underwater Vehicle are presented initially. These equations of motion would be used for comparison and analysis with the equations of motion of the UVMS, which is derived in detail by using the Kane's equation. From the literature review, feedback linearization and sliding mode controllers are applied to the Underwater vehicle and the Underwater vehicle with a 3 link manipulator. A new control technique, $\mathcal{L}_1$ adaptive control is applied to both the models. This $\mathcal{L}_1$ adaptive controller has the ability to achieve fast and robust adaptation which increases the performance. Also, its ability to compensate any uncertainty in the parameters is highly advantageous. Simulations are performed to compare the effectiveness and the advantages of the $\mathcal{L}_1$ adaptive controller against the other two controllers.

ARABIC ABSTRACT

الاسم: احمد الطيب احمد طه

عنوان البحث: تطبيق متحكمة إل ون التكيُّفِية على نظام الغواصة ذات الذراع

التخصص: هندسة النظم

تاريخ البحث: مايو 2013

في هذا البحث تم عرض معادلة الحركة العامة للغواصة بصورة عامة بغرض مقارنتها مع معادلة الحركة العامة للغواصة ذات الذراع التي تم ايجادها بصورة اكثر تفصيلاً باستخدام معادلة كين, ومن ثم تم تطبيق بعض المتحكمات على كلٍ من الغواصة والغواصة ذات الذراع ذو الثلاثة مفاصل. و من امثلة هذه المتحكمات الفيد باك الخطية و متحكمة الاسلايدينغ مود من البحوث السابقة. اما في هذا البحث تم تطبيق متحكمة جديدة (إل ون التكيُّفِية) لأول مرة على هذا النوع من النظم (الغواصة ذات الذراع ذو الثلاثة مفاصل). تم اختيار هذه المتحكمة لانها تمتاز بالسرعة والمتانة ضد تغيرات البيئة المحيطة بالنظام . واخيراً تم مقارنة الاداء والكفاءة لهذه المتحكمة (إل ون التكيُّفِية) مع كلٍ من متحكمة الفيد باك الخطية و متحكمة الاسلايدينغ مود عن طريق النمذجة والمحاكاءة و التي اثبتت تفوق متحكمة إل ون التكيُّفِية.

CHAPTER 1

INTRODUCTION

There is enormous amount of water on the earth's surface and abundant mineral resources, but human capabilities lack to explore them efficiently. The Underwater Vehicle has become an efficient tool in this harsh environment. Thus, underwater vehicle is now widely used in different underwater activities such as, ocean exploration, oil and gas platform maintenance and underwater pipeline inspection. Underwater vehicle has many features depending on its application. In this thesis the UVMS which is made up of underwater vehicle with a robotic arm to do special applications such as finding the black box under the sea and welding pipelines underwater etc. is considered. These kinds of UVMSs need a precise control to enable it to function as expected.

For instance, one of the real application for the UVMS model which is manufactured by Sub-Atlantic company in UK (Comanche ROV) is introduced. This type of UVMS model has 2 n-link manipulators attached to it, see Figure 1.1. It is suitable for applications such as, offshore oil and gas, scientific research in deep

sea, military and homeland security.

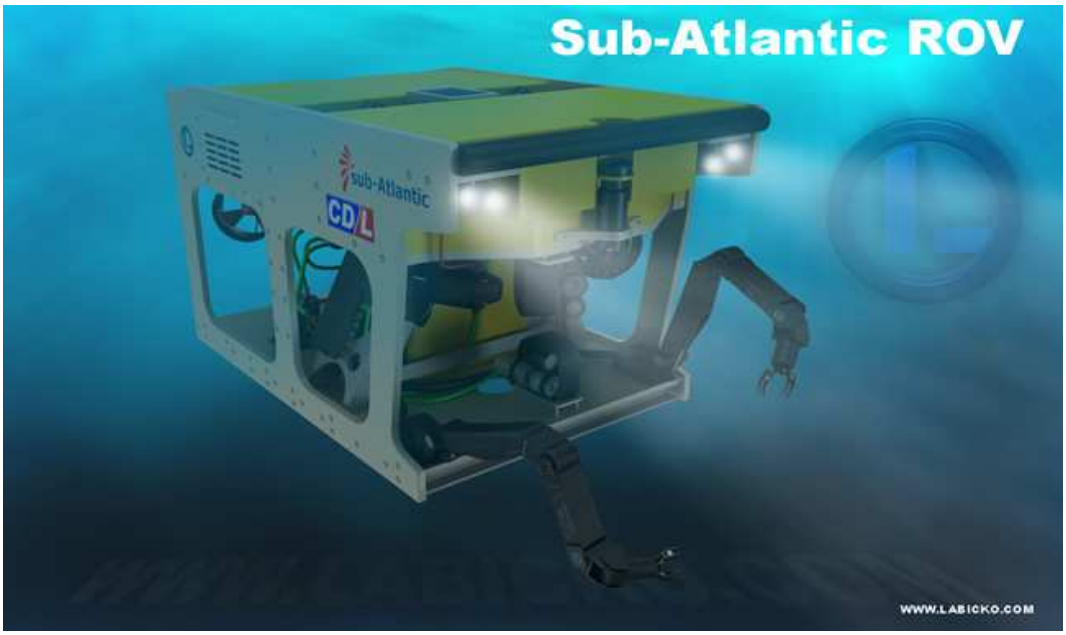

Figure 1.1: Sub-Atlantic ROV [2].

1.1 Motivation

As mentioned above the UVMS considered in this work is composed of the AUV and the underwater manipulator as illustrated in Figure 1.2. The AUV has 6 DOFs while the manipulator has n DOFs, characterized by n successive links. Hence, the total number of DOFs of the UVMS will be $N = 6+n$ DOFs.

In order to design a control system for the UVMS, a mathematical model is needed. According to the literature there are several ways to develop the UVMS model. Newton-Euler and Euler-Lagrange methods are the two most commonly used methods.

However, Kane's method is employed in this thesis to develop the UVMS model

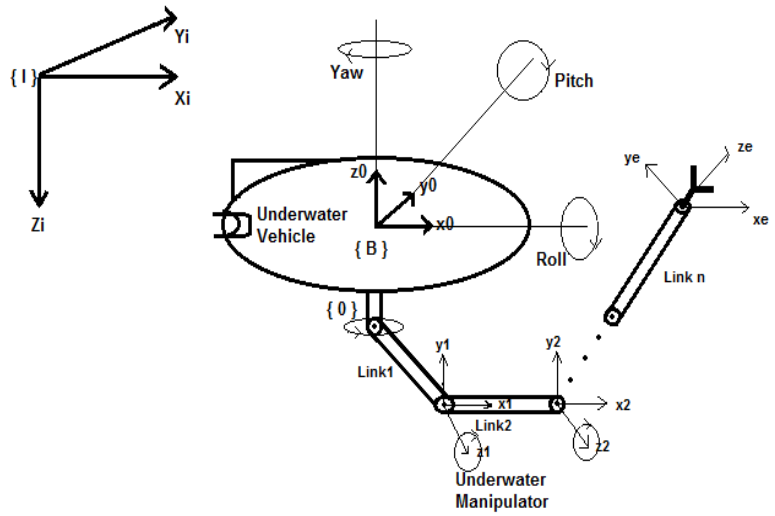

Figure 1.2: Underwater Vehicle Manipulator System.

because there are insufficient details of the dynamic equations for the model in the literature, such as inertia matrix and Coriolis & centripetal term.

In [4], detailed dynamics of the UVMS model are given but there are some difficulties in extracting the Coriolis and centripetal term as a matrix, thus, their approach is used as a reference to develop a model and the computation of Coriolis and centripetal term is adapted from [5].

Controlling the position of the UVMS with 9 DOFs poses some difficulties, most importantly, the disturbance (modeled in the dynamic equation) caused by the interaction forces between the AUV and the manipulator when one of them changes its position. There are several conventional control designs such as feedback linearization, sliding mode and adaptive control to overcome the control problems. Each of these controllers has its own drawbacks. For instance, feedback linearization requires a precise knowledge of the model. However, the UVMS model has many unmodeled dynamics which are usually considered to design a

suitable non-linear controller.

1.2 Thesis Objectives

The objective of this thesis is to identify necessary data and steps to apply Kane's method to develop the UVMS model. The method will be used to find UVMS model with a 3 link manipulator. Furthermore, $\mathcal{L}_1$ adaptive controller for the UVMS model is developed. $\mathcal{L}_1$ adaptive controller is a recent technique that has never been applied to UVMS models. Using this approach for the UVMS model is an original contribution. The result will be benchmarked to recent controllers in the literature such as sliding mode and feedback linearization. The advantage of $\mathcal{L}_1$ adaptive controller stems from its decoupling between robustness and adaptation leading to a robust control. In addition, the technique does not require exact knowledge of the non-linear dynamics. Simulation results and analytical analysis will be used to evaluate the performance.

In the development of modeling and nonlinear control for Underwater Vehicle and UVMS the following objectives will be achieved.

Presenting the kinematics and dynamics equations of Underwater Vehicle. Then, driving the full model of the UVMS by using Kane's method, after developing the model, designing a feedback linearization controller and sliding mode controller for both models. A new controller ($\mathcal{L}_1$ Adaptive controller) is designed for both models, as well as, the comparison of feedback linearization and sliding mode controllers with $\mathcal{L}_1$ adaptive controllers is done. Finally, the stability

analysis for the mentioned controllers is proved.

1.3 Thesis Organization

- Chapter 1 gives a brief introduction about the UVMS model supported by some motivations and real applications and the organization of the thesis.
- Chapter 2 consists of the literature about the modeling and control of the UVMS model.
- Chapter 3 presents the general idea about the Kane's equation which is used throughout this thesis.
- Chapter 4 Introduces the general form of Underwater Vehicle model which is used as a basis for the development of the UVMS model.
- Chapter 5 presents UVMS model in detail by using Kane's equation.
- Chapter 6 presents of $\mathcal{L}_1$ Adaptive Controller, feedback linearization and sliding mode controller for Underwater Vehicle and UVMS, as well as the simulation results.
- Chapter 7 concludes the thesis.

CHAPTER 2

LITERATURE REVIEW

There are two main parts in this section; the first one is the modeling of UVMS and this part is very important because of the lack of information in this area in the literature. The second part is the control of the UVMS model. Due to the lack of sufficient information, Jason vehicle and three link manipulator have been used as an example to develop the UVMS model with full data by using the Kane's method [6].

2.1 Modeling of UVMS

Schjolberg (1994) used iterative Euler-Lagrange algorithm to develop the UVMS model [7]. A general structure of the dynamic equation for the UVMS model in the body and earth reference frames was presented and the interaction forces between the vehicle and the manipulator were introduced through matrices. Although the dynamic equations are presented, the weakness is that the matrices elements are not given, such as the elements of matrix of the reactions forces and moments

between the vehicle and the manipulator.

Gregg Allan Shoults (1996) developed the UVMS model by using Kane's equation [6]. Kane's equation is used to find the generalized active forces and generalized inertia forces for each link in the system. Three link (Puma 560) manipulator attached to the vehicle (Jason) is selected as an example for the simulations purpose. The difficulties in this work appeared while trying to calculate the Coriolis and Centripetal term.

T.J. Tam and S.P Yang (1997)[8] developed the model of the Underwater Robotic Vehicle (URV) with Multiple Manipulators (two 3-link manipulators) by using Kane's method. This work is similar to Gregg (1996) and the difference is instead of using one 3-link manipulator, two 3-link manipulators were used and attached to the vehicle. The difficulties in this work again appeared while trying to extract the Coriolis and Centripetal term.

F. Fahimi (2008) explained how to select the Coriolis and Centripetal term by using an example of the two link robotic arm. the selection of C matrix of the system is introduced while proving the stability conditions of the sliding mode controller of the system. See page 154 [5].

2.2 Controlling of UVMS

Armstrong, Brian and Khatib, Oussama and Burdick, Joel (1986) [9] obtained the explicit model of the PUMA arm in detail.

Ingrid and T.I. Fossen [7](1994) proposed a feedback linearization controller

for trajectory control of the UVMS system which transforms the non-linear system dynamics into a linear system. The control law is selected to perform zero tracking error. The problem in using feedback linearization controller is that it requires a precise knowledge of the system. The UVMS model is highly non-linear system and it has many unmodeled dynamics, thus a feedback linearization controller will not be a good choice.

Gianluca Antonelli, Fabrizio Caccavale, Stefano Chiaverini, and Luigi Villani (2000) [10] designed an adaptive controller to track a desired motion trajectory of the UVMS model without using direct velocity feedback. Therefore, the observer is used to estimate the velocity of the UVMS system which is required by a tracking control law. Thus, the controller and observer are designed to achieve exponential convergence to zero of motion tracking as well as estimation errors.

Antonelli, G. [11] (2006) presented the dynamic and kinematic control of UVMSs. Six controllers, such as feedback linearization, sliding mode control, adaptive control and output feedback control have been compared with respect to their behaviour in presence of modeling uncertainty and presence of ocean current.

E. Xargay, N. Hovakimyan, and C. Cao (2009) [12] ,made a comparison between conventional adaptive control and recently developed technique ($\mathcal{L}_1$ adaptive control) by using two examples as a benchmark (Rohr's example and two cart example). $\mathcal{L}_1$ adaptive controller has two architectures; the first one is state feedback setting and another one is output feedback setting. Both were applied in this paper, the first one is applied to Rohr's example and the other one is applied

to the two cart example. the advantages of this new technique were shown by the qualitative analysis.

B. Ferreira, M. Pinto, A. Matos, and N. Cruz, (2009) [13] started by presenting, the kinematic, modeling and Lyapunov fundamental concepts. Then, they achieved the decoupled motions of the MARES AUV, via control of horizontal and vertical positions and velocities and the performance of these controllers was demonstrated by simulations and experiments.

A. Matos and N. Cruz, (2009)[14] gave full descriptions and specifications (such as mechanical parts, power and energy, computational system, On-board software and control) of the MARES AUV, or Modular Autonomous Robot for Environment Sampling which can dive down to 100 m in depth.

Das, SK and Pal, D and Nandy, S and Kumar, V and Shome, SN and Mahanti, B (2010) [15] presented the general control architecture which will be required for autonomous navigation and guidance control of an autonomous underwater vehicle, such as, hardware and software architecture for the AUV-150.

N. Hovakimyan and C. Cao (2010) [16] introduced $\mathcal{L}_1$ adaptive controller architecture and its applications on different type of systems, such as linear systems, linear time-varying systems and non-linear systems as well as its stability analysis.

D. Maalouf, V. Creuze, A. Chemori, et al (2012) [17] applied $\mathcal{L}_1$ adaptive controller to the Underwater vehicle, but they applied this controller to control only two degree of freedom (pitch and depth) out of six DOFs. The interesting part in this work is that they applied it to the real underwater vehicle AC-ROV

and the proposed controller was able to compensate for the external disturbances as well as the change in bouncing.

Therefore, the main objective of this work is to contribute to the literature by filling in the following gaps: Firstly, due to the lack of the information related to the modeling of the Underwater Vehicle-Manipulator Systems (UVMS), a full model of the UVMS needs to be derived by using Kane's equation,then the comparison and analysis has to be carried out between the general form of the Underwater Vehicle model which is already available in the literature and the general form of the UVMS model. Secondly, apply $\mathcal{L}_1$ Adaptive Controller for UVMS model to be as a benchmark in the literature and compare it with the existing controllers in the literature such as, Feedback Linearization and Sliding Mode controller.

CHAPTER 3

KANE'S EQUATION

3.1 Advantages of Kane's Method

Basically all the methods to obtain the equations of motion are similar. However, some of them are more suitable for the multibody dynamics than the others. The Newton-Euler method provides a complete solution for all the forces and kinematic variables, yet it is inefficient. The Newton-Euler method needs the forces and moment balances to be applied for each body by considering all the interactive and constraint forces. Thus, when only a few of the systems forces are to be solved for, this method is inefficient.

A method is provided by Lagranges Equations which disregards all the interactive and constraint forces that do not perform work. But, this method requires differentiating the scalar energy functions which is considered as a disadvantage. For small multibody systems, this is not a big issue; however, for large multibody systems it creates an efficiency problem.

Kane's method has all the features of both the methods (Newton-Euler and Lagrange's Equations) and it can also overcome the above mentioned challenges without having any other disadvantages. It uses generalized forces and thus the need to examine the interactive and constraint forces is eliminated. The differentiation problem does not appear in this method as it does not use the energy functions. To obtain the velocities and acceleration, algorithms based on vector products are used instead of differentiation. Kane's method is an organized approach to develop the dynamic equations of multibody systems which almost classifies it as an automated numerical computation. See [18] for a brief synopsis of Kane's method supported by a common applications, such as spring-mass-pendulum.

3.2 Kane's Equation

Assigned a system S having N degrees of freedom inside a Newtonian frame, now let, $\dot{q_1} \dots \dot{q_N}$, as the N generalized speeds with regard to S. Let $\mathbf{F}_1 \dots \mathbf{F}_N$, be the generalized active Forces with regard to S, as well as $\mathbf{F}_1^* \dots \mathbf{F}_N^*$, be the generalized inertia forces related to S. After that all of the motions associated with S tend to be Influenced through the equations [6].

$$\mathbf{F}_r + \mathbf{F}_r^* = 0 \tag{3.1}$$

Where, $r = 1 \dots N$.

Suppose there is a rigid body B belonging to S, therefore, the body forces acting on B are seen as the torque T and force R applied at a point Q in B, thus $(F_r)_B$, represents the contribution in F_r, has the following formula:

$$(\mathbf{F}_r)_B = \omega_r \cdot \mathbf{T} + v_{Q_r} \cdot \mathbf{R} \tag{3.2}$$

Where,

$$v_{Q_r} = \frac{\partial v_Q}{\partial \dot{q}_r} \tag{3.3}$$

is the r^{th} partial linear velocity of Q. Similarly

$$\omega_r = \frac{\partial \omega}{\partial \dot{q}_r} \tag{3.4}$$

is the r^{th} partial angular velocity of B.

Similarly,

$$(\mathbf{F}_r^*)_B = \omega_r \cdot \mathbf{T}^* + v_r \cdot \mathbf{R}^* \tag{3.5}$$

Where, T^* and R^* are respectively torque and the inertia force of the rigid body B, as well as v_r is the r^{th} partial linear velocity of the centre of mass of B. The inertia torque and the inertia force of the rigid body B are respectively formulated as follows:

$$\mathbf{T}^* = -\alpha \cdot \mathbf{I} - \omega \times \mathbf{I} \cdot \omega \tag{3.6}$$

$$\mathbf{R}^* = -\mathbf{ma} \tag{3.7}$$

Where, ω and α are respectively the angular and acceleration of the rigid body B, I is the central inertia matrix of B, m and a are the mass and acceleration of B.

CHAPTER 4

MODELING OF UNDERWATER VEHICLE

The general dynamics and kinematics equations for Underwater Vehicle system are presented below.

4.1 Underwater Vehicle Kinematics Equation

To represent the motion of underwater vehicle with six DOFs, the generalized coordinates are needed to show the position and the attitude of the vehicle in space. These six DOFs are surge, sway, heave, yaw, pitch, roll according to [19]. The motion of underwater vehicle is represented by the following vectors.

$$\eta = [\eta_{\mathbf{1}}^{\top}\ \eta_{\mathbf{2}}^{\top}]^{\top} \qquad \eta_{\mathbf{1}} = [x\ y\ z]^{\top} \qquad \eta_2 = [\psi\ \theta\ \phi]^{\top}$$

$$\nu = [\nu_{\mathbf{1}}^{\top}\ \nu_{\mathbf{2}}^{\top}]^{\top} \qquad \nu_{\mathbf{1}} = [\nu_x\ \nu_y\ \nu_z]^{\top} \qquad \nu_2 = [\omega_x\ \omega_y\ \omega_z]^{\top}$$

$$\tau = [\tau_{\mathbf{1}}^{\top}\ \tau_{\mathbf{2}}^{\top}]^{\top} \qquad \tau_{\mathbf{1}} = [X\ Y\ Z]^{\top} \qquad \tau_2 = [K\ L\ M]^{\top} \tag{4.1}$$

Where, $\eta = [\eta_{\mathbf{1}}^{\top}\ \eta_{\mathbf{2}}^{\top}]^{\top}$ includes the position $\eta_{\mathbf{1}}^{\top}$ and the attitude $\eta_{\mathbf{2}}^{\top}$ of the underwater vehicle in Earth frame, $\nu = [\nu_{\mathbf{1}}^{\top}\ \nu_{\mathbf{2}}^{\top}]^{\top}$ represents linear $\nu_{\mathbf{1}}^{\top}$ and angular $\nu_{\mathbf{2}}^{\top}$ velocities of underwater vehicle in the body frame and $\tau = [\tau_{\mathbf{1}}^{\top}\ \tau_{\mathbf{2}}^{\top}]^{\top}$ is input torques $\tau_{\mathbf{1}}$ and moments $\tau_{\mathbf{2}}$ acting on underwater vehicle in the body frame.

Thus, by integrating 4.2 gives η in the Earth frame.

$$\dot{\eta} = \mathbf{R}_{\mathbf{B}}^{\mathbf{I}}(\eta)\nu \tag{4.2}$$

Where, $\mathbf{R}_{\mathbf{B}}^{\mathbf{I}}(\eta)$ is the transformation matrix which transforms the velocities from the body frame to the Earth frame and it has the following components:

$$\mathbf{R}_{\mathbf{B}}^{\mathbf{I}}(\eta) = \begin{bmatrix} \mathbf{R}_{\mathbf{1}3\times3}(\eta) & \mathbf{0}_{3\times3} \\ \mathbf{0}_{3\times3} & \mathbf{R}_{\mathbf{2}3\times3}(\eta) \end{bmatrix} \tag{4.3}$$

Where, $\mathbf{R}_{\mathbf{1}3\times3}(\eta)$ transforms $\nu_{\mathbf{1}}$ (linear velocity for the underwater vehicle) to

position rates in the earth frame and it has the following matrix form:

$$\mathbf{R_1}(\eta) = \begin{bmatrix} C_\psi C_\theta & C_\phi S_\psi - C_\psi S_\phi S_\theta & -S_\phi S_\psi - C_\phi C_\psi S_\theta \\ C_\theta S_\psi & -C_\phi C_\psi - S_\phi S_\psi S_\theta & C_\psi S_\phi - C_\phi S_\psi S_\theta \\ -S_\theta & -C_\theta S_\phi & -C_\phi S_\theta \end{bmatrix} \tag{4.4}$$

Where, $C_x = cos(x)$, and $S_x = sin(x)$ and $\mathbf{R_2}(\eta)$ transforms $\nu_\mathbf{2}$ (angular velocity for the underwater vehicle) to the Euler rates in the earth frame and it has the following matrix form:

$$\mathbf{R_2}(\eta) = \begin{bmatrix} 0 & -S_\phi/C_\theta & C_\phi/C_\theta \\ 0 & -C_\phi & S_\phi \\ 1 & -S_\phi S_\theta/C_\theta & -C_\phi S_\theta/C_\theta \end{bmatrix} \tag{4.5}$$

4.2 Underwater Vehicle Dynamics Equation

The general equation of motion for the underwater vehicle in the body frame is given by:

$$\mathbf{M}\dot{\nu} + \mathbf{C}(\nu)\nu + \mathbf{D}(\nu)\nu + \mathbf{g}(\eta) = \tau \tag{4.6}$$

Where,

$\mathbf{M} \in \mathbb{R}^{6\times6} \equiv$ Inertia matrix including added mass.

$\mathbf{C}(\nu) \in \mathbb{R}^{6\times6} \equiv$ Matrix of Coriolis and centripetal term including added mass.

$\mathbf{D}(\nu) \in \mathbb{R}^{6\times6} \equiv$ Damping matrix.

$\mathbf{g}(\eta) \in \mathbb{R}^6 \equiv$ Vector of gravitational forces and moments.

$\tau \in \mathbb{R}^6 \equiv$ Control Inputs.

And, the inertia matrix consists of two terms as follows:

$$\mathbf{M} = \mathbf{M_{RB}} + \mathbf{M_A} \tag{4.7}$$

Where, M_{RB} represents the rigid body inertia matrix and M_A stands for the added mass which represents the additional forces and moment coefficients caused by the fluid surrounding the vehicle, and it has the following matrix form:

$$\mathbf{M_{RB}} = \begin{bmatrix} m\mathbf{I}_{3\times3} & -m\mathbf{S}(r_g) \\ m\mathbf{S}(r_g) & \mathbf{I}_0 \end{bmatrix} \tag{4.8}$$

Where, $\mathbf{I}_{3\times3} \equiv$ Identity matrix, $\mathbf{I}_0 \equiv$ Inertia tensor with respect to the body frame origin ($\mathbf{I_0} = \mathbf{I_0^\top} > \mathbf{0}$), $\mathbf{r}_g = [r_{g_1}\ r_{g_2}\ r_{g_3}]^\top$ is the centre of gravity vector and $S(r_g)$ is the Skew Symmetric Matrix, defined below:

$$\mathbf{S(r_g)} = \begin{bmatrix} 0 & -r_{g_3} & r_{g_2} \\ r_{g_3} & 0 & -r_{g_1} \\ -r_{g_2} & r_{g_1} & 0 \end{bmatrix} \tag{4.9}$$

And,

$$\mathbf{M_A} = \begin{bmatrix} X_{\dot{u}} & X_{\dot{v}} & X_{\dot{w}} & X_{\dot{p}} & X_{\dot{q}} & X_{\dot{r}} \\ Y_{\dot{u}} & Y_{\dot{v}} & Y_{\dot{w}} & Y_{\dot{p}} & Y_{\dot{q}} & Y_{\dot{r}} \\ Z_{\dot{u}} & Z_{\dot{v}} & Z_{\dot{w}} & Z_{\dot{p}} & Z_{\dot{q}} & Z_{\dot{r}} \\ K_{\dot{u}} & K_{\dot{v}} & K_{\dot{w}} & K_{\dot{p}} & K_{\dot{q}} & K_{\dot{r}} \\ M_{\dot{u}} & M_{\dot{v}} & M_{\dot{w}} & M_{\dot{p}} & M_{\dot{q}} & M_{\dot{r}} \\ N_{\dot{u}} & N_{\dot{v}} & N_{\dot{w}} & N_{\dot{p}} & N_{\dot{q}} & N_{\dot{r}} \end{bmatrix} \tag{4.10}$$

Where, X, Y, Z, K, M, N are the linear forces and torques applied to the underwater vehicle, therefore, for instance $X_{\dot{u}}$ is the hydrodynamic added mass force due to the acceleration $\dot{u}$ in x direction, thus, the Coriolis and centripetal matrix, can be computed from the inertia matrix, to do so, the inertia matrix should be written in sub-matrcies terms as follows:

$$\mathbf{M} = \begin{bmatrix} \mathbf{M_{11}} & \mathbf{M_{12}} \\ \mathbf{M_{21}} & \mathbf{M_{22}} \end{bmatrix} \tag{4.11}$$

Therefore, the Coriolis and centripetal matrix will be given as:

$$\mathbf{C}(\nu) = \begin{bmatrix} \mathbf{0_{3\times 3}} & -\mathbf{S}(\mathbf{M_{11}}\nu_\mathbf{1} + \mathbf{M_{12}}\nu_\mathbf{2}) \\ -\mathbf{S}(\mathbf{M_{11}}\nu_\mathbf{1} + \mathbf{M_{12}}\nu_\mathbf{2}) & -\mathbf{S}(\mathbf{M_{21}}\nu_\mathbf{1} + \mathbf{M_{22}}\nu_\mathbf{2}) \end{bmatrix} \tag{4.12}$$

And, the damping matrix given by:

$$\mathbf{D}(\nu) = \begin{bmatrix} |\nu_1| & 0 & 0 & 0 & 0 & 0 \\ 0 & |\nu_2| & 0 & 0 & 0 & 0 \\ 0 & 0 & |\nu_3| & 0 & 0 & 0 \\ 0 & 0 & 0 & |\nu_4| & 0 & 0 \\ 0 & 0 & 0 & 0 & |\nu_5| & 0 \\ 0 & 0 & 0 & 0 & 0 & |\nu_6| \end{bmatrix} \tag{4.13}$$

Now, the equation of motion for the underwater vehicle in the Earth frame can be written as follows:

$$\mathbf{M_e}(\eta)\ddot{\eta} + \mathbf{C_e}(\eta,\nu)\dot{\eta} + \mathbf{D_e}(\nu,\eta)\dot{\eta} + \mathbf{g_e}(\eta) = \tau_\mathbf{e} \tag{4.14}$$

Where,

$$\begin{aligned} \mathbf{M_e}(\eta) &= \mathbf{R^{-T}}(\eta)\mathbf{M}(\eta)\mathbf{R^{-1}}(\eta) \in \mathbb{R}^{6\times6} \\ \mathbf{C_e}(\eta,\nu) &= \mathbf{R^{-T}}(\eta)[\mathbf{C}(\eta,\nu) - \mathbf{M}(\eta)\mathbf{R^{-1}}(\eta)\dot{\mathbf{R}}(\eta)]\mathbf{R^{-1}}(\eta) \in \mathbb{R}^{6\times6} \\ \mathbf{D_e}(\nu,\eta) &= \mathbf{R^{-T}}(\eta)\mathbf{D}(\nu)\mathbf{R^{-1}}(\eta) \in \mathbb{R}^{6\times6} \\ \mathbf{g_e}(\eta) &= \mathbf{R^{-T}}(\eta)\mathbf{g}(\eta) \in \mathbb{R}^{6} \\ \tau_\mathbf{e} &= \mathbf{R^{-T}}(\eta)\tau \in \mathbb{R}^{6} \end{aligned}$$

CHAPTER 5

DYNAMIC MODEL FOR THE UVMS

In this chapter, the dynamic model of the underwater vehicle with the n DOFs manipulator is developed through the usage of Kane's method, which was introduced in chapter two. The UVMS belongs to the multi-body dynamic systems; because it is composed from two parts, namely is underwater vehicle which has six DOFs and a manipulator (robotic arm) with n DOFs. Therefore, to apply Kane's method we need first to calculate two types of forces, the first one is called the generalized inertia forces, and the second one is called the generalized active forces. These two types of forces must be computed for the entire system (UVMS).

5.1 Coordinate Systems

The coordinate systems will be selected in this section according to the Denavit-Hartenberg (D-H) convention [20]. The D-H parameters are used to keep the

relationship between adjoining coordinate frames (translation and orientation). As shown in Fig 1.2, the total number of coordinate systems attached to the underwater vehicle is $n+1$, were n coordinate frames are assigned to the manipulator and one coordinate frame is assigned to its center of mass (C.M) labeled as the 0^{th} frame. In addition to these frames an Earth frame is to be as a reference frame.

5.1.1 Homogeneous Coordinates

In this section, two types of coordinate vectors are introduced, the first one is called the physical coordinate vector as can be seen in eq. 5.2 and the second one is called homogeneous coordinate vector as can be seen in eq. 5.2 , and they are different because of the addition of 1 in the fourth element of the homogeneous coordinate vector. The main advantage in using the homogeneous coordinate vector is the capability to represent coordinate transformations, including both rotation and translation, using a compact matrix notation.

$$\mathbf{P} = \begin{bmatrix} p_x \\ p_y \\ p_z \end{bmatrix} \tag{5.1}$$

$$\underline{\mathbf{P}} = \begin{bmatrix} p_x \\ p_y \\ p_z \\ 1 \end{bmatrix} \tag{5.2}$$

For instance, assume having two coordinate frames, i and j, in which frame j is rotating and translating from frame i as shown in Fig 5.1. Therefore, the location of point P, can be described in terms of two vectors, d^i and P^j, expressed as follows:

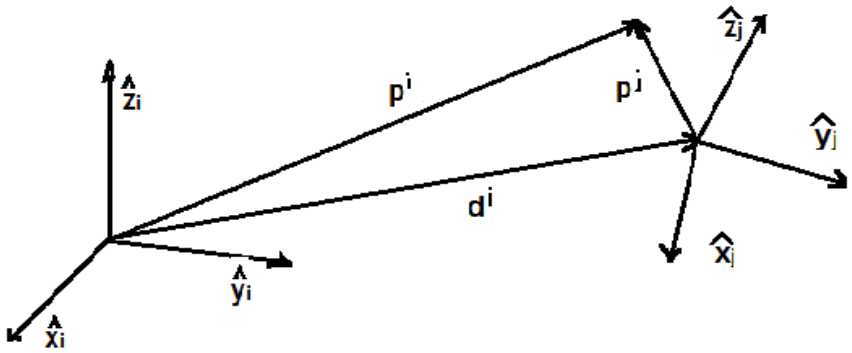

Figure 5.1: Representation of Homogeneous Coordinate Transformations.

$$\begin{bmatrix} p_x \\ p_y \\ p_z \end{bmatrix} = \begin{bmatrix} d_{x_i} \\ d_{y_i} \\ d_{z_i} \end{bmatrix} + \begin{bmatrix} \hat{x}_i \cdot \hat{x}_j & \hat{x}_i \cdot \hat{y}_j & \hat{x}_i \cdot \hat{z}_j \\ \hat{y}_i \cdot \hat{x}_j & \hat{y}_i \cdot \hat{y}_j & \hat{y}_i \cdot \hat{z}_j \\ \hat{z}_i \cdot \hat{x}_j & \hat{z}_i \cdot \hat{y}_j & \hat{z}_i \cdot \hat{z}_j \end{bmatrix} \begin{bmatrix} p_{x_i} \\ p_{y_i} \\ p_{z_i} \end{bmatrix} \tag{5.3}$$

Or, compactly as:

$$\mathbf{P^i} = \mathbf{d^i} + \mathbf{A_i^j P^j} \tag{5.4}$$

Where, $\mathbf{A_i^j}$ represents the direction cosine matrix, containing the information about the orientation of frame j with respect to frame i (without any information about the translation). Thus, a homogeneous transformation will be required because it consists of both orientation and translational information between frame j and i. The homogeneous transformation relating the vector $\mathbf{P^j}$ expressed in the frame j to the vector $\mathbf{P^i}$ expressed in frame i is expressed by the following matrix equation.

$$\begin{bmatrix} p_x \\ p_y \\ p_z \\ 1 \end{bmatrix} = \begin{bmatrix} \hat{x}_i \cdot \hat{x}_j & \hat{x}_i \cdot \hat{y}_j & \hat{x}_i \cdot \hat{z}_j & d_{x_i} \\ \hat{y}_i \cdot \hat{x}_j & \hat{y}_i \cdot \hat{y}_j & \hat{y}_i \cdot \hat{z}_j & d_{y_i} \\ \hat{z}_i \cdot \hat{x}_j & \hat{z}_i \cdot \hat{y}_j & \hat{z}_i \cdot \hat{z}_j & d_{z_i} \\ 0 & 0 & 0 & 1 \end{bmatrix} \begin{bmatrix} p_{x_j} \\ p_{y_j} \\ p_{z_j} \\ 1 \end{bmatrix} \tag{5.5}$$

Or, compactly as:

$$\mathbf{P^i} = \begin{bmatrix} \mathbf{A_i^j} & \mathbf{d^i} \\ \mathbf{0_{1\times 3}} & 1 \end{bmatrix} \begin{bmatrix} \mathbf{P^j} \\ 1 \end{bmatrix} \tag{5.6}$$

It is also possible to rewrite it as:

$$\underline{\mathbf{P}}^{\mathbf{i}} = \underline{\mathbf{A}}_{\mathbf{j}}^{\mathbf{i}} \underline{\mathbf{P}}^{\mathbf{j}} \tag{5.7}$$

Where, $\underline{\mathbf{A}}_{\mathbf{j}}^{\mathbf{i}}$ represents a homogeneous coordinate transformation matrix, which contains the orientation as well as the translation information.

5.1.2 Generalized Coordinates and Speeds

The term "'Generalized Coordinates"' means the states of the dynamic system. Since there are $N = n + 6$ generalized coordinates in the UVMS model, then a vector with N states is used as follows:

$$\eta = \begin{bmatrix} X_v \\ Y_v \\ Z_v \\ \psi_v \\ \theta_v \\ \phi_v \\ \theta_1 \\ \vdots \\ \theta_n \end{bmatrix} \tag{5.8}$$

The generalized coordinates can be computed by integrating the following

differential equation:

$$\dot{\eta} = \mathbf{R}^{\mathbf{I}}_{\mathbf{B}}(\eta)\nu \tag{5.9}$$

Where, $\mathbf{R}^{\mathbf{I}}_{\mathbf{B}}(\eta)$ represents the transformation matrix which transforms the UVMS speed (ν) from the body frame (0^{th}) to the Earth frame ($\mathbf{I}$) $\dot{\eta}$, and it is given as follows:

$$\mathbf{R}^{\mathbf{I}}_{\mathbf{B}}(\eta) = \begin{bmatrix} R_{1_{3\times3}}(\eta) & 0_{3\times3} & 0_{3\times3} \\ 0_{3\times3} & R_{2_{3\times3}}(\eta) & 0_{3\times3} \\ 0_{3\times3} & 0_{3\times3} & R_{3_{n\times n}}(\eta) \end{bmatrix} \tag{5.10}$$

Where, $R_{1_{3\times3}}(\eta)$, $R_{2_{3\times3}}(\eta)$ and $R_{3_{n\times n}}(\eta)$, are respectively expressed by the following matrix equations:

$$\mathbf{R_1}(\eta) = \begin{bmatrix} C_\psi C_\theta & C_\phi S_\psi - C_\psi S_\phi S_\theta & -S_\phi S_\psi - C_\phi C_\psi S_\theta \\ C_\theta S_\psi & -C_\phi C_\psi - S_\phi S_\psi S_\theta & C_\psi S_\phi - C_\phi S_\psi S_\theta \\ -S_\theta & -C_\theta S_\phi & -C_\phi S_\theta \end{bmatrix} \tag{5.11}$$

$$\mathbf{R_2}(\eta) = \begin{bmatrix} 0 & -S_\phi/C_\theta & C_\phi/C_\theta \\ 0 & -C_\phi & S_\phi \\ 1 & -S_\phi S_\theta/C_\theta & -C_\phi S_\theta/C_\theta \end{bmatrix} \tag{5.12}$$

$$\mathbf{R_3}_{n\times n}(\eta) = \begin{bmatrix} 1 & & 0 \\ & \ddots & \\ 0 & & 1 \end{bmatrix} = \mathbf{I}_{nXn} \tag{5.13}$$

Where, $C_x = cos(x)$, and $S_x = sin(x)$ and ν represents the generalized speed and can be expressed by the following vector:

$$\nu = \begin{bmatrix} v_x \\ v_y \\ v_z \\ w_x \\ w_y \\ w_z \\ \dot{\theta}_1 \\ \vdots \\ \dot{\theta}_n \end{bmatrix} \tag{5.14}$$

5.2 Kinematic Analysis

In this section, linear and angular velocities are computed, as well as linear and angular accelerations for each link, which are required to calculate the inertia forces of the system according to Kane's equation represented in chapter two.

5.2.1 Position Vector to a Link's C.M

Keep in mind that each link has its own coordinate frame located at its C.M. In addition to the 0^{th} coordinate frame located at the underwater vehicle C.M., thus, the total number of coordinate frames is equal to $n + 1$. Therefore, the function of the position vector is to transform the C.M. of each link from the local link coordinate frames to the 0^{th} coordinate frame of the vehicle. Thus, the concept of the homogeneous transformation is used to find the position vectors. The homogeneous transformation between successive links is governed by the link Denavit-Hartenberg (D-H) parameters and it is given by the following matrix equation:

$$\underline{\mathbf{A}}^{\mathbf{i}}_{\mathbf{i-1}} = \begin{bmatrix} cos(\theta_i) & -cos(\alpha_i)sin(\theta_i) & sin(\alpha_i)sin(\theta_i) & \alpha_i cos(\theta_i) \\ sin(\theta_i) & cos(\alpha_i)cos(\theta_i) & -sin(\alpha_i)cos(\theta_i) & \alpha_i sin(\theta_i) \\ 0 & sin(\alpha_i) & cos(\alpha_i) & d_i \\ 0 & 0 & 0 & 1 \end{bmatrix} \tag{5.15}$$

Where, θ_i is the rotation angle between frame i and $i-1$ measured about the positive $\hat{z}_{i-1}$ axis, α_i is the twist angle of link i, d_i is the distance parameter of link i and a_i is the length parameter of link i [20].

As a special case, the homogeneous transformation between link 1 and the 0^{th}

frame of the vehicle is given as follows:

$$\underline{\mathbf{A_0^1}} = \begin{bmatrix} cos(\theta_1) & -cos(\alpha_1)sin(\theta_1) & sin(\alpha_1)sin(\theta_1) & c_{x_0} \\ sin(\theta_1) & cos(\alpha_1)cos(\theta_1) & -sin(\alpha_1)cos(\theta_1) & c_{y_0} \\ 0 & sin(\alpha_1) & cos(\alpha_1) & c_{z_0} \\ 0 & 0 & 0 & 1 \end{bmatrix} = \begin{bmatrix} \mathbf{A_0^1} & \mathbf{c_0^0} \\ \mathbf{0_{1\times 3}} & 1 \end{bmatrix} \tag{5.16}$$

Where, $\mathbf{c_0^0}$ is the position vector from the C.M. of the vehicle to the first link coordinate frame expressed in the 0^{th} coordinate frame. Thus, the position vector of the C.M of link 1 expressed in 0^{th} frame will be as follows:

$$\underline{\mathbf{P_1^0}} = \underline{\mathbf{A_0^1}}\underline{\mathbf{c_1^1}} \tag{5.17}$$

Where, $\mathbf{c_1^1}$ is the homogeneous position vector to the C.M. of link 1 expressed in its local coordinate frame, therefore, in general, $\mathbf{c_j^j}$ will represent the homogeneous position vector to the C.M. of link j expressed in its own local coordinate frame.

The position vector of the C.M of link 2 expressed in 0^{th} frame will be as follows:

$$\underline{\mathbf{P_2^0}} = \underline{\mathbf{A_0^1}}\underline{\mathbf{A_1^2}}\underline{\mathbf{c_2^2}} \tag{5.18}$$

In the same manner, a general form of the positions vectors of k links are given

by:

$$\underline{\mathbf{P}}_{\mathbf{j}}^{\mathbf{0}} = \left(\prod_{\mathbf{k=1}}^{\mathbf{j}} \underline{\mathbf{A}}_{\mathbf{k-1}}^{\mathbf{k}} \right) \underline{\mathbf{c}}_{\mathbf{j}}^{\mathbf{j}} \tag{5.19}$$

5.2.2 Angular Velocity

In this chapter, the following notations are used, ($\mathbf{w}_{\mathbf{j}}^{\mathbf{i}}$, $\mathbf{v}_{\mathbf{j}}^{\mathbf{i}}$, $\alpha_{\mathbf{j}}^{\mathbf{i}}$ and $\mathbf{a}_{\mathbf{j}}^{\mathbf{i}}$) and represent the angular and linear velocities as well as the angular and linear accelerations of the C.M of link j, respectively, with respect to the Earth frame expressed in the 0^{th} coordinate frame, ($\hat{\mathbf{x}}$, $\hat{\mathbf{y}}$ and $\hat{\mathbf{z}}$) are represent the unit vectors, as special cases ($\mathbf{w}_{\mathbf{0}}^{\mathbf{i}}$, $\mathbf{v}_{\mathbf{0}}^{\mathbf{i}}$, $\alpha_{\mathbf{0}}^{\mathbf{i}}$ and $\mathbf{a}_{\mathbf{0}}^{\mathbf{i}}$) are represent the angular and linear velocities as well as the angular and linear accelerations of the C.M of vehicle with respect to the Earth frame expressed in the 0^{th} coordinate frame. Therefore, the angular velocity for the AUV will be as follows:

$$\mathbf{w}_{\mathbf{0}}^{\mathbf{i}} = w_x \hat{\mathbf{x}}_{\mathbf{0}} + w_y \hat{\mathbf{y}}_{\mathbf{0}} + w_z \hat{\mathbf{z}}_{\mathbf{0}} \tag{5.20}$$

In the same manner, the angular velocities for the manipulator links will be as follows:

$$
\begin{aligned}
\mathbf{w_1^i} &= \mathbf{w_0^i} + \mathbf{w_1^i} = \mathbf{w_0^i} + \dot{\theta}_1 \hat{\mathbf{z}}_\mathbf{0} \qquad 1^{st} \text{ link} \\
\mathbf{w_2^i} &= \mathbf{w_0^i} + \mathbf{w_1^i} + \mathbf{A_0^1 w_2^1} \qquad 2^{nd} \text{ link} \\
&= \mathbf{w_0^i} + \dot{\theta}_\mathbf{1} \hat{\mathbf{z}}_\mathbf{0} + \mathbf{A_0^1} \dot{\theta}_2 \hat{\mathbf{z}}_\mathbf{0} \\
&\vdots \\
\mathbf{w_j^i} &= \mathbf{w_0^i} + \mathbf{w_1^0} + \sum_{l=1}^{j-1} \prod_{m=1}^{l} \mathbf{A_{m-1}^m w_{l+1}^l} \qquad j^{th} \text{ link}
\end{aligned} \tag{5.21}
$$

Where,

$\mathbf{w_{l+1}^l} = [0\ 0\ \ \dot{\theta}_{l+1}]^\top$ is the angular velocity of link $l+1$ with respect to the $\hat{\mathbf{z}}_\mathbf{l}$ axis.

5.2.3 Linear Velocity

The linear velocity for the vehicle is given by the the following equation:

$$
\mathbf{v_0^i} = v_x \hat{\mathbf{x}}_\mathbf{0} + v_y \hat{\mathbf{y}}_\mathbf{0} + v_z \hat{\mathbf{z}}_\mathbf{0} \tag{5.22}
$$

While, the linear velocities of the manipulator's links are given as follows:

$$\begin{aligned}
\mathbf{v_1^0} &= \mathbf{v_0^0} + \frac{\mathbf{dP_1^0}}{\mathbf{dt}} + \mathbf{w_0^i} \times \mathbf{P_1^0} && 1^{st} \text{ link} \\
\mathbf{v_2^0} &= \mathbf{v_0^0} + \frac{\mathbf{dP_2^0}}{\mathbf{dt}} + \mathbf{w_0^i} \times \mathbf{P_2^0} && 2^{nd} \text{ link} \\
&\vdots \\
\mathbf{v_j^0} &= \mathbf{v_0^0} + \frac{\mathbf{dP_j^0}}{\mathbf{dt}} + \mathbf{w_0^i} \times \mathbf{P_j^0} && j^{th} \text{ link}
\end{aligned} \tag{5.23}$$

5.2.4 Angular Acceleration

The angular acceleration for the vehicle is given by the the following equation:

$$\alpha_{\mathbf{0}}^{\mathbf{i}} = \frac{\mathbf{dw_0^i}}{\mathbf{dt}} = \dot{w}_x \hat{\mathbf{x}}_\mathbf{0} + \dot{w}_y \hat{\mathbf{y}}_\mathbf{0} + \dot{w}_z \hat{\mathbf{z}}_\mathbf{0} \tag{5.24}$$

While the angular acceleration of the manipulator's links are given as follows:

$$\begin{aligned}
\alpha_{\mathbf{1}}^{\mathbf{i}} &= \frac{\mathbf{dw_1^i}}{\mathbf{dt}} + \mathbf{w_0^i} \times \mathbf{w_1^i} && 1^{st} \text{ link} \\
\alpha_{\mathbf{2}}^{\mathbf{i}} &= \frac{\mathbf{dw_2^i}}{\mathbf{dt}} + \mathbf{w_0^i} \times \mathbf{w_2^i} && 2^{nd} \text{ link} \\
&\vdots \\
\alpha_{\mathbf{j}}^{\mathbf{i}} &= \frac{\mathbf{dw_j^i}}{\mathbf{dt}} + \mathbf{w_0^i} \times \mathbf{w_j^i} && j^{th} \text{ link}
\end{aligned} \tag{5.25}$$

5.2.5 Linear Acceleration

The linear acceleration for the vehicle is given by the the following equation:

$$\mathbf{a_0^0} = \frac{\mathbf{dv_0^0}}{\mathbf{dt}} + \mathbf{w_0^i} \times \mathbf{v_0^0} \tag{5.26}$$

While the linear acceleration of the manipulator's links are given as follows:

$$\begin{aligned}
\mathbf{a_1^0} &= \frac{\mathbf{dv_1^0}}{\mathbf{dt}} + \mathbf{w_0^i} \times \mathbf{v_1^0} && 1^{st} \text{ link} \\
\mathbf{a_2^0} &= \frac{\mathbf{dv_2^0}}{\mathbf{dt}} + \mathbf{w_0^i} \times \mathbf{v_2^0} && 2^{nd} \text{ link} \\
&\vdots \\
\mathbf{a_j^0} &= \frac{\mathbf{dv_j^0}}{\mathbf{dt}} + \mathbf{w_0^i} \times \mathbf{v_j^0} && j^{th} \text{ link}
\end{aligned} \tag{5.27}$$

5.3 Inertia Forces

The inertia force $\mathbf{R_0^*}$ of the vehicle is given by the following equation:

$$\mathbf{R_0^*} = -\mathbf{m_0}\ \mathbf{a_0^0} \tag{5.28}$$

Where, $\mathbf{m_0}$ and $\mathbf{a_0^0}$ represents the mass and the linear acceleration of the vehicle, respectively.

The inertia force $\mathbf{R_j^*}$ for the manipulator's links is given by the following equa-

tion:

$$\mathbf{R_j^*} = -\mathbf{m_j}\ \mathbf{a_j^0} \tag{5.29}$$

Where, $\mathbf{m_j}$ and $\mathbf{a_j^0}$ represents the mass and the linear acceleration of the manipulator link j, respectively.

The inertia torque $\mathbf{T_0^*}$ of the vehicle is given by the following equation:

$$\mathbf{T_0^*} = -\alpha_\mathbf{0}^\mathbf{0} \cdot \mathbf{I_0^0} - \mathbf{w_j^i} \times \mathbf{I_0^0} \cdot \mathbf{w_0^i} \tag{5.30}$$

Where, $\mathbf{I_0^0}$is the central inertia matrix of the vehicle.

The inertia torque $\mathbf{T_j^*}$ of the manipulator's links are given by the following equation:

$$\mathbf{T_j^*} = -\alpha_\mathbf{j}^\mathbf{0} \cdot \mathbf{I_j^0} - \mathbf{w_j^i} \times \mathbf{I_j^0} \cdot \mathbf{w_j^i} \tag{5.31}$$

Where, $\mathbf{I_j^0}$ is the central inertia matrix of the manipulator link J which can be computed by using the following formula:

$$\mathbf{I_j^0} = \mathbf{A_0^j I_j^j} (\mathbf{A_0^j})^\top \tag{5.32}$$

Where, $\mathbf{A_0^j}$ is the direction cosine matrix connecting frame j to the 0^{th} frame and $\mathbf{I_j^j}$ is the central inertia matrix of link j expressed in its frame.

Thus, the generalized inertia force for the total system (UVMS) according to the Kane's equation introduced in chapter 2, can be written as follows:

$$\mathbf{F_r^*} = \sum_{\mathbf{j=0}}^{\mathbf{n}} (\frac{\partial \mathbf{w_j^i}}{\partial \nu_\mathbf{r}} \cdot \mathbf{T_j^*} + \frac{\partial \mathbf{v_j^i}}{\partial \nu_\mathbf{r}} \cdot \mathbf{R_j^*}) \tag{5.33}$$

Where, $r = 1, \cdots, N$ represents the number of DOFs.

5.4 Gravity Forces

Gravity force categorized as the active force, due to its acting on the C.M. of each link in the UVMS system. Therefore, the force of the gravity $\mathbf{R_{g_i}}$, acting on an arbitrary link j with mass $\mathbf{m_j}$, is given by the following formula:

$$\mathbf{R_{g_i}} = \mathbf{m_j}\ \mathbf{g_{0_j}} \tag{5.34}$$

The generalized active force of gravity $(\mathbf{F_r})_\mathbf{g}$ for the entire UVMS sysrem is given by:

$$(\mathbf{F_r})_\mathbf{g} = \sum_{\mathbf{j=0}}^{\mathbf{n}} \mathbf{m_j} \frac{\partial \mathbf{v_j^0}}{\partial \nu_\mathbf{r}} \cdot \mathbf{g_{0_j}} \tag{5.35}$$

Where,

$$\mathbf{g_{0_j}} = \begin{bmatrix} g_{x_j} \\ g_{y_j} \\ g_{z_j} \end{bmatrix} \tag{5.36}$$

Represents the gravity force vector for the arbitrary Link expressed in the vehicle coordinate frame (0^{th} frame).

Therefore, for the UVMS system the gravity vector expressed in the vehicle coordinate frame (0^{th} frame) will be as follows:

$$\mathbf{g_{0_j}} = \mathbf{R_1^{-1}} * \mathbf{g} + \mathbf{R_1^{-1}} * (\sum_{\mathbf{l=1}}^{\mathbf{j-1}} \prod_{\mathbf{m=1}}^{\mathbf{l}} \mathbf{A_{m-1}^{m}} * \mathbf{g}) \tag{5.37}$$

Where,

$$\mathbf{g} = \begin{bmatrix} 0 \\ 0 \\ 9.8 \end{bmatrix}, \tag{5.38}$$

Is the gravity vector in the Earth frame.

Thus, by substituting eq. 5.37 into eq. 5.35 the generalized active force of the gravity for the entire UVMS sysrem will be obtained.

5.5 Hydrodynamic Forces

The hydrodynamic forces are listed in terms of added mass, buoyancy, fluid acceleration, and drag, which are generally caused by the motion of the vehicle in an underwater environment which results in a highly nonlinear dynamics of the vehicle. Along this section, these hydrodynamic forces are computed using Kane's equation.

5.5.1 Added Mass

The added mass represents the additional forces and moments coefficients, caused by the fluid surrounding the vehicle and the manipulator's links, this phenomenon will be seen as the virtual mass (added mass), as a result of that, this added mass must be taken into account in the dynamic equation of the UVMS system [21].

The inertia force $\mathbf{R}^*_{\mathbf{A_j}}$ and torque $\mathbf{T}^*_{\mathbf{A_j}}$ have been shown and extracted in [6, 21, 22] where, the added mass phenomenon of a submerged body is given by the following equation matrix form:

$$\begin{bmatrix} \mathbf{R}^*_{\mathbf{A_j}} \\ \mathbf{T}^*_{\mathbf{A_j}} \end{bmatrix} = \mathbf{I}^{\mathbf{0}}_{\mathbf{A_j}} \begin{bmatrix} \dot{\mathbf{v}}^{\mathbf{0}}_{\mathbf{j}} \\ \dot{\mathbf{w}}^{\mathbf{i}}_{\mathbf{j}} \end{bmatrix} - \begin{bmatrix} \tilde{\mathbf{w}}^{\mathbf{i}}_{\mathbf{j}} & \mathbf{0_{3\times 3}} \\ \tilde{\mathbf{v}}^{\mathbf{0}}_{\mathbf{j}} & \tilde{\mathbf{w}}^{\mathbf{i}}_{\mathbf{j}} \end{bmatrix} \mathbf{I}^{\mathbf{0}}_{\mathbf{A_j}} \begin{bmatrix} \mathbf{v}^{\mathbf{0}}_{\mathbf{j}} \\ \mathbf{w}^{\mathbf{i}}_{\mathbf{j}} \end{bmatrix} \tag{5.39}$$

Where, $\tilde{\mathbf{v}}^{\mathbf{0}}_{\mathbf{j}}$ and $\tilde{\mathbf{w}}^{\mathbf{i}}_{\mathbf{j}}$ are skew symmetric matrices and $\mathbf{I}^{\mathbf{0}}_{\mathbf{A_j}}$ is the 6×6 added mass matrix.

And, $\dot{\mathbf{v}}^{\mathbf{0}}_{\mathbf{j}}$ and $\dot{\mathbf{w}}^{\mathbf{i}}_{\mathbf{j}}$ are extracted by just rewriting eq. 5.27 and 5.25 to be in the

following forms:

$$\dot{\mathbf{v}}_{\mathbf{j}}^{\mathbf{0}} = \mathbf{a}_{\mathbf{j}}^{\mathbf{0}} - \mathbf{w}_{\mathbf{0}}^{\mathbf{i}} \times \mathbf{v}_{\mathbf{j}}^{\mathbf{0}} \tag{5.40}$$

$$\dot{\mathbf{w}}_{\mathbf{j}}^{\mathbf{i}} = \alpha_{\mathbf{j}}^{\mathbf{i}} - \mathbf{w}_{\mathbf{0}}^{\mathbf{i}} \times \mathbf{w}_{\mathbf{j}}^{\mathbf{i}} \tag{5.41}$$

Substituting the above two equations into equation 5.39 leads to:

$$\begin{bmatrix} \mathbf{R}_{\mathbf{A_j}}^{*} \\ \mathbf{T}_{\mathbf{A_j}}^{*} \end{bmatrix} = -\mathbf{I}_{\mathbf{A_j}}^{\mathbf{0}} \begin{bmatrix} \mathbf{a}_{\mathbf{j}}^{\mathbf{0}} \\ \alpha_{\mathbf{j}}^{\mathbf{i}} \end{bmatrix} + \mathbf{I}_{\mathbf{A_j}}^{\mathbf{0}} \begin{bmatrix} \mathbf{w}_{\mathbf{j}}^{\mathbf{i}} \times \mathbf{v}_{\mathbf{j}}^{\mathbf{0}} \\ \mathbf{w}_{\mathbf{0}}^{\mathbf{i}} \times \mathbf{w}_{\mathbf{j}}^{\mathbf{i}} \end{bmatrix} - \begin{bmatrix} \tilde{\mathbf{w}}_{\mathbf{j}}^{\mathbf{i}} & \mathbf{0_{3\times 3}} \\ \tilde{\mathbf{v}}_{\mathbf{j}}^{\mathbf{0}} & \tilde{\mathbf{w}}_{\mathbf{j}}^{\mathbf{i}} \end{bmatrix} \mathbf{I}_{\mathbf{A_j}}^{\mathbf{0}} \begin{bmatrix} \mathbf{v}_{\mathbf{j}}^{\mathbf{0}} \\ \mathbf{w}_{\mathbf{j}}^{\mathbf{i}} \end{bmatrix} \tag{5.42}$$

The relative velocity and acceleration of the fluid are computed by the following formulas:

$$\begin{aligned} \nu_{\mathbf{j}}^{\mathbf{0}} &= \mathbf{v}_{\mathbf{j}}^{\mathbf{0}} - \mathbf{v}_{\mathbf{f}}^{\mathbf{0}} \\ \sigma_{\mathbf{j}}^{\mathbf{0}} &= \mathbf{a}_{\mathbf{j}}^{\mathbf{0}} - \mathbf{a}_{\mathbf{f}}^{\mathbf{0}} \end{aligned} \tag{5.43}$$

Where, $\mathbf{v}_{\mathbf{f}}^{\mathbf{0}}$ and $\mathbf{a}_{\mathbf{f}}^{\mathbf{0}}$ are the velocity and the acceleration of the fluid, respectively.

Therefore, by substituting eq. 5.43 into eq. 5.42 the final form of the inertia force and torque will be:

$$\begin{bmatrix} \mathbf{R}_{\mathbf{A_j}}^{*} \\ \mathbf{T}_{\mathbf{A_j}}^{*} \end{bmatrix} = -\mathbf{I}_{\mathbf{A_j}}^{\mathbf{0}} \begin{bmatrix} \sigma_{\mathbf{j}}^{\mathbf{0}} \\ \alpha_{\mathbf{j}}^{\mathbf{i}} \end{bmatrix} + \mathbf{I}_{\mathbf{A_j}}^{\mathbf{0}} \begin{bmatrix} \mathbf{w}_{\mathbf{j}}^{\mathbf{i}} \times \nu_{\mathbf{j}}^{\mathbf{0}} \\ \mathbf{w}_{\mathbf{0}}^{\mathbf{i}} \times \mathbf{w}_{\mathbf{j}}^{\mathbf{i}} \end{bmatrix} - \begin{bmatrix} \tilde{\mathbf{w}}_{\mathbf{j}}^{\mathbf{i}} & \mathbf{0_{3\times 3}} \\ \tilde{\nu}_{\mathbf{j}}^{\mathbf{0}} & \tilde{\mathbf{w}}_{\mathbf{j}}^{\mathbf{i}} \end{bmatrix} \mathbf{I}_{\mathbf{A_j}}^{\mathbf{0}} \begin{bmatrix} \nu_{\mathbf{j}}^{\mathbf{0}} \\ \mathbf{w}_{\mathbf{j}}^{\mathbf{i}} \end{bmatrix} \tag{5.44}$$

The generalized inertia force $(\mathbf{F}_{\mathbf{r}}^{*})_{\mathbf{AM}}$ caused by the added mass (represents the contribution of the hydrodynamic force and torque for the dynamic model)

for the total system (UVMS system) is obtained as follows:

$$(\mathbf{F_r^*})_{\mathbf{AM}} = \sum_{\mathbf{j=0}}^{\mathbf{n}} (\frac{\partial \mathbf{w_j^i}}{\partial \nu_\mathbf{r}} \cdot \mathbf{T_{A_j}^*} + \frac{\partial \mathbf{v_j^0}}{\partial \nu_\mathbf{r}} \cdot \mathbf{R_{A_j}^*}) \tag{5.45}$$

Now, the inertia matrix $\mathbf{M}(\eta)$ for the total system (UVMS) can be extracted, by summing the generalized inertia forces (see eq. 5.33) with the generalized inertia forces caused by the added mass (see eq. 5.45), then applying the Jacobian for this summation with respect to the acceleration (see eq. 5.46)

$$(\mathbf{M}(\eta))_{\mathbf{i,j}} = -\frac{\partial((\mathbf{F_i^*}) + (\mathbf{F_i^*})_{\mathbf{AM}})}{\partial \dot{\nu}_\mathbf{j}} \tag{5.46}$$

For the purpose of the analysis, the inertia matrix of the total system is

$$\mathbf{M_{N\times N}}(\eta) = \left[\begin{array}{c|c} \mathbf{M_v} + \mathbf{H}(\eta) & \mathbf{M_c}(\eta) \\ \hline \mathbf{M_c^\top}(\eta) & \mathbf{M_m}(\eta) \end{array}\right] \tag{5.47}$$

Where, $\mathbf{M_c}(\eta)$ is the reaction inertia matrix between the vehicle and the manipulator, $\mathbf{M_v}$ is the inertia matrix for vehicle, $\mathbf{H}(\eta)$ is the added inertia due to the manipulator, and $\mathbf{M_m}(\eta)$ is the inertia matrix for the manipulator.

Since, the inertia matrix for the UVMS system $\mathbf{M_{N\times N}}(\eta)$ is known, therefore, the Coriolis and centripetal matrix $\mathbf{C_{n\times n}}(\nu, \eta)$ can be selected according to [5] page 154, as the following equation:

$$\mathbf{C_{ij}} = \frac{\mathbf{1}}{\mathbf{2}}\dot{\mathbf{M}}_{\mathbf{ij}}(\eta) + \frac{\mathbf{1}}{\mathbf{2}}\sum_{\mathbf{k=1}}^{\mathbf{n}}(\frac{\partial \mathbf{M_{ik}}(\eta)}{\partial \eta_{\mathbf{j}}} - \frac{\partial \mathbf{M_{jk}}(\eta)}{\partial \eta_{\mathbf{i}}})\dot{\eta}_{\mathbf{k}} \tag{5.48}$$

At this point, the inertia, Coriolis & centripetal matrices have been calculated.

5.5.2 Buoyancy

Buoyancy force is the net force on a rigid body caused by the pressure differences in the surrounding water caused by gravity, and it acts through the centre of gravity or the centre of mass. Therefore, if the centre of buoyancy is not on the same vertical line as the centre of gravity, there will be a resulting torque. [**?**].

Thus, for a homogeneous symmetric shape, the centre of mass and the centre of buoyancy are identical. In this thesis the buoyancy force $\mathbf{R_{B_j}}$ is assumed to be acting through the centre of mass of the vehicle and the manipulator's links, and it is expressed by the following formula:

$$\mathbf{R_{B_j}} = -\rho \mathbf{V_j} \mathbf{g_{0_j}} \tag{5.49}$$

Where, ρ represents the density of the fluid, $\mathbf{V_j}$ represents the volume of the fluid displaced by link j and $\mathbf{g_{0_j}}$ is the gravity vector for the arbitrary Link expressed in the AUV frame (0^{th} frame).

So, the generalized active force caused by the buoyancy $(\mathbf{F_r})_{\mathbf{Buoy}}$ for the total

system (UVMS model) as follows:

$$(\mathbf{F_r})_{\mathbf{Buoy}} = -\rho \sum_{\mathbf{j=0}}^{\mathbf{n}} \mathbf{V_j} \frac{\partial \mathbf{v_j^0}}{\partial \nu_\mathbf{r}} \cdot \mathbf{g_{0_j}} \tag{5.50}$$

Where, $r = 1, \cdots, N$

Thus, at this point the net gravity forces acting on the total system (UVMS model) can be computed by summing both forces namely, the generalized active force as a result of the gravity (eq. 5.35) with the generalized active force caused by the buoyancy (eq. 5.50) which leads to following gravity vector force:

$$(\mathbf{F_g})_{\mathbf{N\times 1}} = (\mathbf{F_r})_\mathbf{g} + (\mathbf{F_r})_{\mathbf{Buoy}} \tag{5.51}$$

Thus, the final form of the gravity force vector will look like the following:

$$\mathbf{g}(\eta)_{\mathbf{N\times 1}} = \begin{bmatrix} \mathbf{g_v}(\eta)_{\mathbf{6\times 1}} + \mathbf{g_E}(\eta)_{\mathbf{6\times 1}} \\ \\ \mathbf{g_m}(\eta)_{\mathbf{n\times 1}} \end{bmatrix} \tag{5.52}$$

Where, $\mathbf{g_v}(\eta)_{\mathbf{N\times 1}}$ is the gravity forces and moments vector for the vehicle, $\mathbf{g_E}(\eta)_{\mathbf{6\times 1}}$ is the gravity forces and moments vector on the vehicle due to manipulator and $\mathbf{g_m}(\eta)_{\mathbf{n\times 1}}$ is the gravity forces and moments vector for the manipulator.

5.5.3 Fluid Acceleration

Fluid acceleration is the rate of change in the fluid velocity. it is assumed that it is acting through the C.M of the vehicle and the manipulator's links.

The fluid acceleration force $\mathbf{R_{Fl_j}}$ can be written as the following:

$$\mathbf{R_{Fl_j}} = \rho \mathbf{V_j} \mathbf{a_{Fl}^0} \tag{5.53}$$

Where, $\mathbf{a_{Fl}^0}$ represents the acceleration of the fluid.

Therefore, the generalized active force $(\mathbf{F_r})_{\mathbf{FluidAccel}}$ caused by the fluid acceleration is given by the following equation:

$$(\mathbf{F_r})_{\mathbf{FluidAccel}} = \rho \sum_{\mathbf{j=0}}^{\mathbf{n}} \mathbf{V_j} \frac{\partial \mathbf{v_j^0}}{\partial \nu_\mathbf{r}} \cdot \mathbf{a_{Fl}^0} \tag{5.54}$$

Where, $r = 1, \cdots, N$

5.5.4 Drag Force

In general, the drag force is proportional to the square of the relative velocity of the rigid body irrespective to the medium (water, gas, air, and so on), and it depends on the geometric shape of the rigid body and the density of the medium. The drag force consists of profile drag, skin friction drag, and lift forces.

The profile drag force and torque acting on an infinitesimal part of the link are given by the following expressions respectively:

$$\mathbf{dR_{Drag_j}} = -0.5 \rho C_D b_i \| \mathbf{v_j^0}(\mathbf{l})^\perp \| \mathbf{v_j^0}(\mathbf{l})^\perp \mathbf{dl} \tag{5.55}$$

$$\mathbf{dT_{Drag_j}} = -0.5\rho C_D b_i \|\mathbf{v_j^0}(\mathbf{l})^{\perp}\|(\mathbf{A_0^j l\hat{x}_j} \times \mathbf{v_j^0}(\mathbf{l})^{\perp})\mathbf{dl} \tag{5.56}$$

Where, $\mathbf{l}$ is the link length, $\mathbf{dl}$ is the length of the infinitesimal element, b_j is the width of the rectangle that circumscribes the frontal projection of the infinitesimal element of link j, $\mathbf{v_j^0}(\mathbf{l})^{\perp}$ is the relative velocity of link j with respect to the fluid normal to the link along the length.

And, C_D is the drag coefficient (it is a function of the link geometry $C_{D,basic}$ see [23] for different link shapes, and fluid flow angle σ), it has the following formula:

$$C_D = C_{D,basic} sin^2(\sigma) \tag{5.57}$$

Therefore, to find the force and moment on link j caused by profile drag, the surface integral in eq. 5.55 and eq. 5.56 should be converted to a line integral by using strip theory, which leads to:

$$\begin{aligned} \mathbf{R_{Drag_j}} &= -0.5\rho \int_0^L \|\mathbf{v_j^0}(\mathbf{l})^{\perp}\| \mathbf{v_j^0}(\mathbf{l})^{\perp} C_D b_i \mathbf{dl} \\ \mathbf{T_{Drag_j}} &= -0.5\rho \int_0^L \|\mathbf{v_j^0}(\mathbf{l})^{\perp}\| (\mathbf{A_0^j l\hat{x}_j} \times \mathbf{v_j^0}(\mathbf{l})^{\perp}) C_D b_i \mathbf{dl} \end{aligned} \tag{5.58}$$

The generalized active force caused by the drag force and torque for the total system (UVMS) is given by the following equation:

$$(\mathbf{F_r})_{\mathbf{Drag}} = \sum_{\mathbf{j=0}}^{\mathbf{n}} (\frac{\partial \mathbf{w_j^i}}{\partial \nu_\mathbf{r}} \cdot \mathbf{T_{Drag_i}} + \frac{\partial \mathbf{v_j^0}}{\partial \nu_\mathbf{r}} \cdot \mathbf{R_{Drag_i}}) \tag{5.59}$$

with $r = 1, \cdots, N$

Therefore, the drag matrix $(\mathbf{D}(\nu,\eta))_{\mathbf{N\times N}}$ for the total system (UVMS model) extracted by computing the Jacobian for the drag force with respect to the acceleration $\dot{\nu}$ is given by the following equation:

$$(\mathbf{D}(\nu,\eta))_{\mathbf{i,j}} = -\frac{\partial(\mathbf{F_i})_{\mathbf{Drag}}}{\partial\dot{\nu}_{\mathbf{j}}} \tag{5.60}$$

Finally, the damping matrix will have the following form:

$$\mathbf{D}(\nu,\eta)_{\mathbf{N\times N}} = \begin{bmatrix} \mathbf{D_v}(\nu,\eta)_{\mathbf{6\times 6}} & \mathbf{0} \\ \mathbf{0} & \mathbf{D_m}(\nu,\eta)_{\mathbf{n\times n}} \end{bmatrix} \tag{5.61}$$

Where, $\mathbf{D_v}(\nu,\eta)$ is the damping matrix for the vehicle and $\mathbf{D_m}(\nu,\eta)_{\mathbf{n\times 1}}$ is the damping matrix for the manipulator.

5.6 Dynamic model

The closed form of the dynamic model for the UVMS according to Kane's equation, can be written as follows:

$$\mathbf{M}(\eta)\dot{\nu} + \mathbf{C}(\eta,\nu)\nu + \mathbf{D}(\nu,\eta)\nu + \mathbf{g}(\eta) = \tau \tag{5.62}$$

Where, τ, represents the external input forces vector, and $\tau_{\mathbf{v}}$ and $\tau_{\mathbf{m}}$ represent the input forces for the vehicle and the input forces for the manipulator, respectively.

Similarly, the equation of motion for the UVMS in the earth fixed reference

frame can be written as follows:

$$\mathbf{M_e}(\eta)\ddot{\eta} + \mathbf{C_e}(\eta,\nu)\dot{\eta} + \mathbf{D_e}(\nu,\eta)\dot{\eta} + \mathbf{g_e}(\eta) = \tau_\mathbf{e} \tag{5.63}$$

where,

$$\begin{aligned}
\mathbf{M_e}(\eta) =& \mathbf{R^{-T}}(\eta)\mathbf{M}(\eta)\mathbf{R^{-1}}(\eta) \in \mathbf{R^{(6+n)\times(6+n)}} \\
\mathbf{C_e}(\eta,\nu) =& \mathbf{R^{-T}}(\eta)[\mathbf{C}(\eta,\nu) - \mathbf{M}(\eta)\mathbf{R^{-1}}(\eta)\dot{\mathbf{R}}(\eta)]\mathbf{R^{-1}}(\eta) \in \mathbf{R^{(6+n)\times(6+n)}} \\
\mathbf{D_e}(\nu,\eta) =& \mathbf{R^{-T}}(\eta)\mathbf{D}(\nu)\mathbf{R^{-1}}(\eta) \in \mathbf{R^{(6+n)\times(6+n)}} \\
\mathbf{g_e}(\eta) =& \mathbf{R^{-T}}(\eta)\mathbf{g}(\eta) \in \mathbf{R^{6+n}} \\
\tau_\mathbf{e} =& \mathbf{R^{-T}}(\eta)\tau \in \mathbf{R^{6+n}}
\end{aligned}$$

And, n represents the number of DOFs of the manipulator.

5.7 Properties of Equation of Motion

For both vehicle and UVMS systems, the following properties hold:

The inertia matrix for the total system is symmetric and strictly positive definite

$\mathbf{M}(\eta) = \mathbf{M}^\top(\eta) > \mathbf{0}$

The Damping matrix for the total system is strictly positive definite

$\mathbf{D}(\eta,\nu) > \mathbf{0}$

Finally for the total system

$\mathbf{x}^\top[\dot{\mathbf{M}}(\eta) - 2\mathbf{C}(\eta,\nu)]\mathbf{x} = \mathbf{0}$ is true

Where, $\mathbf{x}$ is an arbitrary vector.

5.8 Example: 3 links Manipulator attached to the Underwater Vehicle

In this section, the model of underwater vehicle with 3 links manipulator has been developed by applying Kane's method by following the all steps presented in the previous section, see [6] chapter 5.

The parameters of the UVMS model selected to be matched with Jason Underwater Vehicle [1], as well as, with the first 3 links of the Puma 560 manipulator, therefore, the UVMS model has 9 DOFs, see tables (7.1 and 7.2). All equations presented in the previous section solved by using MATLAB 12 b in this section.

5.8.1 Coordinate Systems for the UVMS

Since, there are 9 DOFs, therefore, there will be 9 states of the model which are described in the Earth frame as follows:

$$\eta = \begin{bmatrix} X_v \\ Y_v \\ Z_v \\ \psi_v \\ \theta_v \\ \phi_v \\ \theta_1 \\ \theta_2 \\ \theta_3 \end{bmatrix} \tag{5.64}$$

And, the generalized speed vector,

$$\nu = \begin{bmatrix} v_x \\ v_y \\ v_z \\ w_x \\ w_y \\ w_z \\ \dot{\theta}_1 \\ \dot{\theta}_2 \\ \dot{\theta}_3 \end{bmatrix} \tag{5.65}$$

The equation of motion of the UVMS will be formulated in the 0^{th} frame.

5.8.2 Kinematic Analysis of the UVMS

The aim of the Kinematic Analysis is to calculate the inertia forces of the UVMS, to achieve this task, first, the following items must be calculated according to the section 5.2:

1. Position Vectors

2. Angular Velocities

3. Linear Velocities

4. Angular Accelerations

5. Linear Accelerations

The dimensions of the Jason Underwater Vehicle are given as in the following tables: The first joint of the manipulator located on the vehicle at point,

Length	$L = 2.2m$
Height	$H = 1.2m$
Width	$W = 1.1m$

Table 5.1: Dimension of Jason Underwater Vehicle [1]

$(0.5L \quad 0 \quad 0.5H)$, where, L and H represent the Vehicle's Length and Height, respectively. Therefore, the position vector from the C.M. of the vehicle the first joint of the manipulator can be written as the follows:

$$\mathbf{c_0^0} = [c_{x_0} \quad c_{y_0} \quad c_{z_0}]^\top = [0.5L \quad 0 \quad 0.5H]^\top = [1.1 \quad 0 \quad 0.6]^\top \text{meters} \tag{5.66}$$

The Denavit-Hartenberg (D-H) parameters for the three links of the Puma 560 are given in the following table: Thus, the homogeneous transformation between

Joint	θ	α	d	a
1^{st}	θ_1	-90	0	0
2^{nd}	θ_2	0	0	0.4318
3^{rd}	θ_3	90	0.1505	0

Table 5.2: D-H Parameters for the three links Puma 560

frame 0 (vehicle frame) and frame 1 (first link) is given by the following transformation matrix:

$$\underline{\mathbf{A}}_{\mathbf{0}}^{\mathbf{1}} = \begin{bmatrix} cos(\theta_1) & 0 & -sin(\theta_1) & 1.1 \\ sin(\theta_1) & 0 & cos(\theta_1) & 0 \\ 0 & -1 & 0 & 0.6 \\ 0 & 0 & 0 & 1 \end{bmatrix} \tag{5.67}$$

Therefore, table 5.2 will be used to find the rest homogeneous transformations as follows:

$$\underline{\mathbf{A}}_{\mathbf{0}}^{\mathbf{2}} = \begin{bmatrix} cos(\theta_2) & -sin(\theta_2) & 0 & 0.4318cos(\theta_2) \\ sin(\theta_2) & cos(\theta_2) & 0 & 0.4318sin(\theta_2) \\ 0 & 0 & 1 & 0 \\ 0 & 0 & 0 & 1 \end{bmatrix} \tag{5.68}$$

$$\underline{\mathbf{A}}_{\mathbf{0}}^{\mathbf{3}} = \begin{bmatrix} cos(\theta_3) & 0 & sin(\theta_3) & 0 \\ sin(\theta_3) & 0 & -cos(\theta_2) & 0 \\ 0 & 1 & 0 & 0.1505 \\ 0 & 0 & 0 & 1 \end{bmatrix} \tag{5.69}$$

1. Position Vector to the C.M of the Link

To compute the position vector of the C.M. of each link with respect to the 0^{th} frame, the position vectors of the C.M of each link expressed in local link coordinate required, and it's given as follows [24]:

$$\mathbf{c_1^1} = \begin{bmatrix} 0 & 0.3088 & 0 \end{bmatrix}^\top \tag{5.70}$$

$$\mathbf{c_2^2} = \begin{bmatrix} -0.3289 & 0 & 0.2038 \end{bmatrix}^\top \tag{5.71}$$

$$\mathbf{c_3^3} = \begin{bmatrix} 0 & 0 & 0 \end{bmatrix}^\top \tag{5.72}$$

As an example, the position vector of the C.M of the first link expressed in 0^{th}

can be found by substitution eq. 5.70 and eq. 5.67 in to eq. 5.17 which leads to:

$$\mathbf{P}_1^0 = \mathbf{A_0^1 c_1^1} = \begin{bmatrix} 0 \\ 0 \\ -0.31 \end{bmatrix} \tag{5.73}$$

2. Angular Velocity to C.M of the Link

The angular velocity to C.M of each link can be computed from eq. 5.21, for instance.

$$\mathbf{w}_1^i = \begin{bmatrix} qd4 \\ qd5 \\ qd7 + qd6 \end{bmatrix} \tag{5.74}$$

where, as an example, $qd4$ represents $\dot{q}_4$.

3. Linear Velocity to C.M of the Link

The linear velocity to C.M of each link can be computed from eq. **??**, for example.

$$\mathbf{v}_1^0 = \begin{bmatrix} qd1 + 0.29 * qd5 \\ qd2 - 0.29 * qd4 + 1.1 * qd6 \\ qd3 - 1.1 * qd5 \end{bmatrix} \tag{5.75}$$

4. Angular Acceleration to C.M of the Link

The angular acceleration to C.M of each link can be computed from eq. 5.25, for

instance.

$$\alpha_1^i = \begin{bmatrix} qd5 * (qd7 + qd6) - 1.0 * qd5 * qd6 + qdd4 \\ qd4 * qd6 - 1.0 * qd4 * (qd7 + qd6) + qdd5 \\ qdd7 + qdd6 \end{bmatrix} \tag{5.76}$$

5. Linear Acceleration to C.M of the Link

The linear acceleration to C.M of each link can be computed from eq. 5.27, for instance.

$$\mathbf{a}_1^0 = \begin{bmatrix} \Big[qdd1 + (0.29 * qdd5) - qd6 * (qd2 - (0.29 * qd4) + \\ (1.1 * qd6)) + qd5 * (qd3 - (1.1 * qd5))\Big] \\ \Big[qdd2 - (0.29 * qdd4) + (1.1 * qdd6) - qd4 * (qd3 - \\ (1.1 * qd5)) + qd6 * (qd1 + (0.29 * qd5))\Big] \\ \Big[qdd3 - (1.1 * qdd5) + qd4 * (qd2 - (0.29 * qd4) + \\ (1.1 * qd6)) - qd5 * (qd1 + (0.29 * qd5))\Big] \end{bmatrix} \tag{5.77}$$

5.8.3 Masses and Inertias for the UVMS model

The mass and inertia properties of the Jason underwater vehicle and Puma 560 manipulator are listed in the following table:

Link	Mass kg	$I_{xx} kg.m^2$	$I_{yy} kg.m^2$	$I_{zz} kg.m^2$
Vehicle	1200	265	628	605
Link 1	12.96	1.0981	0.1774	1.1112
Link 2	22.37	0.4036	0.9684	0.9664
Link 3	5.01	0.0746	0.0755	0.0075

Table 5.3: Mass and Inertia Properties of the UVMS

5.8.4 Gravity Force

The generalized active force caused by gravity can be computed from eq. 5.35, as an example,

$$
\begin{aligned}
\mathbf{g_{0_1}} =& m0 * ((98 * sin(e5))/(5 * (cos(e5)^2 + sin(e5)^2))+ \\
& (49 * cos(e4) * cos(e5) * sin(e7))/(5 * (cos(e4)^2 * cos(e5)^2+ \\
& cos(e4)^2 * sin(e5)^2 + cos(e5)^2 * sin(e4)^2 + sin(e4)^2 * sin(e5)^2))- \\
& (49 * cos(e5) * cos(e7) * sin(e4))/(5 * (cos(e4)^2 * cos(e5)^2 + cos(e4)^2 * sin(e5)^2+ \\
& cos(e5)^2 * sin(e4)^2 + sin(e4)^2 * sin(e5)^2))- \\
& (49 * cos(e4) * cos(e5) * sin(e9))/(5 * (cos(e4)^2 * cos(e5)^2+ \\
& cos(e4)^2 * sin(e5)^2 + cos(e5)^2 * sin(e4)^2 + sin(e4)^2 * sin(e5)^2))+ \\
& (49 * cos(e5) * cos(e9) * sin(e4))/(5 * (cos(e4)^2 * cos(e5)^2 + cos(e4)^2 * sin(e5)^2+ \\
& cos(e5)^2 * sin(e4)^2 + sin(e4)^2 * sin(e5)^2))) + m1 * ((98 * sin(e5))/(5 * (cos(e5)^2+ \\
& sin(e5)^2)) + (49 * cos(e4) * cos(e5) * sin(e7))/(5 * (cos(e4)^2 * cos(e5)^2+ \\
& cos(e4)^2 * sin(e5)^2 + cos(e5)^2 * sin(e4)^2 + sin(e4)^2 * sin(e5)^2))- \\
& (49 * cos(e5) * cos(e7) * sin(e4))/(5 * (cos(e4)^2 * cos(e5)^2 + cos(e4)^2 * sin(e5)^2+ \\
& cos(e5)^2 * sin(e4)^2 + sin(e4)^2 * sin(e5)^2))- \\
& (49 * cos(e4) * cos(e5) * sin(e9))/(5 * (cos(e4)^2 * cos(e5)^2 + cos(e4)^2 * sin(e5)^2+ \\
& cos(e5)^2 * sin(e4)^2 + sin(e4)^2 * sin(e5)^2))+
\end{aligned}
$$

$$(49 * cos(e5) * cos(e9) * sin(e4))/(5 * (cos(e4)^2 * cos(e5)^2 + cos(e4)^2 * sin(e5)^2 +$$

$$cos(e5)^2 * sin(e4)^2 + sin(e4)^2 * sin(e5)^2))) + m2 * ((98 * sin(e5))/(5 * (cos(e5)^2 +$$

$$sin(e5)^2)) + (49 * cos(e4) * cos(e5) * sin(e7))/(5 * (cos(e4)^2 * cos(e5)^2 +$$

$$cos(e4)^2 * sin(e5)^2 + cos(e5)^2 * sin(e4)^2 + sin(e4)^2 * sin(e5)^2)) -$$

$$(49 * cos(e5) * cos(e7) * sin(e4))/(5 * (cos(e4)^2 * cos(e5)^2 + cos(e4)^2 * sin(e5)^2 +$$

$$cos(e5)^2 * sin(e4)^2 + sin(e4)^2 * sin(e5)^2)) -$$

$$(49 * cos(e4) * cos(e5) * sin(e9))/(5 * (cos(e4)^2 * cos(e5)^2 + cos(e4)^2 * sin(e5)^2 +$$

$$cos(e5)^2 * sin(e4)^2 + sin(e4)^2 * sin(e5)^2)) +$$

$$(49 * cos(e5) * cos(e9) * sin(e4))/(5 * (cos(e4)^2 * cos(e5)^2 + cos(e4)^2 * sin(e5)^2 +$$

$$cos(e5)^2 * sin(e4)^2 + sin(e4)^2 * sin(e5)^2))) +$$

$$m3 * ((98 * sin(e5))/(5 * (cos(e5)^2 + sin(e5)^2)) +$$

$$(49 * cos(e4) * cos(e5) * sin(e7))/(5 * (cos(e4)^2 * cos(e5)^2 + cos(e4)^2 * sin(e5)^2 +$$

$$cos(e5)^2 * sin(e4)^2 + sin(e4)^2 * sin(e5)^2)) -$$

$$(49 * cos(e5) * cos(e7) * sin(e4))/(5 * (cos(e4)^2 * cos(e5)^2 +$$

$$cos(e4)^2 * sin(e5)^2 + cos(e5)^2 * sin(e4)^2 + sin(e4)^2 * sin(e5)^2)) -$$

$$(49 * cos(e4) * cos(e5) * sin(e9))/(5 * (cos(e4)^2 * cos(e5)^2 + cos(e4)^2 * sin(e5)^2 +$$

$$cos(e5)^2 * sin(e4)^2 + sin(e4)^2 * sin(e5)^2)) +$$

$$(49 * cos(e5) * cos(e9) * sin(e4))/(5 * (cos(e4)^2 * cos(e5)^2 +$$

$$cos(e4)^2 * sin(e5)^2 + cos(e5)^2 * sin(e4)^2 + sin(e4)^2 * sin(e5)^2)))$$

where, $m0$, $m1$, $m2$ and $m3$ represent the vehicle mass and the manipulator links masses and $e4$ represents η_4.

5.8.5 Hydrodynamic Forces

1. Hydrodynamic Added Mass

The hydrodynamic coefficients of the vehicle developed by approximating the vehicle shape as an ellipsoid (as shown in Fig 5.2) which is governed by the following formula:

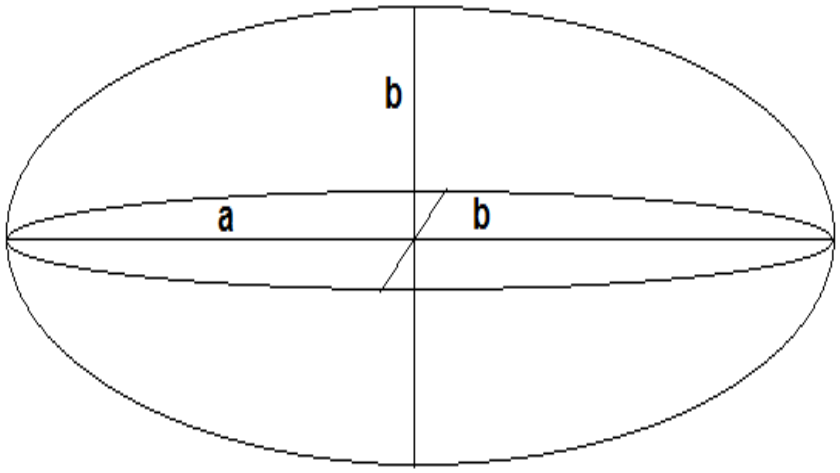

Figure 5.2: Ellipsoid Model for Vehicle Hydrodynamic Added Mass.

$$\frac{x^2}{a^2} + \frac{y^2}{b^2} + \frac{z^2}{b^2} = 1 \tag{5.78}$$

where, a and b represent semi major axis oriented along the vehicle ($\hat{x}_0$) and ($\hat{y}_0$ and $\hat{z}_0$), respectively. By defining the eccentricity e and m of the water displaced

by the ellipsoid as given in the following equation,

$$e = 1 - (\frac{b}{a})^2 \tag{5.79}$$

$$m = \frac{4}{3}\pi\rho a b^2 \tag{5.80}$$

β_0 and α_0 are defined as constant in the following equation,

$$\alpha_0 = \frac{2(1-e^2)}{e^3}(0.5 \ln \frac{1+e}{1-e} - e) \tag{5.81}$$

$$\beta_0 = \frac{1}{e^2} - \frac{1-e^2}{2e^3} \ln \frac{1+e}{1-e} \tag{5.82}$$

Therefore, the diagonal terms of the hydrodynamic added mass for the vehicle will be as follows,

$$(\mathbf{I}^0_{A_0})_{11} = - \frac{\alpha_0}{2-\alpha_0} m \tag{5.83}$$

$$(\mathbf{I}^0_{A_0})_{22} = - \frac{\beta 0}{2-\beta 0} m \tag{5.84}$$

$$(\mathbf{I}^0_{A_0})_{33} = (\mathbf{I}^0_{A_0})_{22} \tag{5.85}$$

$$(\mathbf{I}^0_{A_0})_{44} = 0 \tag{5.86}$$

$$(\mathbf{I}^0_{A_0})_{55} = - 0.1 \frac{(b^2-a^2)^2(\alpha_0 - \beta_0)}{(b^2-a^2) + (b^2+a^2)(\beta_0 - \alpha_0)} m \tag{5.87}$$

$$(\mathbf{I}^0_{A_0})_{66} = (\mathbf{I}^0_{A_0})_{55} \tag{5.88}$$

The added mass coefficients for the manipulator can be computed by approximating the links as cylinders.

$$\mathbf{I}_{A_j}^{j} = \begin{bmatrix} k_j & 0 & 0 & 0 & 0 & 0 \\ 0 & k_j & 0 & 0 & 0 & 0 \\ 0 & 0 & 0 & 0 & 0 & 0 \\ 0 & 0 & 0 & \frac{k_j L_j^2}{3} & 0 & 0 \\ 0 & 0 & 0 & 0 & \frac{k_j L_j^2}{3} & 0 \\ 0 & 0 & 0 & 0 & 0 & 0 \end{bmatrix} \tag{5.89}$$

where, $k_j = \frac{\rho \pi r_j L_j}{4}$, L_j and r_j are the length and radius of the cylinder, respectively.

5.8.6 Buoyancy Force

The generalized active force caused by buoyancy can be computed from eq. 5.50, for instance,

$$(\mathbf{F}_r)_{Buoy_1} = -m0 * ((98 * sin(e5))/(5 * (cos(e5)^2 + sin(e5)^2))+$$

$$(49 * cos(e4) * cos(e5) * sin(e7))/(5 * (cos(e4)^2 * cos(e5)^2+$$

$$cos(e4)^2 * sin(e5)^2 + cos(e5)^2 * sin(e4)^2 + sin(e4)^2 * sin(e5)^2))-$$

$$(49 * cos(e5) * cos(e7) * sin(e4))/(5 * (cos(e4)^2 * cos(e5)^2+$$

$$cos(e4)^2 * sin(e5)^2 + cos(e5)^2 * sin(e4)^2 + sin(e4)^2 * sin(e5)^2))-$$

$$(49 * cos(e4) * cos(e5) * sin(e9))/(5 * (cos(e4)^2 * cos(e5)^2+$$

$$cos(e4)^2 * sin(e5)^2 + cos(e5)^2 * sin(e4)^2 + sin(e4)^2 * sin(e5)^2))+$$

$$(49 * cos(e5) * cos(e9) * sin(e4))/(5 * (cos(e4)^2 * cos(e5)^2 + cos(e4)^2 * sin(e5)^2+$$

$$cos(e5)^2 * sin(e4)^2 + sin(e4)^2 * sin(e5)^2)))-$$

$$(99 * m1 * ((98 * sin(e5))/(5 * (cos(e5)^2 + sin(e5)^2))+$$

$$(49 * cos(e4) * cos(e5) * sin(e7))/(5 * (cos(e4)^2 * cos(e5)^2+$$

$$cos(e4)^2 * sin(e5)^2 + cos(e5)^2 * sin(e4)^2 + sin(e4)^2 * sin(e5)^2))-$$

$$(49 * cos(e5) * cos(e7) * sin(e4))/(5 * (cos(e4)^2 * cos(e5)^2+$$

$$cos(e4)^2 * sin(e5)^2 + cos(e5)^2 * sin(e4)^2 + sin(e4)^2 * sin(e5)^2))-$$

$$(49 * cos(e4) * cos(e5) * sin(e9))/(5 * (cos(e4)^2 * cos(e5)^2 + cos(e4)^2 * sin(e5)^2+$$

$$cos(e5)^2 * sin(e4)^2 + sin(e4)^2 * sin(e5)^2))+$$

$$(49 * cos(e5) * cos(e9) * sin(e4))/(5 * (cos(e4)^2 * cos(e5)^2 + cos(e4)^2 * sin(e5)^2+$$

$$cos(e5)^2 * sin(e4)^2 + sin(e4)^2 * sin(e5)^2))))/100-$$

$$(99 * m2 * ((98 * sin(e5))/(5 * (cos(e5)^2 + sin(e5)^2))+$$

$$(49 * cos(e4) * cos(e5) * sin(e7))/(5 * (cos(e4)^2 * cos(e5)^2 + cos(e4)^2 * sin(e5)^2+$$

$$cos(e5)^2 * sin(e4)^2 + sin(e4)^2 * sin(e5)^2))-$$

$$(49 * cos(e5) * cos(e7) * sin(e4))/(5 * (cos(e4)^2 * cos(e5)^2+$$

$$cos(e4)^2 * sin(e5)^2 + cos(e5)^2 * sin(e4)^2 + sin(e4)^2 * sin(e5)^2))-$$

$$(49 * cos(e4) * cos(e5) * sin(e9))/(5 * (cos(e4)^2 * cos(e5)^2 + cos(e4)^2 * sin(e5)^2+$$

$$cos(e5)^2 * sin(e4)^2 + sin(e4)^2 * sin(e5)^2))+$$

$$(49 * cos(e5) * cos(e9) * sin(e4))/(5 * (cos(e4)^2 * cos(e5)^2 + cos(e4)^2 * sin(e5)^2+$$

$$cos(e5)^2 * sin(e4)^2 + sin(e4)^2 * sin(e5)^2))))/100-$$

$$(99 * m3 * ((98 * sin(e5))/(5 * (cos(e5)^2 + sin(e5)^2))+$$

$$(49 * cos(e4) * cos(e5) * sin(e7))/(5 * (cos(e4)^2 * cos(e5)^2+$$

$$cos(e4)^2 * sin(e5)^2 + cos(e5)^2 * sin(e4)^2 + sin(e4)^2 * sin(e5)^2))-$$

$$(49 * cos(e5) * cos(e7) * sin(e4))/(5 * (cos(e4)^2 * cos(e5)^2 + cos(e4)^2 * sin(e5)^2+$$

$$cos(e5)^2 * sin(e4)^2 + sin(e4)^2 * sin(e5)^2))-$$

$(49 * cos(e4) * cos(e5) * sin(e9))/(5 * (cos(e4)^2 * cos(e5)^2 + cos(e4)^2 * sin(e5)^2 +$

$cos(e5)^2 * sin(e4)^2 + sin(e4)^2 * sin(e5)^2)) +$

$(49 * cos(e5) * cos(e9) * sin(e4))/(5 * (cos(e4)^2 * cos(e5)^2 +$

$cos(e4)^2 * sin(e5)^2 + cos(e5)^2 * sin(e4)^2 + sin(e4)^2 * sin(e5)^2))))/100$

5.8.7 Profile Drag Force

The drag and torque motivated by the vehicle relative velocity in the fluid is given by the following formulas,

$$\mathbf{R}_{Drag_0} = -0.5 C_{D_0} \rho v_0^2 S_0 \tag{5.90}$$

$$\mathbf{T}_{Drag_0} = 0 \tag{5.91}$$

where, S_0 represents frontal reference area of the vehicle which has sphere shape, v_0 is the relative velocity of the vehicle with respect to the fluid and C_D represents the drag coefficient for the shape of the vehicle.

The drag and torque induced by the manipulator relative velocity in the fluid is given by eq. 5.58, by selecting the value of $C_D = 1.1$, as in [23].

$$\mathbf{R_{Drag_j}} = -0.5\rho \int_0^L \|\mathbf{v_j^0}(\mathbf{l})^\perp\| \mathbf{v_j^0}(\mathbf{l})^\perp C_D 2 r_j \mathbf{dl}$$

$$\mathbf{T_{Drag_j}} = -0.5\rho \int_0^L \|\mathbf{v_j^0}(\mathbf{l})^\perp\| (\mathbf{A_0^j l \hat{x}_j} \times \mathbf{v_j^0}(\mathbf{l})^\perp) C_D 2 r_j \mathbf{dl}$$

where, r_j is the radius of j.

CHAPTER 6

CONTROLLER DESIGN FOR THE UNDERWATER VEHICLE

6.1 Feedback Linearization for the Underwater Vehicle

Let us start with the general dynamic model of the AUV presented in 4.14. Here, we define the new control input u as, see [5]:

$$\mathbf{u} = \mathbf{M}(\eta)^{-\mathbf{1}}[\tau - \mathbf{C_e}(\nu, \eta)\nu - \mathbf{D_e}(\nu)\nu - \mathbf{g_e}(\eta)] \tag{6.1}$$

By substituting 6.1 in the general equation of motion 4.14 leads to the following simple system, which seems similar to a linear system:

$$\ddot{\eta} = \mathbf{u} \tag{6.2}$$

At this point, we need to design a control law for this simple system 6.2. Therefore, we defined $\mathbf{e} = \eta - \eta_{\mathbf{d}}$ to be the tracking error. Now, we can show that the control law is;

$$\mathbf{u} = \ddot{\eta}_{\mathbf{d}} + \lambda_{\mathbf{1}}\dot{\mathbf{e}} + \lambda_{\mathbf{2}}\mathbf{e} \tag{6.3}$$

By selecting $(\lambda_{\mathbf{1}},\ \lambda_{\mathbf{2}}) > 0$, this leads to an exponentially stable closed-loop dynamics. By substituting 6.3 into 6.2 we can get the closed-loop error dynamics, which results in:

$$\ddot{\mathbf{e}} + \lambda_{\mathbf{1}}\dot{\mathbf{e}} + \lambda_{\mathbf{2}}\mathbf{e} = \mathbf{0} \tag{6.4}$$

Now, the control law is designed for the linear system 6.2. Thus, we can transform it to the initial control input by using 6.1:

$$\tau = \mathbf{M}(\eta)\mathbf{u} + \mathbf{C}_{\mathbf{e}}(\nu, \eta)\nu + \mathbf{D}_{\mathbf{e}}(\nu)\nu + \mathbf{g}_{\mathbf{e}}(\eta) \tag{6.5}$$

The main drawback of the feedback linearization is that is assumes, that the dynamic model in 6.5 is exact. Thus, if there are uncertainties in determining the dynamic parameters of the AUV or the parameters of the AUV changes, this results in the performance of the controller being adversely affected [5].

6.1.1 Simulation Results for the Underwater Vehicle

Figure 6.1 shows the overall control block diagram of the feedback linearization controller.

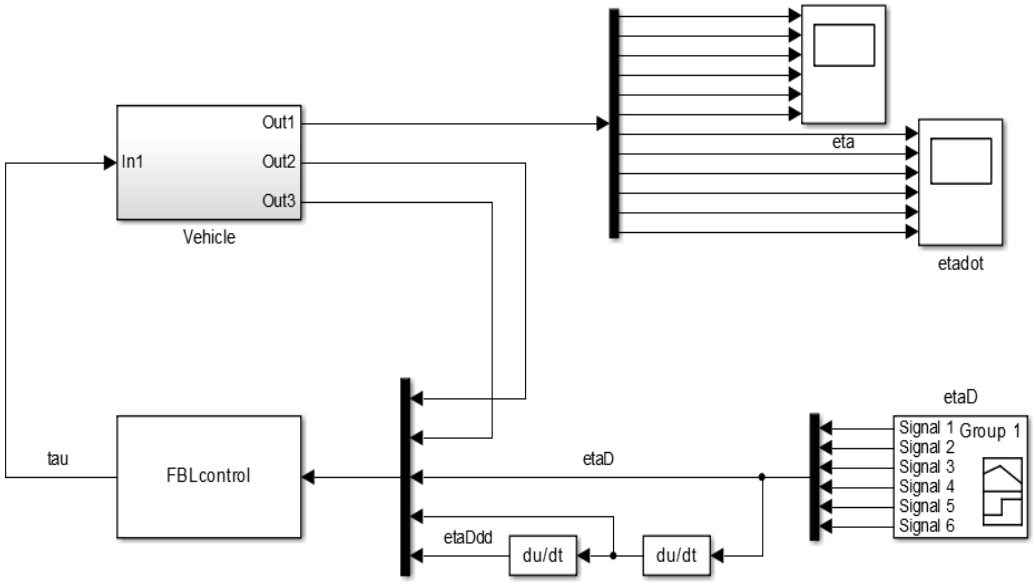

Figure 6.1: Simulink Block Diagram for the Underwater Vehicle.

The designed feedback linearization controller is implemented on the Modular Autonomous Robot for Environment Sampling (MARES) AUV model and the following simulation are obtained.

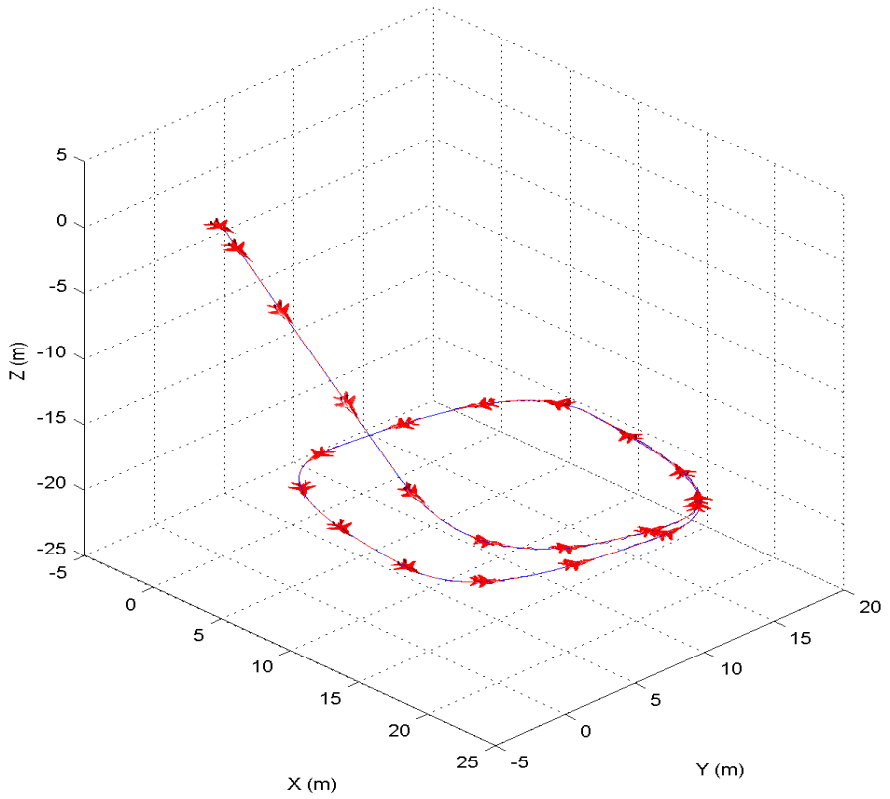

Figure 6.2: 3D tracking of the MARES AUV without uncertainty.

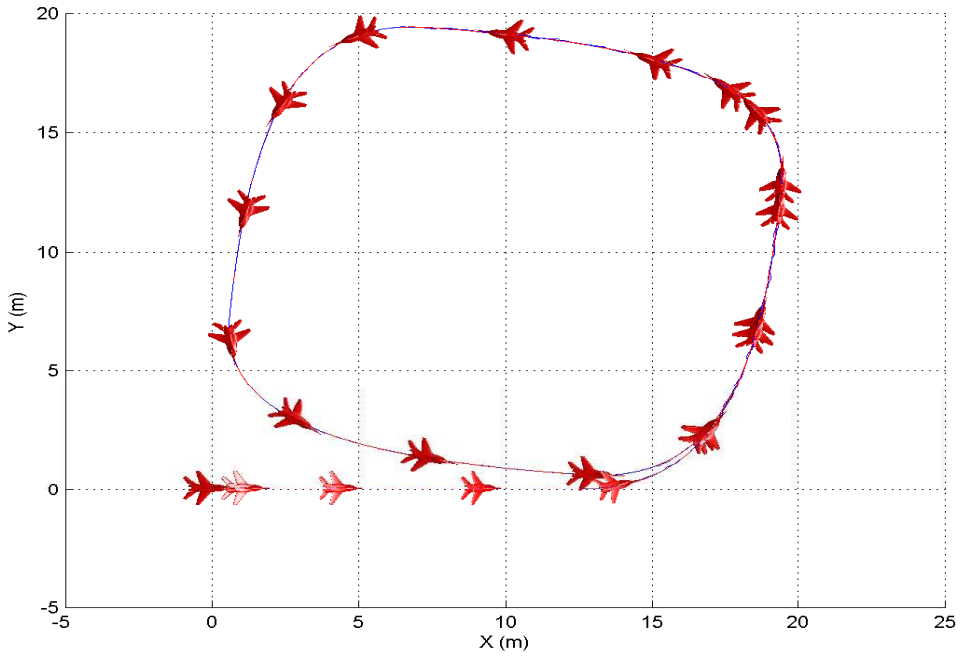

Figure 6.3: X-Y Semi Circle trajectory tracking of the MARES AUV without uncertainty.

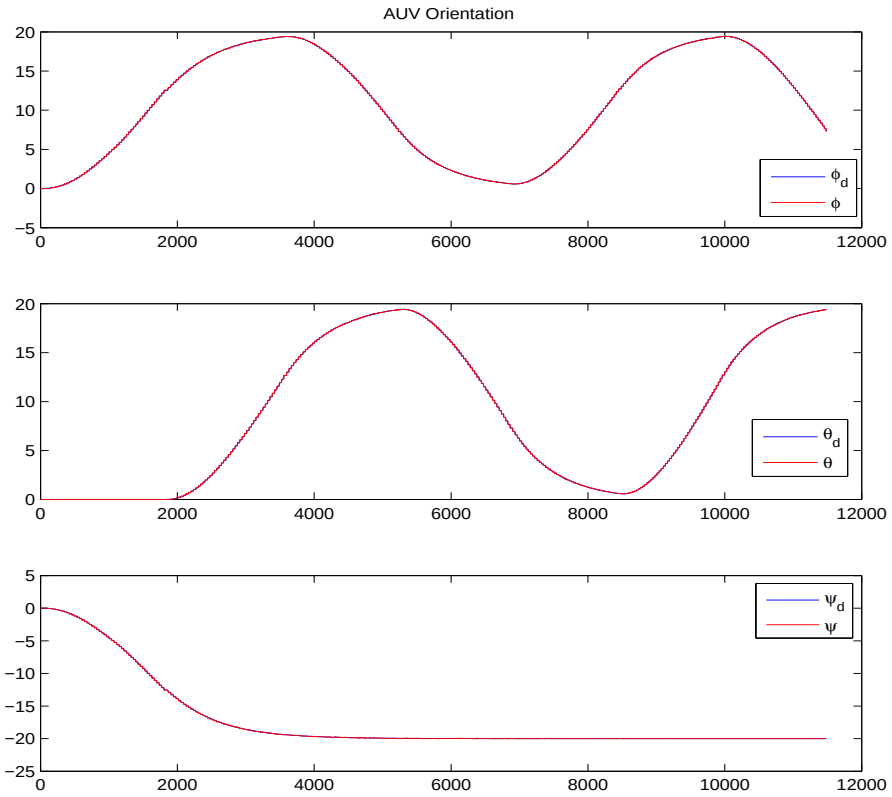

Figure 6.4: Orientation of the MARES AUV without uncertainty.

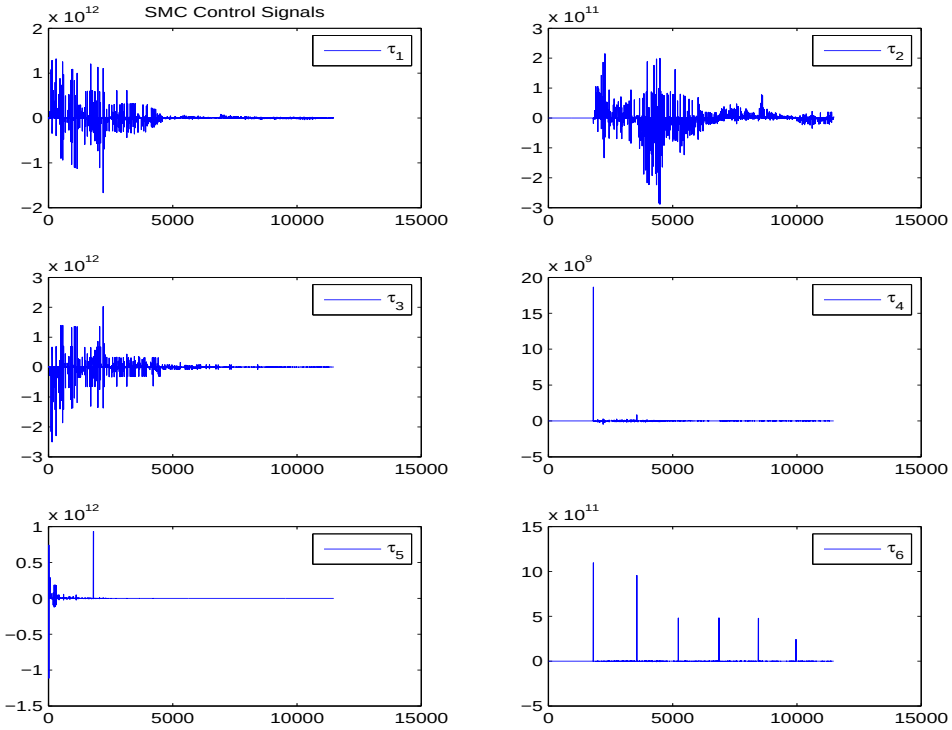

Figure 6.5: Control Signals of the MARES AUV without uncertainty.

The uncertainty in parameters (ρ and $\mathbf{M}$ represent water density and the inertia matrix for the AUV, respectively) was not considered in the above simulation, but now it is considered (10% error in ρ and 25% error in $\mathbf{M}$).

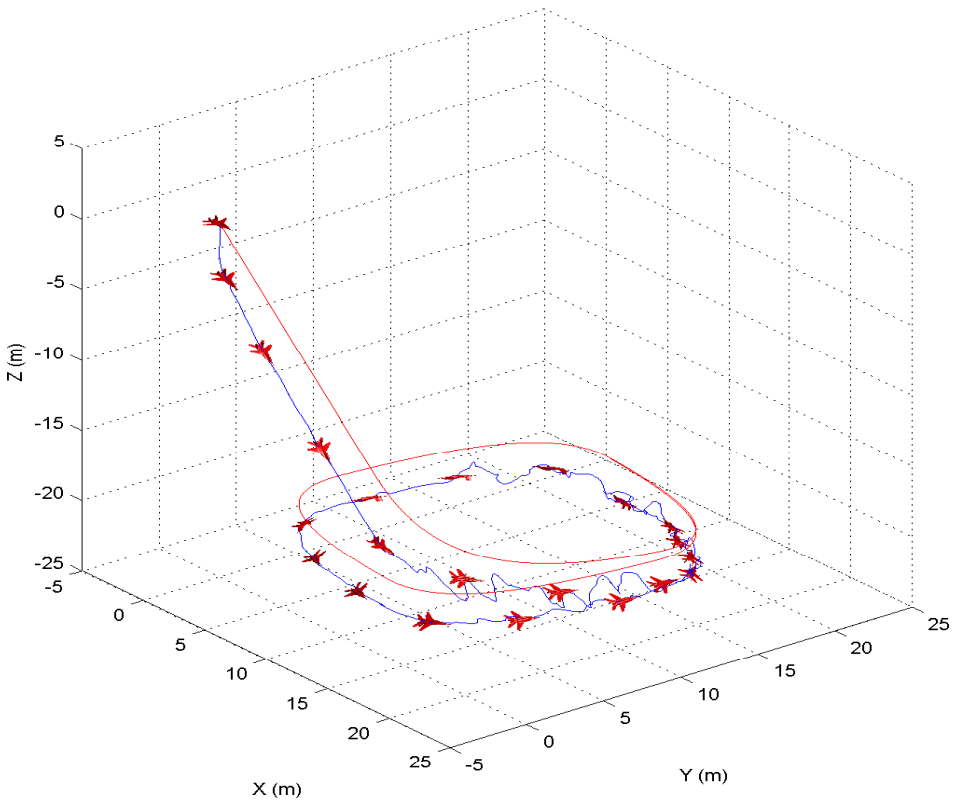

Figure 6.6: 3D tracking of the MARES AUV with uncertainty in parameters.

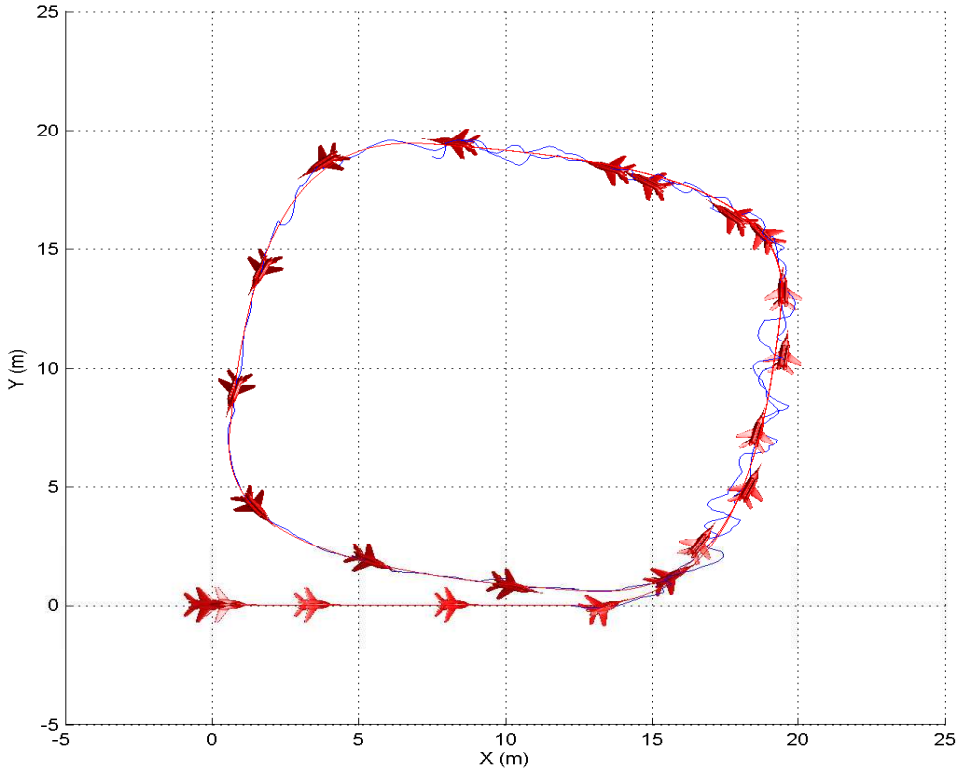

Figure 6.7: X-Y Semi Circle of the MARES AUV with uncertainty in parameters.

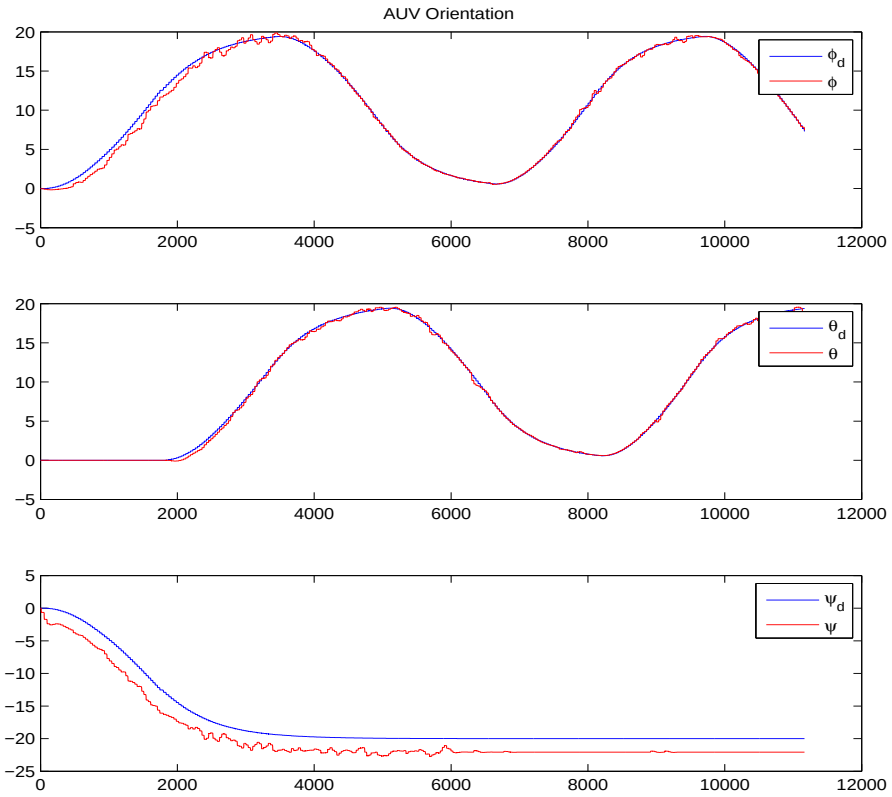

Figure 6.8: Orientation of the MARES AUV with uncertainty in parameters.

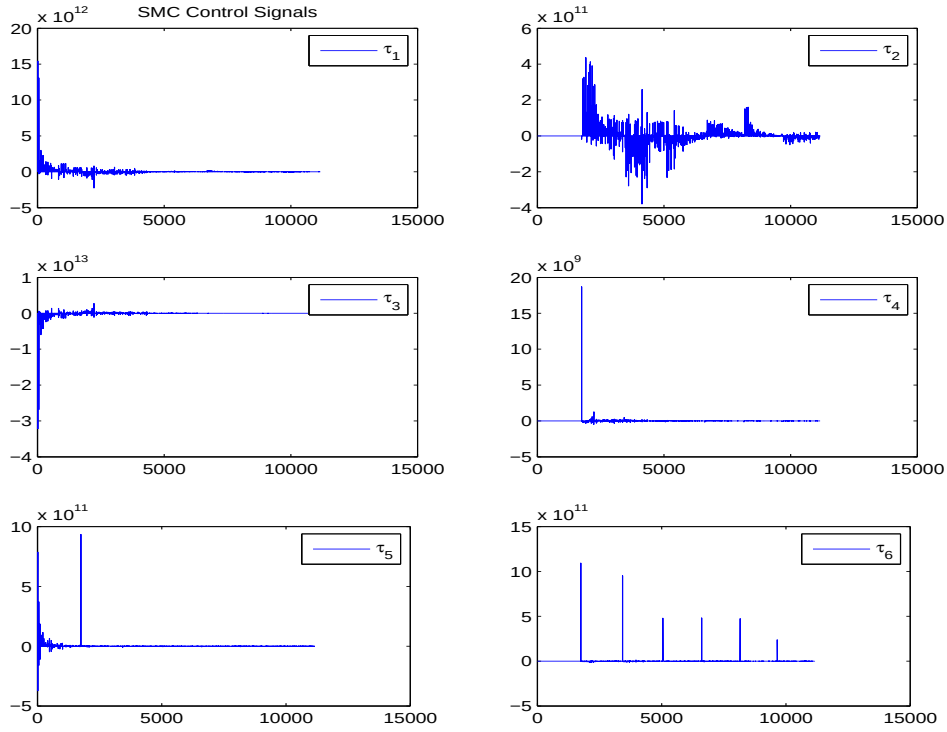

Figure 6.9: Control Signals of the MARES AUV with uncertainty in parameters.

6.2 Sliding Mode Control for the Underwater Vehicle

The required behavior of the closed-loop system in sliding mode control; generally is governed by the scalar equation, $s_m(x,t) = 0$, (see [25] page 278), where,

$$s_m(x,t) = (\frac{d}{dt} + \lambda_m)^{n-1} e_m \tag{6.6}$$

Where, $\mathbf{S}(\mathbf{x},\mathbf{t}) = [s_1(x,t),\ldots,s_m(x,t)]^\top$ is the time-varying surface in the state space $\mathbb{R}^n$, x is the state of the system, λ_m is a strictly positive constant, n is the system's order , m is the number of surfaces ($m = n$) and e_m is the tracking error. Therefore, for a second order system, where $n = 2$, Eq. 6.6 will become

$$\mathbf{s}(\mathbf{x},\mathbf{t}) = (\frac{\mathbf{d}}{\mathbf{dt}} + \lambda)\mathbf{e} \tag{6.7}$$

The idea behind the sliding mode control design is as follows. If we can derive a controller such that $s(x,t) = 0$, thus, regardless of bounded uncertainties of the AUV model, the state η of the AUV will follow the desired behavior η_d [5]. Thus,

$$(\frac{\mathbf{d}}{\mathbf{dt}} + \lambda)\mathbf{e} = \mathbf{0} \tag{6.8}$$

Eq. 6.8, is called the sliding surface.

6.2.1 Sliding Model Controller Design for AUV

We will assume that Eq. 4.14 and Eq. 6.9 represent the real dynamic and the nominal dynamic models of AUV, respectively. We followed the same steps as in [5] chapter 5.

$$\hat{\mathbf{M}}_\mathbf{e}(\eta)\ddot{\eta} + \hat{\mathbf{C}}_\mathbf{e}(\eta,\nu)\dot{\eta} + \hat{\mathbf{D}}_\mathbf{e}(\nu,\eta)\dot{\eta} + \hat{\mathbf{g}}_\mathbf{e}(\eta) = \tau_\mathbf{e} \tag{6.9}$$

The "hat" on the matrices means that these matrices are computed using the nominal parameters of the AUV.

Now, let us define $\mathbf{e} = \eta - \eta_{\mathbf{d}}$, and, for the purpose of simplicity, we can rewrite Eq. 6.7 as follows

$$\mathbf{s}(\mathbf{x}, \mathbf{t}) = \dot{\eta} - \mathbf{s_r} \tag{6.10}$$

Where,

$$\mathbf{s_r} = \dot{\eta}_{\mathbf{d}} - \lambda \mathbf{e} \tag{6.11}$$

Thus, Eq. 6.8 becomes as follows

$$\dot{\eta} - \mathbf{s_r} = \mathbf{0} \tag{6.12}$$

From Eq. 6.9 and Eq. 6.12 we can write

$$\hat{\tau} = \hat{\mathbf{M}}_{\mathbf{e}} \dot{\mathbf{s}}_{\mathbf{r}} + \hat{\mathbf{C}}_{\mathbf{e}} \mathbf{s_r} + \hat{\mathbf{D}}_{\mathbf{e}} \mathbf{s_r} + \hat{\mathbf{g}}_{\mathbf{e}} \tag{6.13}$$

A complete sliding mode control law can be written as follows

$$\tau = \hat{\tau} - \mathbf{K}\mathbf{sgn}(\mathbf{s}) \tag{6.14}$$

The first part of the control law $\hat{\tau}$ is called an equivalent control and the second part is a discontinuous function of $\mathbf{s}$.

Where, K is a diagonal controller discontinuity gain matrix.

Or,

$$\tau = (\hat{\mathbf{M}}_\mathbf{e}\dot{\mathbf{s}}_\mathbf{r} + \hat{\mathbf{C}}_\mathbf{e}\mathbf{s}_\mathbf{r} + \hat{\mathbf{D}}_\mathbf{e}\mathbf{s}_\mathbf{r} + \hat{\mathbf{g}}_\mathbf{e}) - \mathbf{K}\mathbf{sgn}(\mathbf{s}) \tag{6.15}$$

Now, to stabilize $\mathbf{s}$, the candidate Lyapunov function will be selected as

$$V(s) = \frac{\mathbf{1}}{\mathbf{2}}(\mathbf{s}^\top\mathbf{M}\mathbf{s}) \tag{6.16}$$

Thus,

$$\dot{V} = \frac{\mathbf{1}}{\mathbf{2}}(\dot{\mathbf{s}}^\top\mathbf{M}_\mathbf{e}\mathbf{s}) + \frac{\mathbf{1}}{\mathbf{2}}(\mathbf{s}^\top\dot{\mathbf{M}}\mathbf{s}) + \frac{\mathbf{1}}{\mathbf{2}}(\mathbf{s}^\top\mathbf{M}\dot{\mathbf{s}}) \tag{6.17}$$

Since, the matrix M is symmetric and postive definite and $\dot{\eta} = s + s_r$ therefore, Eq. 6.17 becomes

$$\begin{aligned}
\dot{V} &= \mathbf{s}^\top\mathbf{M}_\mathbf{e}\dot{\mathbf{s}} + \frac{\mathbf{1}}{\mathbf{2}}(\mathbf{s}^\top\dot{\mathbf{M}}_\mathbf{e}\mathbf{s}) = \mathbf{s}^\top\mathbf{M}_\mathbf{e}(\ddot{\eta} - \dot{\mathbf{s}_\mathbf{r}}) + \frac{\mathbf{1}}{\mathbf{2}}(\mathbf{s}^\top\dot{\mathbf{M}}\mathbf{s}) \\
&= \mathbf{s}^\top\mathbf{M}_\mathbf{e}\ (\mathbf{M}_\mathbf{e}^{-\mathbf{1}}[\tau_\mathbf{e} - \mathbf{C}(\mathbf{s}+\mathbf{s}_\mathbf{r}) - \mathbf{D}(\mathbf{s}+\mathbf{s}_\mathbf{r}) - \mathbf{g}_\mathbf{e}] - \dot{\mathbf{s}_\mathbf{r}}) + \frac{\mathbf{1}}{\mathbf{2}}(\mathbf{s}^\top\dot{\mathbf{M}}\mathbf{s}) \\
&= \mathbf{s}^\top([\tau_\mathbf{e} - \mathbf{C}\mathbf{s}_\mathbf{r} - \mathbf{D}\mathbf{s}_\mathbf{r} - \mathbf{g}_\mathbf{e}] - \mathbf{M}_\mathbf{e}\dot{\mathbf{s}_\mathbf{r}}) - \mathbf{s}^\top\mathbf{D}_\mathbf{e}\mathbf{s} + \frac{\mathbf{1}}{\mathbf{2}}\mathbf{s}^\top(\dot{\mathbf{M}}_\mathbf{e} - \mathbf{2C})\mathbf{s}
\end{aligned}$$

From section 5.7 we have proparty say, $s^\top(\dot{M}_e - 2C)s = 0$, thus

$$\dot{V} = -\mathbf{s}^\top \mathbf{D_e s} + \mathbf{s}^\top([\tau_\mathbf{e} - \mathbf{C s_r} - \mathbf{D s_r} - \mathbf{g_e}] - \mathbf{M_e \dot{s}_r}) \tag{6.18}$$

By substituting the value of τ_e from eq. 4.14 in to eq. 6.18 lead to

$$\dot{V} = -\mathbf{s}^\top \mathbf{D_e s} + \mathbf{s}^\top[(\hat{\mathbf{M}}_\mathbf{e} - \mathbf{M_e})\mathbf{s_r} + (\hat{\mathbf{C}}_\mathbf{e} - \mathbf{C_e})\mathbf{s_r} + (\hat{\mathbf{D}}_\mathbf{e} - \mathbf{D_e})\mathbf{s_r} + (\hat{\mathbf{g}}_\mathbf{e} - \mathbf{g_e}) - \mathbf{K sgn(s)}]$$

Thus,

$$\dot{V} = -\mathbf{s}^\top \mathbf{D_e s} + \mathbf{s}^\top(\tilde{\mathbf{M}}_\mathbf{e}\mathbf{s_r} + \tilde{\mathbf{C}}_\mathbf{e}\mathbf{s_r} + \tilde{\mathbf{D}}_\mathbf{e}\mathbf{s_r} + \tilde{\mathbf{g}}_\mathbf{e}) - \mathbf{s}^\top \mathbf{K sgn(s)}$$

Where,

$$\tilde{\mathbf{M}}_\mathbf{e} = \hat{\mathbf{M}}_\mathbf{e} - \mathbf{M_e},\ \tilde{\mathbf{C}}_\mathbf{e} = \hat{\mathbf{C}}_\mathbf{e} - \mathbf{C_e},\ \tilde{\mathbf{D}}_\mathbf{e} = \hat{\mathbf{D}}_\mathbf{e} - \mathbf{D_e} \text{ and } \tilde{\mathbf{g}}_\mathbf{e} = \hat{\mathbf{g}}_\mathbf{e} - \mathbf{g_e} \tag{6.19}$$

Then,

$$\dot{V} = -\mathbf{s}^\top \mathbf{D_e s} + \sum_{\mathbf{i=1}}^{\mathbf{n}} \mathbf{s_i}(\tilde{\mathbf{M}}_\mathbf{e}\mathbf{s_r} + \tilde{\mathbf{C}}_\mathbf{e}\mathbf{s_r} + \tilde{\mathbf{D}}_\mathbf{e}\mathbf{s_r} + \tilde{\mathbf{g}}_\mathbf{e})_\mathbf{i} - \mathbf{K_i}|\mathbf{s_i}|$$

OR,

$$\dot{V} \leq -\mathbf{s}^\top \mathbf{D_e s} + \sum_{\mathbf{i=1}}^{\mathbf{n}} |\mathbf{s_i}|.|(\tilde{\mathbf{M}}_\mathbf{e}\mathbf{s_r} + \tilde{\mathbf{C}}_\mathbf{e}\mathbf{s_r} + \tilde{\mathbf{D}}_\mathbf{e}\mathbf{s_r} + \tilde{\mathbf{g}}_\mathbf{e})_\mathbf{i}| - |\mathbf{K_i}||\mathbf{s_i}|$$

$$\dot{V} \leq -\mathbf{s}^\top \mathbf{D_e s} - \sum_{\mathbf{i=1}}^{\mathbf{n}} |\mathbf{s_i}|\ (\mathbf{K_i} - |(\tilde{\mathbf{M}}_\mathbf{e}\mathbf{s_r} + \tilde{\mathbf{C}}_\mathbf{e}\mathbf{s_r} + \tilde{\mathbf{D}}_\mathbf{e}\mathbf{s_r} + \tilde{\mathbf{g}}_\mathbf{e})_\mathbf{i}|)$$

The discontinuity gains $\mathbf{K_i}$'s are selected such that,

$$\mathbf{K_i} \geq |(\tilde{\mathbf{M}}_\mathbf{e}\mathbf{s_r} + \tilde{\mathbf{C}}_\mathbf{e}\mathbf{s_r} + \tilde{\mathbf{D}}_\mathbf{e}\mathbf{s_r} + \tilde{\mathbf{g}}_\mathbf{e})_\mathbf{i}| + \mathbf{\Gamma_i} \tag{6.20}$$

Where, $\mathbf{\Gamma_i}$'s are arbitrary positive constants, thus,

$$\dot{V} \leq -(\mathbf{s}^\top \mathbf{D_e s}) - (\sum_{\mathbf{i=1}}^{\mathbf{n}} |\mathbf{s_i}|.\mathbf{\Gamma_i}) \leq \mathbf{0} \tag{6.21}$$

As long as, the discontinuity gains $\mathbf{K_i}$'s are selected according to eq. 6.20, the derivative of the Lyapunov function defined in eq. 6.21 is always negative.
Since, eq. 6.21 is satisfied, s approaches to zero as time goes on, irrespective of its initial value and irrespective of any uncertainties in the dynamic model defined in eq. 6.19.

6.3 Simulation Results

Figure 6.10 shows the overall control block diagram of the sliding mode controller.

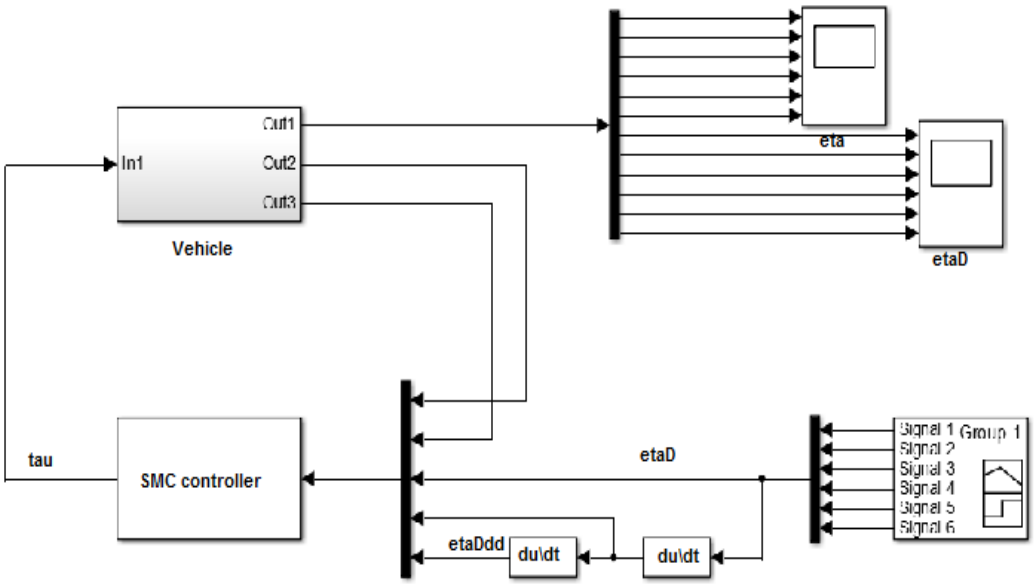

Figure 6.10: Simulink Block Diagram for the Underwater Vehicle.

The designed sliding mode controller is implemented on the MARES AUV model and the following simulation are obtained.

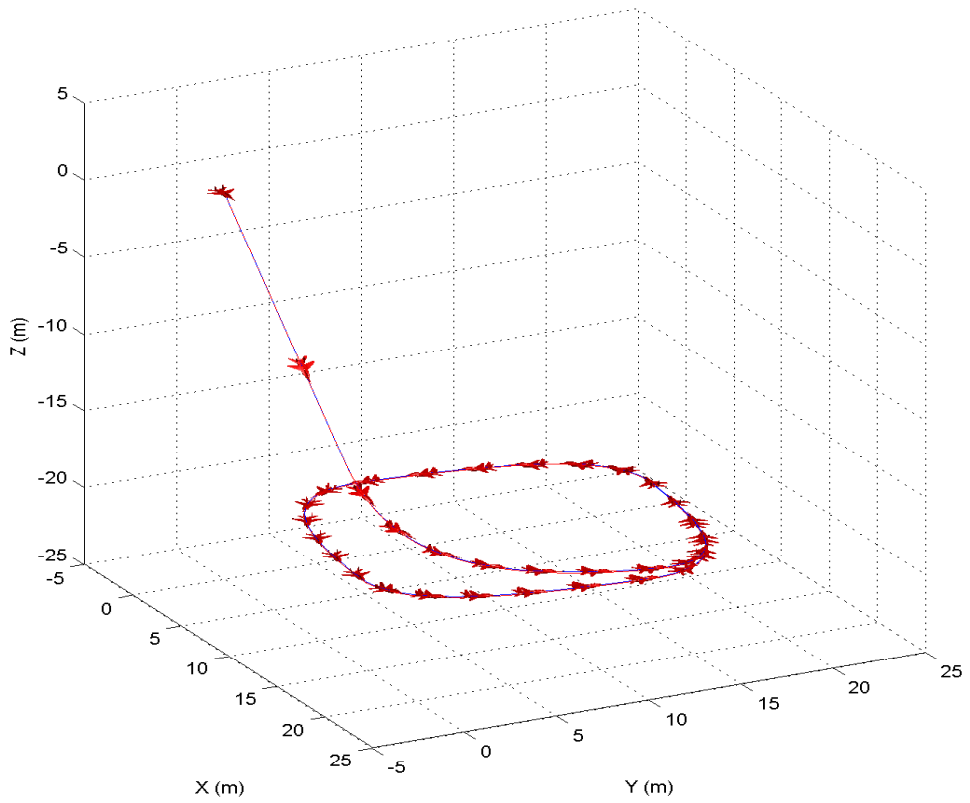

Figure 6.11: 3D trajectory tracking of the MARES AUV without uncertainty.

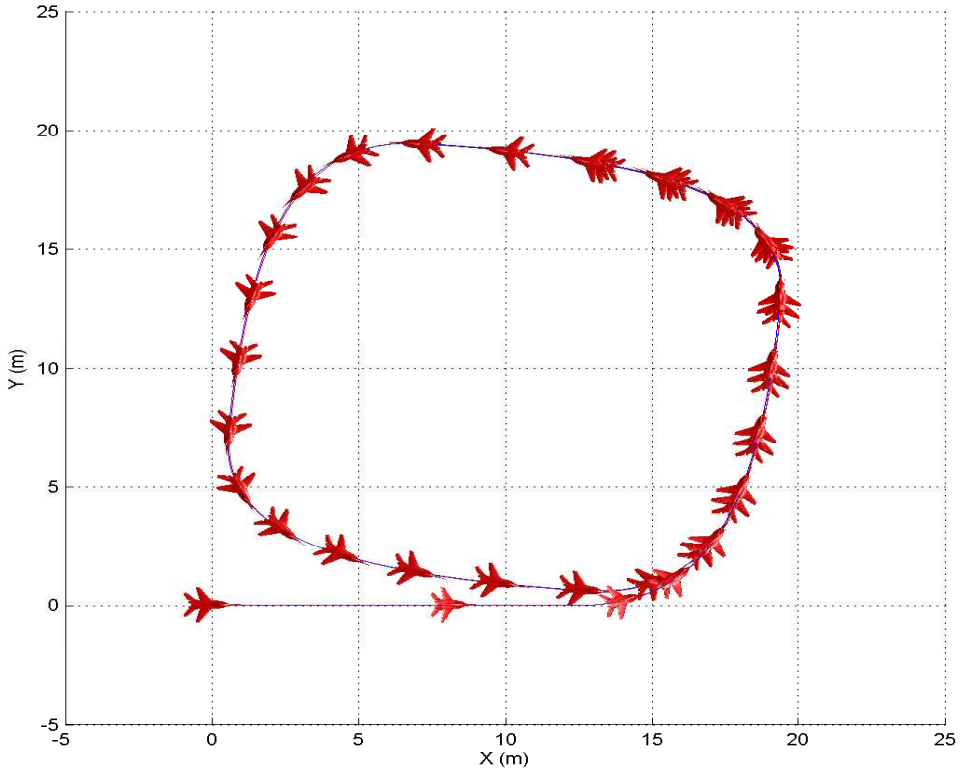

Figure 6.12: X-Y Semi Circle trajectory tracking of the MARES AUV without uncertainty.

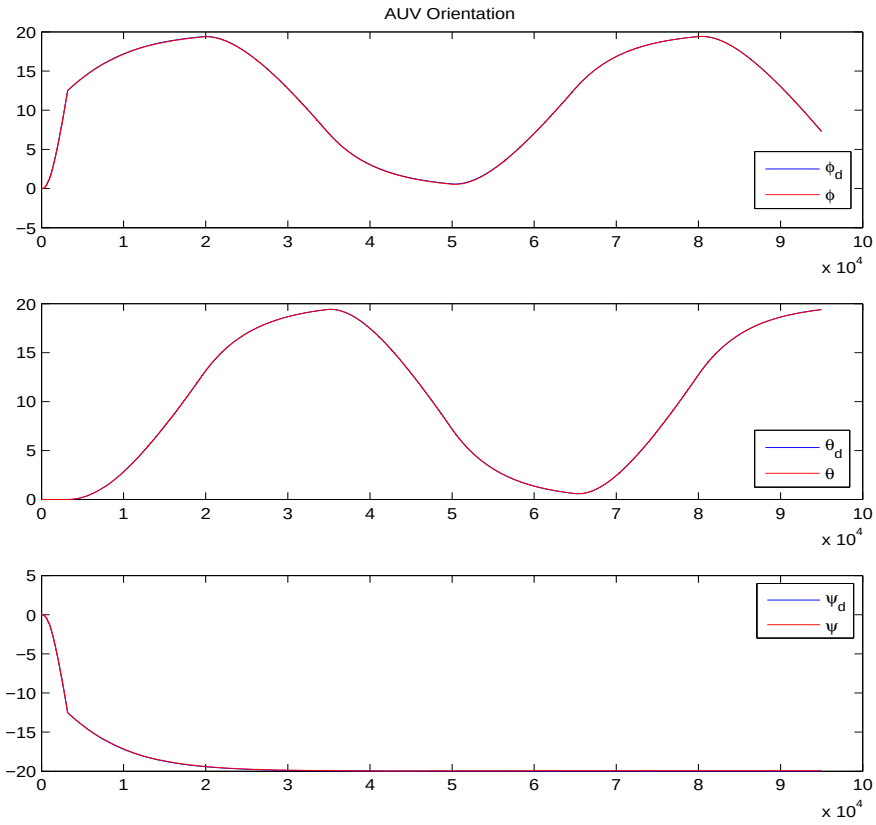

Figure 6.13: Orientation of the MARES AUV without uncertainty.

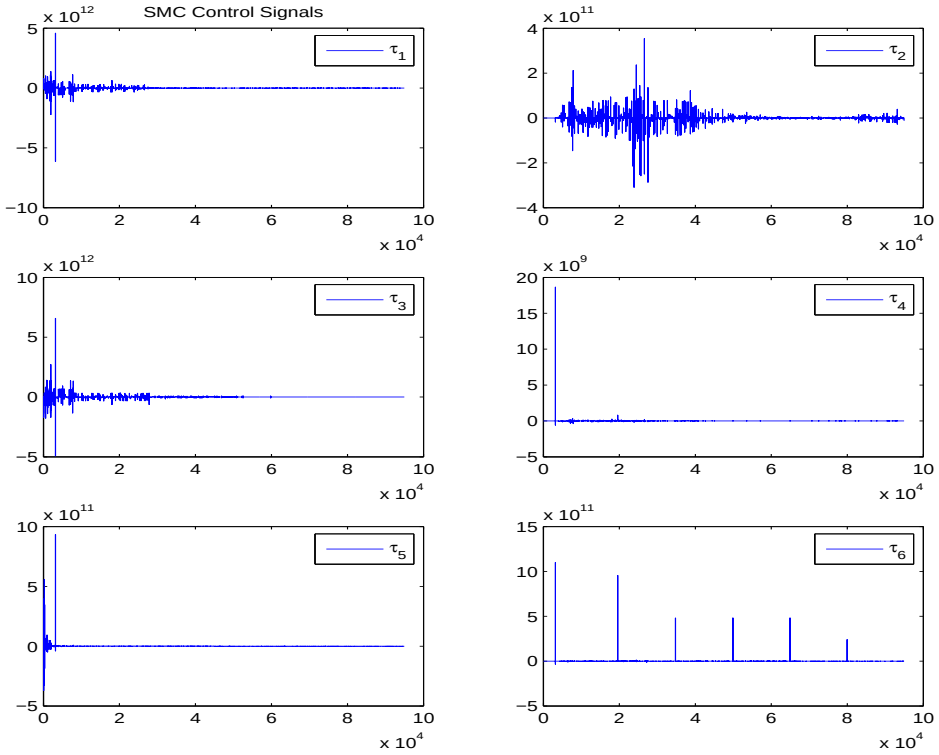

Figure 6.14: Control Signals of the MARES AUV without uncertainty.

The uncertainty in parameters (ρ and $\mathbf{M}$ represent Water density and the Inertia matrix for the AUV, respectively) was not considered in the above simulation, but now it is considered (10% error in ρ and 25% error in $\mathbf{M}$).

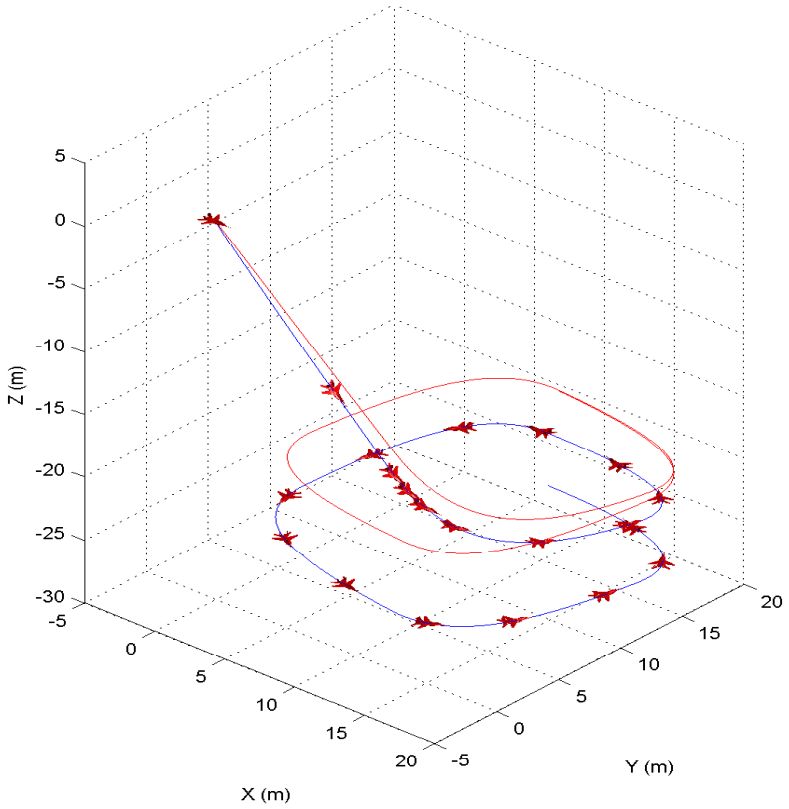

Figure 6.15: 3D tracking of the MARES AUV with uncertainty in parameters.

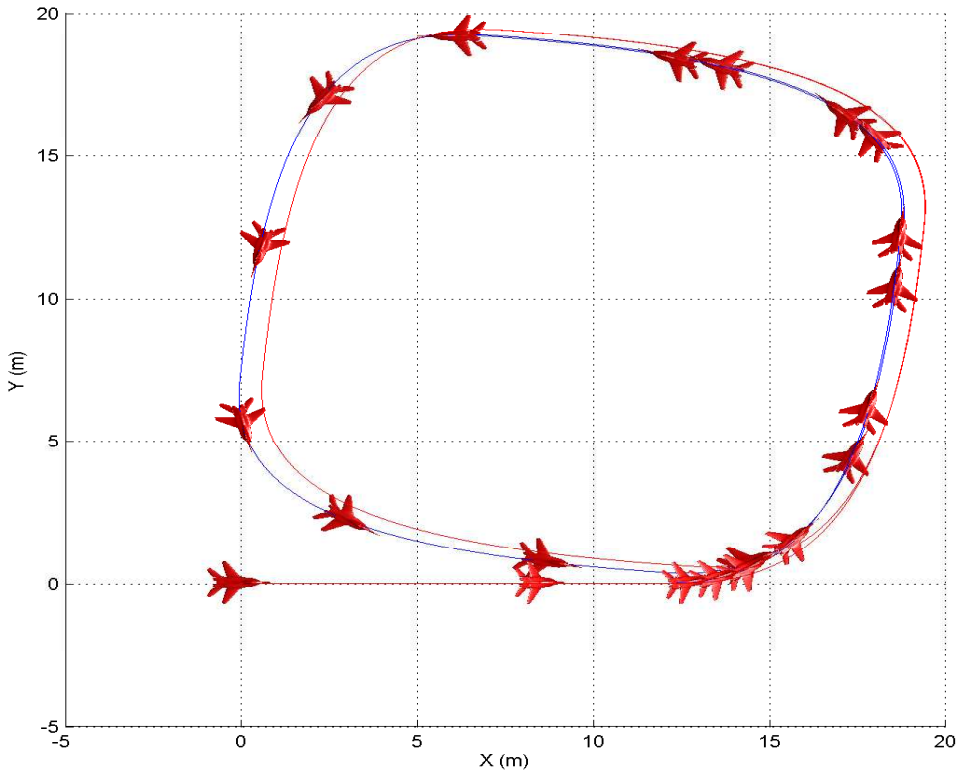

Figure 6.16: X-Y Semi Circle trajectory tracking of the MARES AUV with uncertainty in parameters.

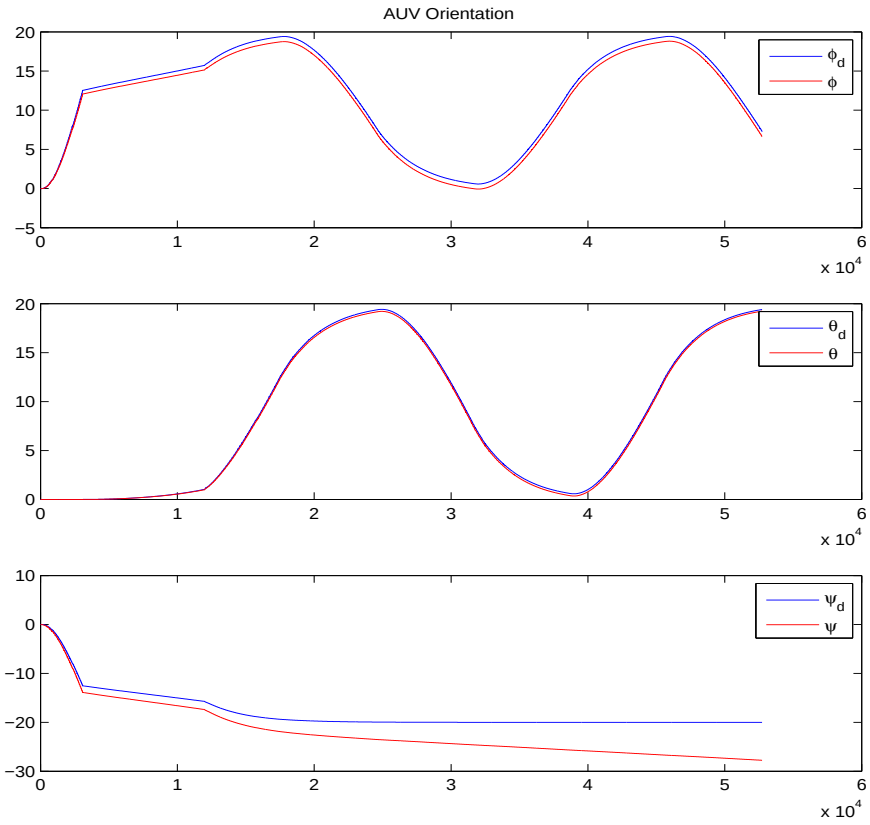

Figure 6.17: Orientation of the MARES AUV with uncertainty in parameters.

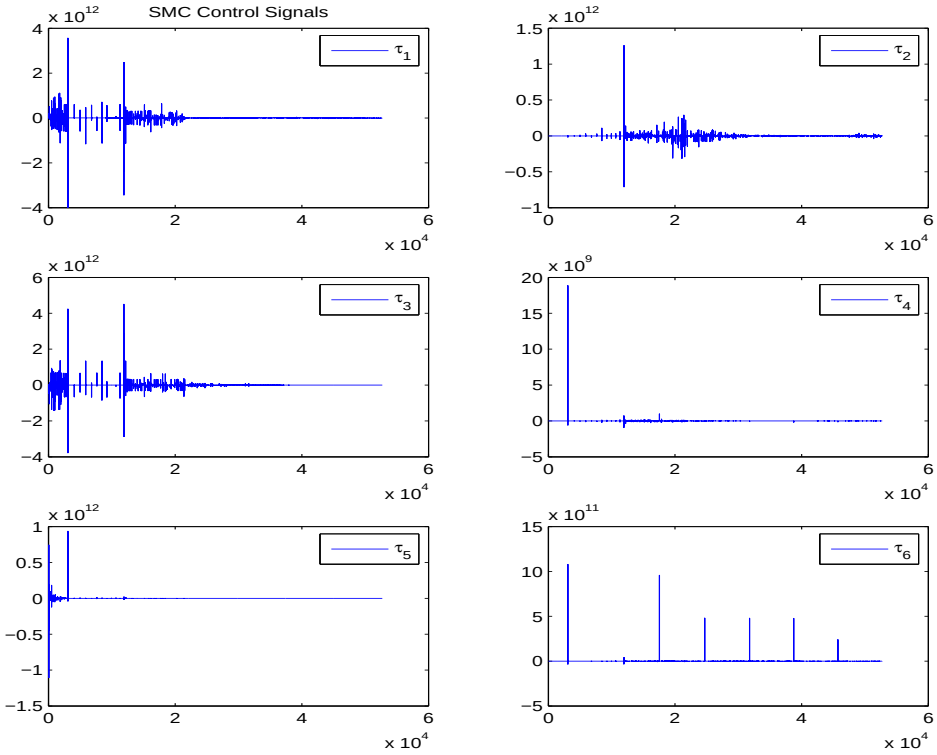

Figure 6.18: Control Signals of the MARES AUV with uncertainty in parameters.

6.4 $\mathcal{L}_1$ Adaptive Control for the Underwater Vehicle

The attractive point of using $\mathcal{L}_1$ adaptive controller in this thesis is its ability for fast and robust adaptation which increase the system's performance for both input and output compared to other controllers in the literature. This capability is done through the separation between adaption and robustness. Using this controller, the uncertainties will be estimated by a fast algorithm, and therefore, compensated uncertainties will pass through a low-pass filter and it will be a part

of the control signal. There are two main functions of this filter, first, guarantee that the control signal remains in the reasonable frequency range, second, separates between adaptation and robustness as well as through this filter we can optimize both, the performance and the robustness [16, 3, 26].

6.4.1 Preliminaries

Given the nonlinear function $\mathbf{f}(\mathbf{t}, \mathbf{x}) : [0,\ \infty) \times \mathbb{R}^n \rightarrow \mathbb{R}$,governed by the following assumptions.

- Assumption 1: (Uniform boundedness of f(t,0)) There exists $B > 0$, such that $|f(t,0)| \ \leq B, \ \ \forall t \geq 0$

- Assumption 2: (Semiglobal uniform boundedness of partial derivatives)

  If the nonlinear function f(t,x) is continuous in its arguments, and furthermore, for arbitrary $\delta \ > 0$, therefore, there will exist $d_{f_t}(\delta) > 0$ and $d_{f_x}(\delta) > 0$, such that $\forall \|x\|_\infty \leq \ \delta$ the partial derivatives of $\mathbf{f}(\mathbf{t}, \mathbf{x})$ with respect to t and x are piecewise continuous and bounded,

  $$\|\tfrac{\partial \mathbf{f}(\mathbf{t},\mathbf{x})}{\partial \mathbf{x}}\|_{\mathbf{1}} \ \leq \mathbf{d}_{\mathbf{f_x}}(\delta), \ \text{ and } \ |\tfrac{\partial \mathbf{f}(\mathbf{t},\mathbf{x})}{\partial \mathbf{t}}| \ \leq \mathbf{d}_{\mathbf{f_t}}(\delta)$$

- Lemma

  According to the above assumptions, the nonlinear function f(t,x) can be linearly parameterized in two time-varying parameters using $\|x\|_\infty$ as a regressor, as follows:

  $$\mathbf{f}(\mathbf{t}, \mathbf{x}(\mathbf{t})) = \theta(\mathbf{t})\|\mathbf{x}(\mathbf{t})\|_\infty + \sigma(\mathbf{t})$$

Where, $|\theta(\mathbf{t})| < \theta_\rho$, $|\dot{\theta}(\mathbf{t})| < \mathbf{d}_\theta$, $|\sigma(\mathbf{t})| < \sigma_\mathbf{b}$, *and* $|\dot{\sigma}(\mathbf{t})| < \mathbf{d}_\sigma$

Where, $\theta_\rho \triangleq d_{f_x}(\rho)$, $\sigma_b \triangleq B+\epsilon$, by which $(B,\ \epsilon) > 0$ is an arbitrary constant, d_θ *and* d_σ are computable bounds.

- Property 1: (see [27]) Given the vectors $y \in \mathbb{R}^n$, $\theta^* \in \Omega_0 \subset \Omega_1 \subset \mathbb{R}^n$, and $\theta \in \Omega_1$, therefore :

$$(\theta - \theta^*)^\top (\mathbf{proj}(\theta, \mathbf{y}) - \mathbf{y}) \leq \mathbf{0} \tag{6.22}$$

6.4.2 $\mathcal{L}_1$ Adaptive Controller Formulation

In this section, $\mathcal{L}_1$ adaptive controller components are illustrated in figure 6.19 are presented.

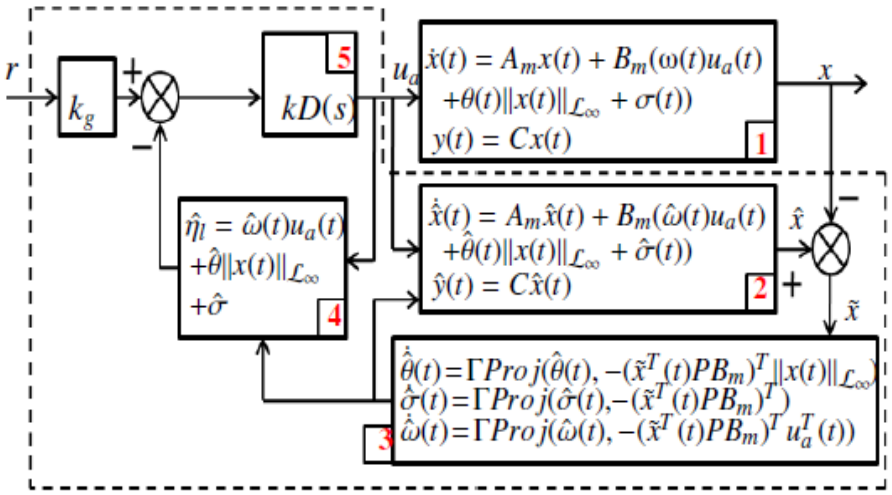

Figure 6.19: Block Diagram of the closed-loop $\mathcal{L}_1$ adaptive controller [3].

To apply $\mathcal{L}_1$ adaptive controller on the AUV, we have to rewrite 4.14 to be in the form of a state-space representation. First, we will consider the following

simple example [16, 17]:

$$\begin{aligned}
&\dot{\mathbf{x}}_\mathbf{1}(\mathbf{t}) = \mathbf{x_2},\ \mathbf{x_1(0)} = \mathbf{x_{1_0}} \\
&\dot{\mathbf{x}}_\mathbf{2}(\mathbf{t}) = \mathbf{A_2 x_2(t)} + \mathbf{f_2(t, x(t))} + \mathbf{B_2 wu},\ \mathbf{x_2(0)} = \mathbf{x_{2_0}} \\
&\mathbf{y(t)} = \mathbf{Cx(t)}
\end{aligned} \tag{6.23}$$

Where, $\mathbf{x(t)} = [\mathbf{x_1(t)},\ \mathbf{x_2(t)}]^\top \in\ \mathbb{R}^{\mathbf{2n}}$ are the states of the system, $\mathbf{A_2} \in\ \mathbb{R}^{\mathbf{n\times n}}$ is a known matrix, $\mathbf{B_2} \in\ \mathbb{R}^{\mathbf{m\times n}}$ is a constant full rank matrix, $\mathbf{u(t)} \in\ \mathbb{R}^{\mathbf{m}}$ is the control input vector, $\mathbf{w} \in\ \mathbb{R}$ is the uncertainty on the input gain, $\mathbf{C} \in\ \mathbb{R}^{\mathbf{m\times n}}$ is a known full rank constant matrix, $\mathbf{y(t)} \in\ \mathbb{R}^{\mathbf{m}}$ is the measured output and $f_2(t)$ is an unknown nonlinear function. We can rewrite 6.23 as:

$$\dot{\mathbf{x}} = \mathbf{Ax(t)} + \mathbf{f(t)} + \mathbf{B_m wu(t)} \tag{6.24}$$

Where,

$$\mathbf{A} = \begin{bmatrix} \mathbf{0_{n\times n}} & \mathbf{I_{n\times n}} \\ \mathbf{0_{n\times n}} & \mathbf{A_2} \end{bmatrix},\quad \mathbf{f} = \begin{bmatrix} \mathbf{0_{n\times 1}} \\ \mathbf{f_2} \end{bmatrix}\quad \textit{and},\ \mathbf{B_m} = \begin{bmatrix} \mathbf{0_{n\times m}} \\ \mathbf{B_2} \end{bmatrix} \tag{6.25}$$

From Eq. 4.14

$$\ddot{\eta} = \mathbf{M_e}(\eta)^{-\mathbf{1}}\ [\tau_\mathbf{e} - \mathbf{C_e}(\eta, \nu)\dot{\eta} - \mathbf{D_e}(\nu, \eta)\dot{\eta} - \mathbf{g_e}(\eta)] \tag{6.26}$$

Say:

$$\eta_{\mathbf{1}} = \eta$$

$$\eta_{\mathbf{2}} = \dot{\eta}, \quad \text{thus}$$

$$\dot{\eta_{\mathbf{1}}} = \dot{\eta} = \eta_{\mathbf{2}}$$

$$\dot{\eta_{\mathbf{2}}} = \ddot{\eta} \tag{6.27}$$

Therefore, from Eqs. 6.26 and 6.27 the state space representation is:

$$\begin{bmatrix} \dot{\eta}_{\mathbf{1}} \\ \dot{\eta}_{\mathbf{2}} \end{bmatrix} = \begin{bmatrix} \mathbf{0_{6\times 6}} & \mathbf{I_{6\times 6}} \\ \mathbf{0_{6\times 6}} & \frac{\mathbf{-D_e}}{\mathbf{M_e}} \end{bmatrix} \begin{bmatrix} \eta_{\mathbf{1}} \\ \eta_{\mathbf{2}} \end{bmatrix} - \begin{bmatrix} \mathbf{0_{6\times 1}} \\ \frac{\mathbf{g_e}}{\mathbf{M_e}} \end{bmatrix} + \begin{bmatrix} \mathbf{0_{6\times 6}} \\ \frac{\mathbf{1}}{\mathbf{M_e}} \end{bmatrix} \tau$$

$$\mathbf{y(t)} = \begin{bmatrix} \mathbf{I_{6\times 6}} & \mathbf{0_{6\times 6}} \\ \mathbf{0_{6\times 6}} & \mathbf{I_{6\times 6}} \end{bmatrix} \begin{bmatrix} \eta_{\mathbf{1}} \\ \eta_{\mathbf{2}} \end{bmatrix} \tag{6.28}$$

Now, we can rewrite Eq. 6.28 to be in the same form as Eq. 6.24. Then, by using the Lemma in sub-section 6.4.1, Eq. 6.24 can be written as follows:

$$\dot{\mathbf{x}}(\mathbf{t}) = \mathbf{A_m x(t)} + \mathbf{B_m}(\mathbf{w(t)u_{ad}} + \theta(\mathbf{t})\|\mathbf{x(t)}\|_\infty + \sigma(\mathbf{t})),\ \mathbf{x(0)} = \mathbf{x_0} \tag{6.29}$$

$$\mathbf{y(t)} = \mathbf{c}^\top \mathbf{x(t)}$$

From Eq. 6.29 the following state predictor is considered;

$$\begin{aligned}\dot{\hat{\mathbf{x}}}(\mathbf{t}) =& \mathbf{A_m}\hat{\mathbf{x}}(\mathbf{t}) + \mathbf{B_m}(\hat{\mathbf{w}}(\mathbf{t})\mathbf{u_{ad}} + \theta(\mathbf{t})\|\mathbf{x}(\mathbf{t})\|_\infty + \hat{\sigma}(\mathbf{t})),\ \mathbf{x(0)} = \mathbf{x_0} \\ \hat{\mathbf{y}}(\mathbf{t}) =& \mathbf{c}^\top\hat{\mathbf{x}}(\mathbf{t})\end{aligned} \tag{6.30}$$

where, $\hat{\mathbf{x}}(t) \in \mathbb{R}^n$ represents the predictor state, $\hat{\mathbf{y}}(t) \in \mathbb{R}^n$ is the predictor output, $\hat{\theta}(\mathbf{t})$ and $\hat{\sigma}(\mathbf{t})$ are the estimated parameters. Therefore, by defining the error $\tilde{\mathbf{x}}(t) = \mathbf{x}(t) - \hat{\mathbf{x}}(t)$, $\tilde{\theta}(t) = \theta(t) - \hat{\theta}(t)$ and $\tilde{\sigma}(t) = \sigma(t) - \hat{\sigma}(t)$, the following error dynamic obtained;

$$\dot{\tilde{x}}(t) = A_m\tilde{x}(t) + B_m(\tilde{w}(t)u_{ad} + \tilde{\theta}(t)\|x(t)\|_\infty + \tilde{\sigma}) \tag{6.31}$$

Consider the following Lyapunov function candidate;

$$V(\tilde{\mathbf{x}}(\mathbf{t}), \tilde{\theta}(\mathbf{t}), \tilde{\sigma}(\mathbf{t}), \dot{\tilde{\sigma}}(\mathbf{t})) = \tilde{\mathbf{x}}^\top(\mathbf{t})\mathbf{P}\tilde{\mathbf{x}}(\mathbf{t}) + \frac{\tilde{\theta}^\top(\mathbf{t})\tilde{\theta}(\mathbf{t})}{\gamma_1} + \frac{\tilde{\sigma}^\top(\mathbf{t})\tilde{\sigma}(\mathbf{t})}{\gamma_2} + \frac{\tilde{\mathbf{w}}^\mathbf{2}(\mathbf{t})}{\gamma_3} \tag{6.32}$$

Thus,

$$\begin{aligned}
\dot{V}(t) =&\dot{\tilde{\mathbf{x}}}^{\top}(\mathbf{t})\mathbf{P}\tilde{\mathbf{x}}(\mathbf{t}) + \tilde{\mathbf{x}}^{\top}(\mathbf{t})\mathbf{P}\dot{\tilde{\mathbf{x}}}(\mathbf{t}) + \frac{1}{\gamma_1}(\dot{\tilde{\theta}}^{\top}(\mathbf{t})\tilde{\theta}(\mathbf{t}) + \tilde{\theta}^{\top}(\mathbf{t})\dot{\tilde{\theta}}(\mathbf{t})) \\
&+\frac{1}{\gamma_2}(\dot{\tilde{\sigma}}^{\top}(\mathbf{t})\tilde{\sigma}(\mathbf{t}) + \tilde{\sigma}^{\top}(\mathbf{t})\dot{\tilde{\sigma}}(\mathbf{t})) + \frac{2}{\gamma_3}(\tilde{\mathbf{w}}(\mathbf{t})\dot{\tilde{\mathbf{w}}}(\mathbf{t})) \\
&=(\mathbf{A_m}\tilde{\mathbf{x}}(\mathbf{t}) + \mathbf{B_m}\tilde{\mathbf{w}}(\mathbf{t})\mathbf{u_{ad}}(\mathbf{t}) + \mathbf{B_m}\tilde{\theta}(\mathbf{t})\|\mathbf{x}\|_{\infty} + \mathbf{B_m}\tilde{\sigma}(\mathbf{t}))^{\top}\mathbf{P}\tilde{\mathbf{x}}(\mathbf{t}) \\
&+\tilde{\mathbf{x}}(\mathbf{t})^{\top}\mathbf{P}(\mathbf{A_m}\tilde{\mathbf{x}}(\mathbf{t}) + \mathbf{B_m}\tilde{\mathbf{w}}(\mathbf{t})\mathbf{u_{ad}}(\mathbf{t}) + \mathbf{B_m}\tilde{\theta}(\mathbf{t})\|\mathbf{x}\|_{\infty} + \mathbf{B_m}\tilde{\sigma}(\mathbf{t})) \\
&+\frac{1}{\gamma_1}(\dot{\tilde{\theta}}^{\top}(\mathbf{t})\tilde{\theta}(\mathbf{t}) + \tilde{\theta}^{\top}(\mathbf{t})\dot{\tilde{\theta}}(\mathbf{t})) + \frac{1}{\gamma_2}(\dot{\tilde{\sigma}}^{\top}(\mathbf{t})\tilde{\sigma}(\mathbf{t}) + \tilde{\sigma}^{\top}(\mathbf{t})\dot{\tilde{\sigma}}(\mathbf{t})) + \frac{2}{\gamma_3}(\tilde{\mathbf{w}}(\mathbf{t})\dot{\tilde{\mathbf{w}}}(\mathbf{t})) \\
&=\tilde{\mathbf{x}}(\mathbf{t})^{\top}\mathbf{A_m}\mathbf{P}\tilde{\mathbf{x}}(\mathbf{t}) + (\mathbf{B_m}\tilde{\mathbf{w}}(\mathbf{t})\mathbf{u_{ad}}(\mathbf{t}) + \mathbf{B_m}\tilde{\theta}(\mathbf{t})\|\mathbf{x}\|_{\infty} + \mathbf{B_m}\tilde{\sigma}(\mathbf{t}))^{\top}\mathbf{P}\tilde{\mathbf{x}}(\mathbf{t}) \\
&+\tilde{\mathbf{x}}(\mathbf{t})^{\top}\mathbf{P}\mathbf{A_m}\tilde{\mathbf{x}}(\mathbf{t}) + \tilde{\mathbf{x}}^{\top}\mathbf{P}(\mathbf{B_m}\tilde{\mathbf{w}}(\mathbf{t})\mathbf{u_{ad}}(\mathbf{t}) + \mathbf{B_m}\tilde{\theta}(\mathbf{t})\|\mathbf{x}\|_{\infty} + \mathbf{B_m}\tilde{\sigma}(\mathbf{t})) \\
&+\frac{2}{\gamma_1}(\tilde{\theta}^{\top}(\mathbf{t})\dot{\tilde{\theta}}(\mathbf{t})) + \frac{2}{\gamma_2}(\tilde{\sigma}^{\top}(\mathbf{t})\dot{\tilde{\sigma}}(\mathbf{t})) + \frac{2}{\gamma_3}(\tilde{\mathbf{w}}(\mathbf{t})\dot{\tilde{\mathbf{w}}}(\mathbf{t}))
\end{aligned}$$

$$\begin{aligned}
&= -\tilde{\mathbf{x}}(\mathbf{t})^{\top}(\mathbf{A_m^{\top}}\mathbf{P} + \mathbf{P}\mathbf{A_m})\tilde{\mathbf{x}}(\mathbf{t}) + \mathbf{2}\tilde{\mathbf{x}}(\mathbf{t})^{\top}\mathbf{P}(\mathbf{B_m}\tilde{\mathbf{w}}(\mathbf{t})\mathbf{u_{ad}}(\mathbf{t}) + \mathbf{B_m}\tilde{\theta}(\mathbf{t})\|\mathbf{x}\|_{\infty} + \mathbf{B_m}\tilde{\sigma}(\mathbf{t})) \\
&+\frac{2}{\gamma_1}(\tilde{\theta}^{\top}(\mathbf{t})\dot{\tilde{\theta}}(\mathbf{t})) + \frac{2}{\gamma_2}(\tilde{\sigma}^{\top}(\mathbf{t})\dot{\tilde{\sigma}}(\mathbf{t})) + \frac{2}{\gamma_3}(\tilde{\mathbf{w}}^{(}\mathbf{t})\dot{\tilde{\mathbf{w}}}(\mathbf{t}))
\end{aligned}$$

Therefore,

$$\begin{aligned}
\dot{V}(t) = &-\tilde{\mathbf{x}}(\mathbf{t})^{\top}\mathbf{Q}\tilde{\mathbf{x}}(\mathbf{t}) + \mathbf{2}\tilde{\mathbf{x}}(\mathbf{t})^{\top}\mathbf{P}\mathbf{B_m}\tilde{\mathbf{w}}(\mathbf{t})\mathbf{u_{ad}}(\mathbf{t}) + \mathbf{2}\tilde{\mathbf{x}}(\mathbf{t})^{\top}\mathbf{P}\mathbf{B_m}\tilde{\theta}(\mathbf{t})\|\mathbf{x}\|_{\infty} \\
&+2\tilde{\mathbf{x}}(\mathbf{t})^{\top}\mathbf{P}\mathbf{B_m}\tilde{\sigma}(\mathbf{t}) + \frac{2}{\gamma_1}(\tilde{\theta}^{\top}(\mathbf{t})\dot{\tilde{\theta}}(\mathbf{t})) + \frac{2}{\gamma_2}(\tilde{\sigma}^{\top}(\mathbf{t})\dot{\tilde{\sigma}}(\mathbf{t})) + \frac{2}{\gamma_3}(\tilde{\mathbf{w}}^{(}\mathbf{t})\dot{\tilde{\mathbf{w}}}(\mathbf{t})) \qquad (6.33)
\end{aligned}$$

The derivatives of the parameters can be written by using the projection operators

as follows:

$$\begin{aligned}
\dot{\tilde{\theta}} =& \gamma_1 Proj(\tilde{\theta}(\mathbf{t}), -\|\mathbf{x}(\mathbf{t})\|\mathbf{B_m^\top P\tilde{x}(t)}) \\
\dot{\tilde{\sigma}} =& \gamma_2 Proj(\tilde{\sigma}(\mathbf{t}), -\mathbf{B_m^\top P\tilde{x}(t)}) \\
\dot{\tilde{\mathbf{w}}} =& \gamma_3 Proj(\tilde{\mathbf{w}}(\mathbf{t}), -\mathbf{x}^\top(\mathbf{t})\mathbf{PB_m u_{ad}})
\end{aligned} \tag{6.34}$$

where, ($\gamma_1,\ \gamma_2$ and γ_3) > 0 are the adaptation laws rate, $\mathbf{P} = \mathbf{P}^\top > 0$ satisfy the Lyapunov equation;

$$\mathbf{A_m^\top P + PA_m} = -\mathbf{Q} \tag{6.35}$$

where, $\mathbf{Q} = \mathbf{Q}^\top > 0$.

Therefore, by substituting eq. 6.34 in to eq. 6.33 leads to eq. 6.36:

$$\begin{aligned}
\dot{V}(t) =& -\mathbf{\tilde{x}(t)}^\top\mathbf{Q\tilde{x}(t)} + \mathbf{2\tilde{x}(t)}^\top\mathbf{PB_m\tilde{w}(t)u_{ad}(t)} + \mathbf{2\tilde{x}(t)}^\top\mathbf{PB_m}\tilde{\theta}(\mathbf{t})\|\mathbf{x}\|_\infty \\
&+2\mathbf{\tilde{x}(t)}^\top\mathbf{PB_m}\tilde{\sigma}(\mathbf{t}) + \mathbf{2}\tilde{\theta}^\top(\mathbf{t})\mathbf{Proj}(\tilde{\theta}(\mathbf{t}), -\|\mathbf{x}(\mathbf{t})\|\mathbf{B_m^\top P\tilde{x}(t)}) \\
&+2\tilde{\sigma}^\top(\mathbf{t})\mathbf{Proj}(\tilde{\sigma}(\mathbf{t}), -\mathbf{B_m^\top P\tilde{x}(t)}) + \mathbf{2\tilde{w}(t)Proj}(\mathbf{\tilde{w}(t)}, -\mathbf{x}^\top(\mathbf{t})\mathbf{PB_m u_{ad}}) \\
=& -\mathbf{\tilde{x}(t)}^\top\mathbf{Q\tilde{x}(t)} + \mathbf{2}\tilde{\theta}^\top(\mathbf{t})\|\mathbf{x}\|_\infty\mathbf{B_m^\top P\tilde{x}(t)} + \mathbf{2}\tilde{\theta}^\top(\mathbf{t})\mathbf{Proj}(\tilde{\theta}(\mathbf{t}), -\|\mathbf{x}(\mathbf{t})\|_\infty\mathbf{B_m^\top P\tilde{x}(t)}) \\
&+ 2\tilde{\sigma}^\top(\mathbf{t})\mathbf{B_m^\top P\tilde{x}(t)} + \mathbf{2}\tilde{\sigma}^\top(\mathbf{t})\mathbf{Proj}(\tilde{\sigma}(\mathbf{t}), -\mathbf{B_m^\top P\tilde{x}(t)}) \\
&+ 2\mathbf{\tilde{w}(t)x}^\top(\mathbf{t})\mathbf{PB_m u_{ad}} + \mathbf{2\tilde{w}(t)Proj}(\mathbf{\tilde{w}(t)}, -\mathbf{x}^\top(\mathbf{t})\mathbf{PB_m u_{ad}})
\end{aligned} \tag{6.36}$$

Therefore, using the property 1 in sub-section 6.4.1 leads to:

$$\dot{V}(t) = -\tilde{\mathbf{x}}(\mathbf{t})^\top \mathbf{Q}\tilde{\mathbf{x}}(\mathbf{t}) + 2\overbrace{\tilde{\theta}(\mathbf{t})^\top[\underbrace{\|\mathbf{x}\|_\infty \mathbf{B_m^\top P}\tilde{\mathbf{x}}(\mathbf{t})}_{-y_1} + Proj(\tilde{\theta}(\mathbf{t}), \underbrace{-\|\mathbf{x}(\mathbf{t})\|_\infty \mathbf{B_m^\top P}\tilde{\mathbf{x}}(\mathbf{t})}_{y_1})]}^{\leq 0}$$
$$+2\overbrace{\tilde{\sigma}(\mathbf{t})^\top[\underbrace{\mathbf{B_m^\top P}\tilde{\mathbf{x}}(\mathbf{t})}_{-y_2} + Proj(\tilde{\sigma}(\mathbf{t}), \underbrace{-\mathbf{B_m^\top P}\tilde{\mathbf{x}}(\mathbf{t})}_{y_2})]}^{\leq 0}$$
$$+2\overbrace{\tilde{\mathbf{w}}(\mathbf{t})[\underbrace{\mathbf{x}^\top(\mathbf{t})\mathbf{P}\mathbf{B_m}\mathbf{u_{ad}}}_{-y_3} + Proj(\tilde{\mathbf{w}}(\mathbf{t}), \underbrace{-\mathbf{x}^\top(\mathbf{t})\mathbf{P}\mathbf{B_m}\mathbf{u_{ad}}}_{y_3})]}^{\leq 0} \tag{6.37}$$

$$\Rightarrow \dot{V}(t) = -\tilde{\mathbf{x}}(\mathbf{t})^\top \mathbf{Q}\tilde{\mathbf{x}}(\mathbf{t}) \leq 0 \tag{6.38}$$

Which means that our systems is asymptotically stable. The Laplace transform of the adaptive control signal is obtained as follows;

$$\mathbf{u_{ad}}(\mathbf{s}) = -\frac{\mathbf{C}(\mathbf{s})}{\omega}(\hat{\mu}(\mathbf{s}) - \mathbf{k_g}\mathbf{r}(\mathbf{s})) \tag{6.39}$$

where, $\hat{\mu}(\mathbf{s})$ and $\mathbf{r}(\mathbf{s})$ are the Laplace transform of $\hat{\mu}(\mathbf{t}) = \hat{\theta}(\mathbf{t})\|\mathbf{x}(\mathbf{t})\|_\infty + \sigma(\mathbf{t})$ and $\mathbf{r}(\mathbf{t})$ is the reference signals, respectively and $\mathbf{k_g} = -\frac{\mathbf{1}}{\mathbf{c}^\top \mathbf{A_m^{-1}}}\mathbf{B_m}$ is the feedforward gain.

Say, the filter $\mathbf{C}(\mathbf{s})$ is selected to be as follows;

$$\mathbf{C}(\mathbf{s}) = \frac{\omega \mathbf{k}\mathbf{D}(\mathbf{s})}{\mathbf{I} + \omega \mathbf{k}\mathbf{D}(\mathbf{s})} \tag{6.40}$$

with, DC gain $\mathbf{C}(\mathbf{0}) = \mathbf{I}$. To be sure that the filter in eq. 6.40 is first order with

strictly proper transfer function $\mathbf{D(s)}$, must be selected to be equal $\frac{\mathbf{I}}{\mathbf{s}}$, leads to;

$$\mathbf{C(s)} = \frac{\omega \mathbf{k}}{\mathbf{sI} + \omega \mathbf{k}} \tag{6.41}$$

By substituting eq. 6.40 into eq. 6.39, the Laplace transform of the adaptive control signal will be as follows;

$$\mathbf{u_{ad}} = -\mathbf{kD(s)}(\omega \mathbf{u_{ad}(s)} + \hat{\mu}(\mathbf{s}) - \mathbf{k_g r(s)}) \tag{6.42}$$

Finally, the $\mathcal{L}_1$ norm condition is given as follows;

$$\|\mathbf{G(s)}\|_{\mathcal{L}_1} \mathbf{L} < 1 \tag{6.43}$$

where,

$$\mathbf{G(s)} = \mathbf{H(s)}(\mathbf{C(s)} - \mathbf{I}), \quad \mathbf{H(s)} = (\mathbf{sI} - \mathbf{A_m})^{-1} \mathbf{B_m} \tag{6.44}$$

And,

$$\|\frac{\partial \mathbf{f(t, x)}}{\partial \mathbf{x}}\| \leq \mathbf{d_{f_x}} = \mathbf{L} \tag{6.45}$$

More details can be found in [16].

6.4.3 Simulation Results

The Modular Autonomous Robot for Environment Sampling (MARES) AUV is selected to perform trajectory tracking. The parameters of the MARES model as follows [13, 28, 29]:

Properties	Value
Length	1.5 m
Diameter	20 cm
Weight in air	32 kg
Depth rating	100 m
Propulsion	2 horizontal + 2 vertical thrusters
Horizontal velocity	0-1.5 m/s, variable
Energy	Li-Ion batteries, 600Wh
Autonomy/Range	about 10 hrs / 40 km

Table 6.1: MARES General Characteristic

Properties	Value by m	Description
$[x_{cg}, y_{cg}, z_{cg}]$	[0 0 0]	Center of gravity
$[x_{cb}, y_{cb}, z_{cb}]$	[0 0 (0.0044)]	Center of buoyancy

Table 6.2: MARES Location of center of gravity and buoyancy

Properties	Value $[kg.m^2]$
I_{xx}	$1.55.10^{-1}$
I_{yy}	4.73
I_{zz}	4.73

Table 6.3: MARES Moment Inertia

Properties	Value	Unit
$X_{\dot{u}}$	-1.74	kg
$Y_{\dot{v}}$	4.28.10	kg
$Z_{\dot{w}}$	-4.12.10	kg
$K_{\dot{p}}$	$-8.61.10^{-3}$	$kg.m^2$
$M_{\dot{q}}$	-6.07	$kg.m^2$
$N_{\dot{r}}$	-6.40	$kg.m^2$
$X_{\dot{q}}$	$-3.05.10^{-2}$	kg.m
$Y_{\dot{p}}$	$3.05.10^{-2}$	kg.m
$K_{\dot{v}}$	$3.05.10^{-2}$	kg.m
$M_{\dot{u}}$	$-3.05.10^{-2}$	kg.m
$Y_{\dot{r}}$	$1.13.10^{-1}$	kg.m
$Z_{\dot{q}}$	$-1.23.10^{-1}$	kg.m
$M_{\dot{w}}$	$-1.23.10^{-1}$	kg.m
$N_{\dot{v}}$	$1.13.10^{-1}$	kg.m

Table 6.4: MARES Added Masses

The above designed $\mathcal{L}_1$ adaptive controller is implemented, with the following parameters (controller parameters);

$\gamma_1 = 10^4, \quad \gamma_2 = 10^4, \quad \gamma_3 = 10^4 \quad \text{and} \quad k = 10^3.$

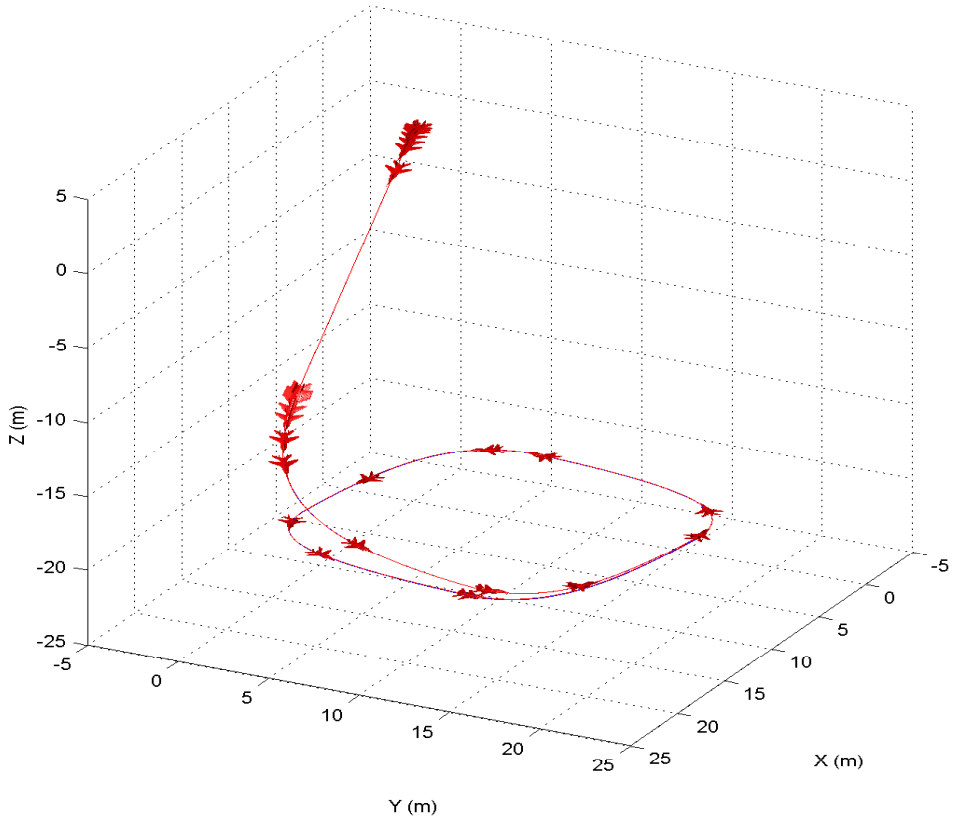

Figure 6.20: 3D trajectory tracking of the MARES AUV without uncertainty.

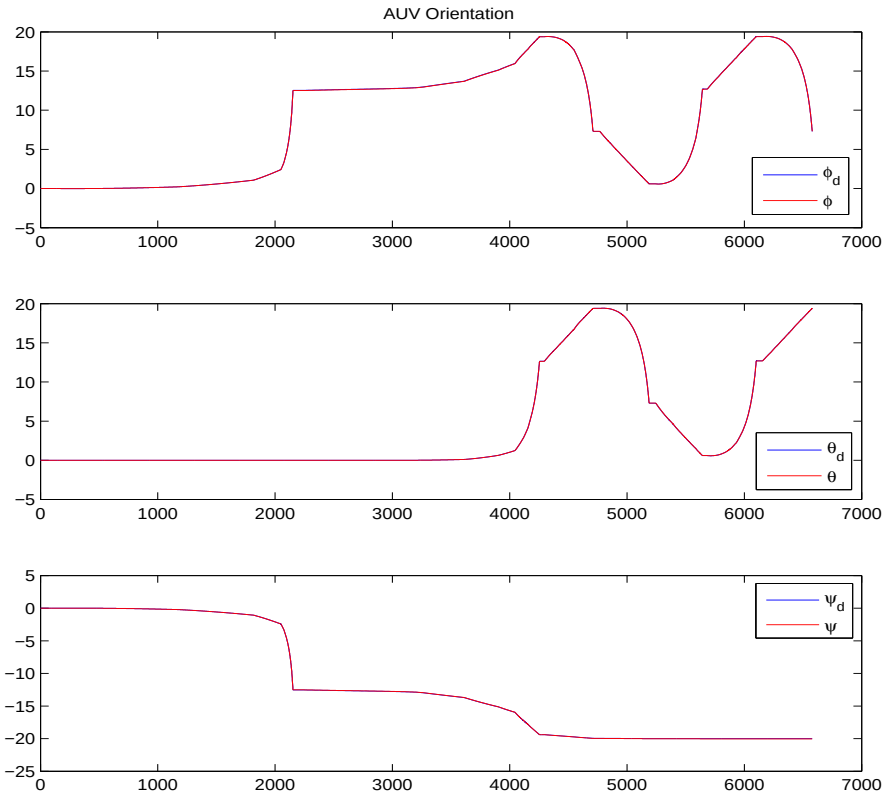

Figure 6.21: Orientation of the MARES AUV without uncertainty.

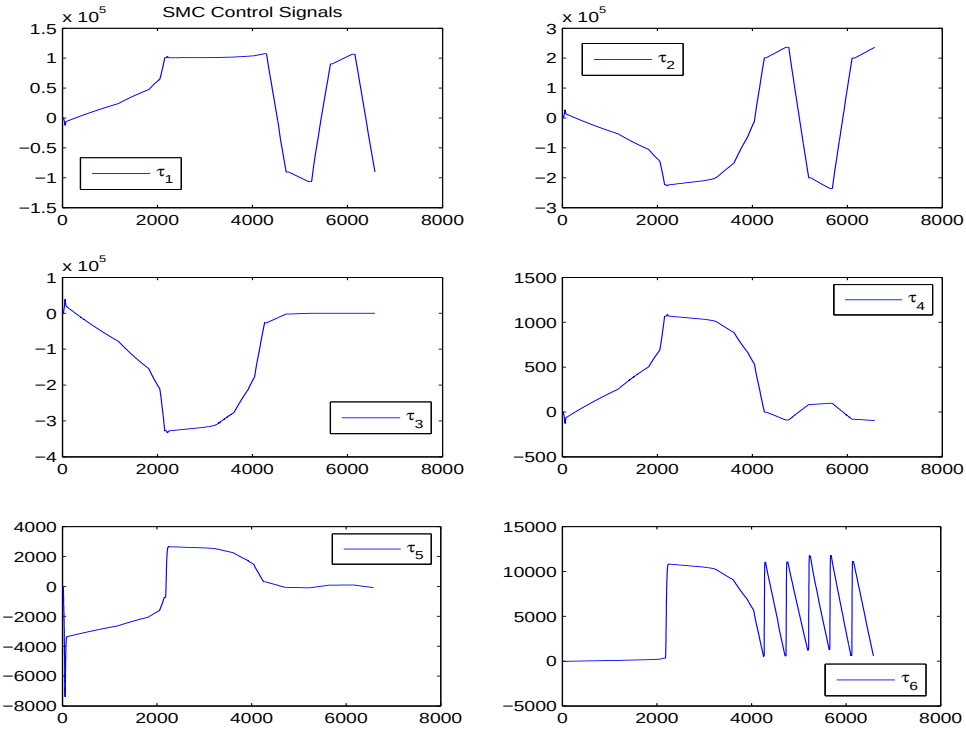

Figure 6.22: Control Signals of the MARES AUV without uncertainty.

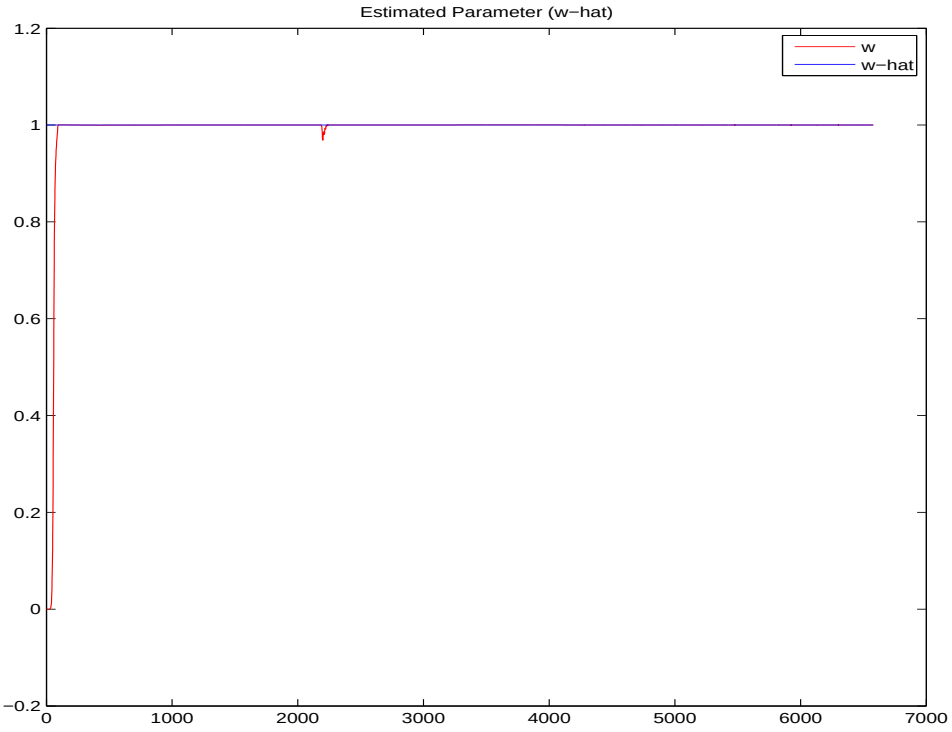

Figure 6.23: Estimated Parameter ($\hat{w}$) without uncertainty.

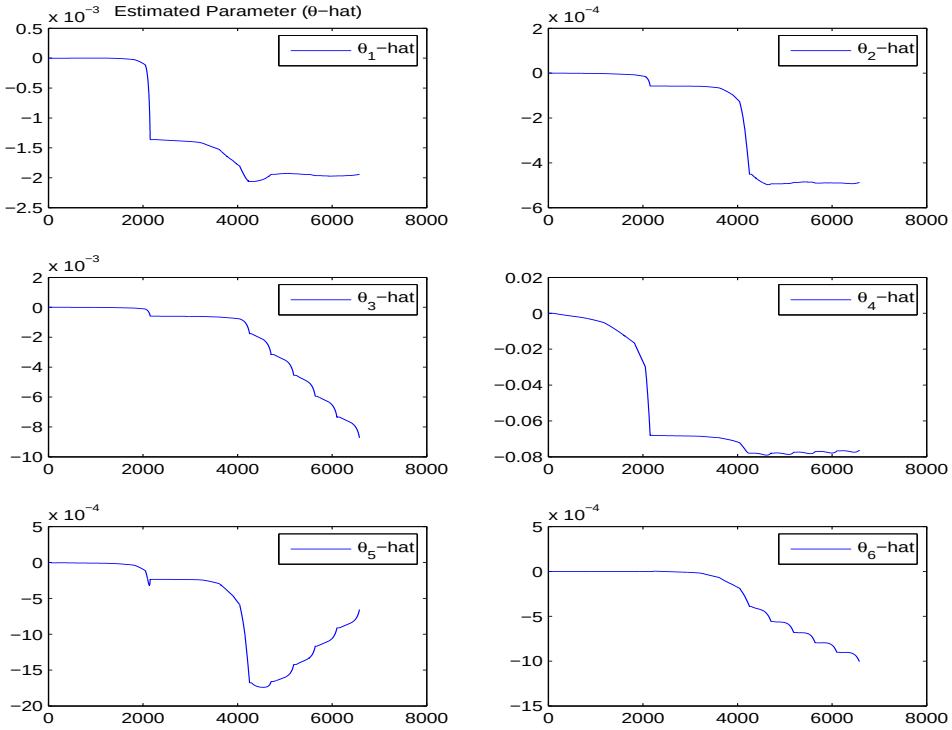

Figure 6.24: Estimated Parameter ($\hat{\theta}$) without uncertainty.

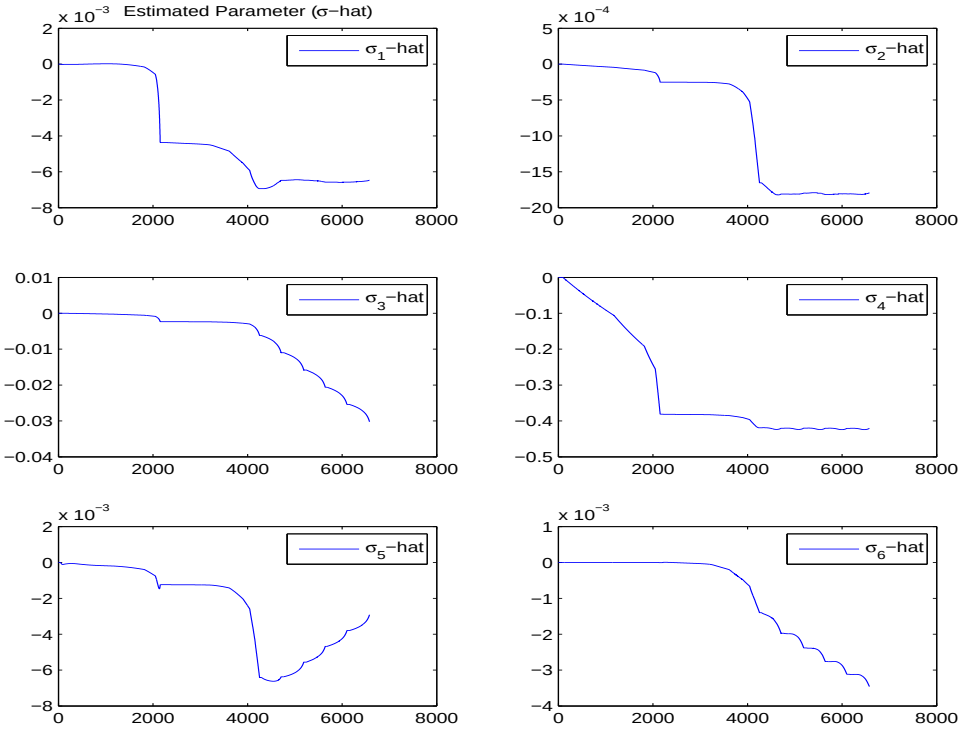

Figure 6.25: Estimated Parameter ($\hat{\sigma}$) without uncertainty.

The uncertainty in parameters (ρ and $\mathbf{M}$ represent water density and the inertia matrix for the AUV, respectively) was not considered in the above simulation, but now it is considered (25% error in ρ and 100% error in $\mathbf{M}$).

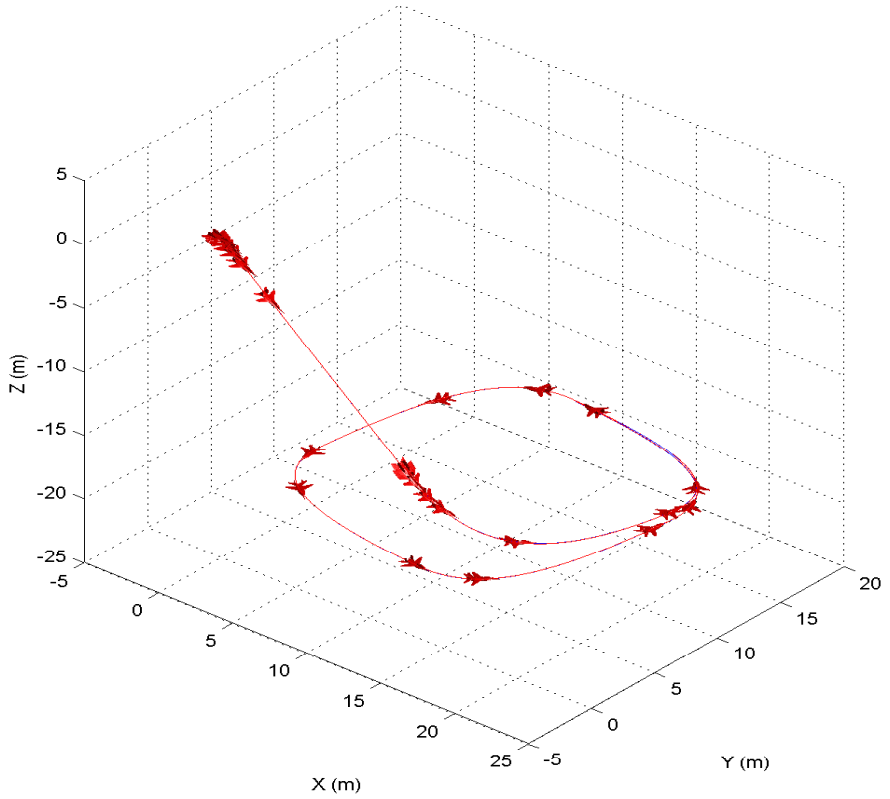

Figure 6.26: 3D trajectory tracking of the MARES AUV with uncertainty in parameters.

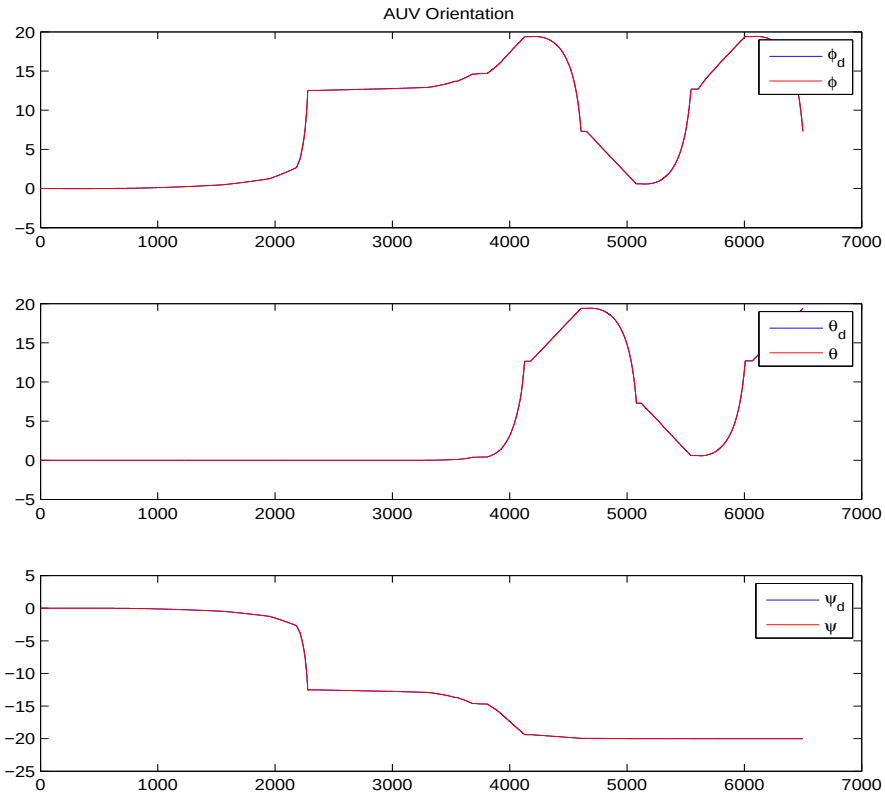

Figure 6.27: Orientation of the MARES AUV with uncertainty in parameters.

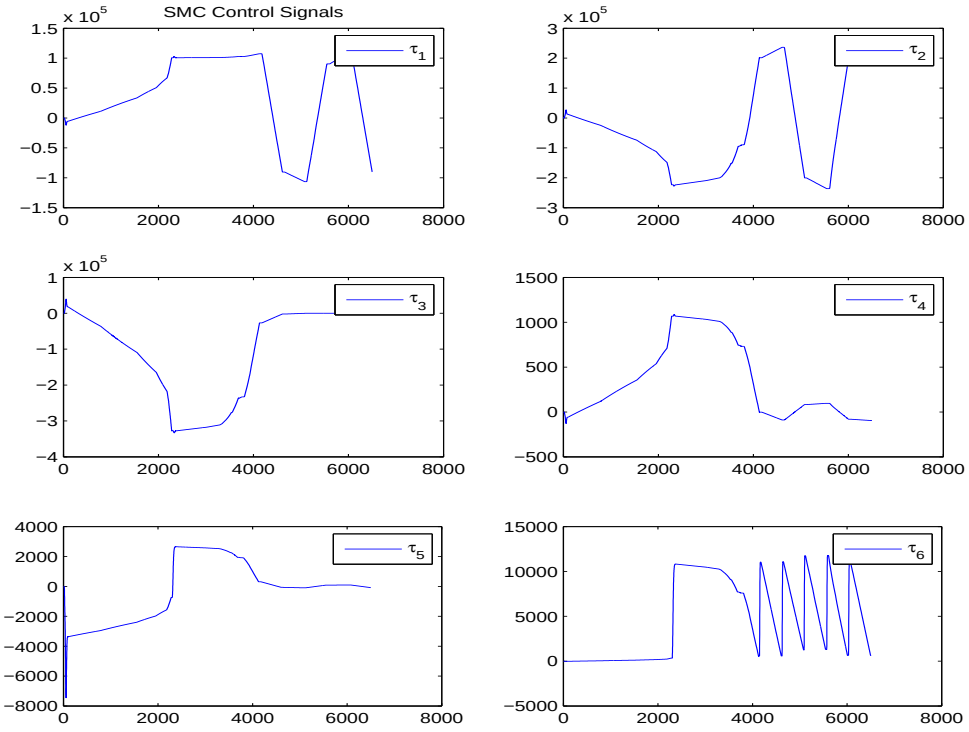

Figure 6.28: Control Signals of the MARES AUV with uncertainty in parameters.

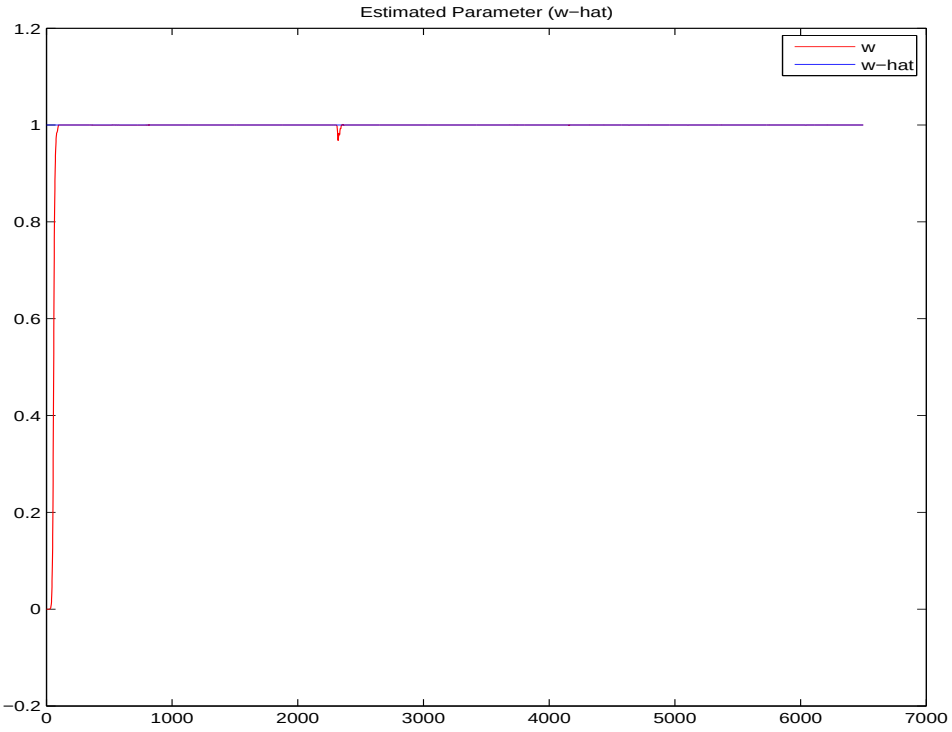

Figure 6.29: Estimated Parameter ($\hat{w}$) with uncertainty in parameters.

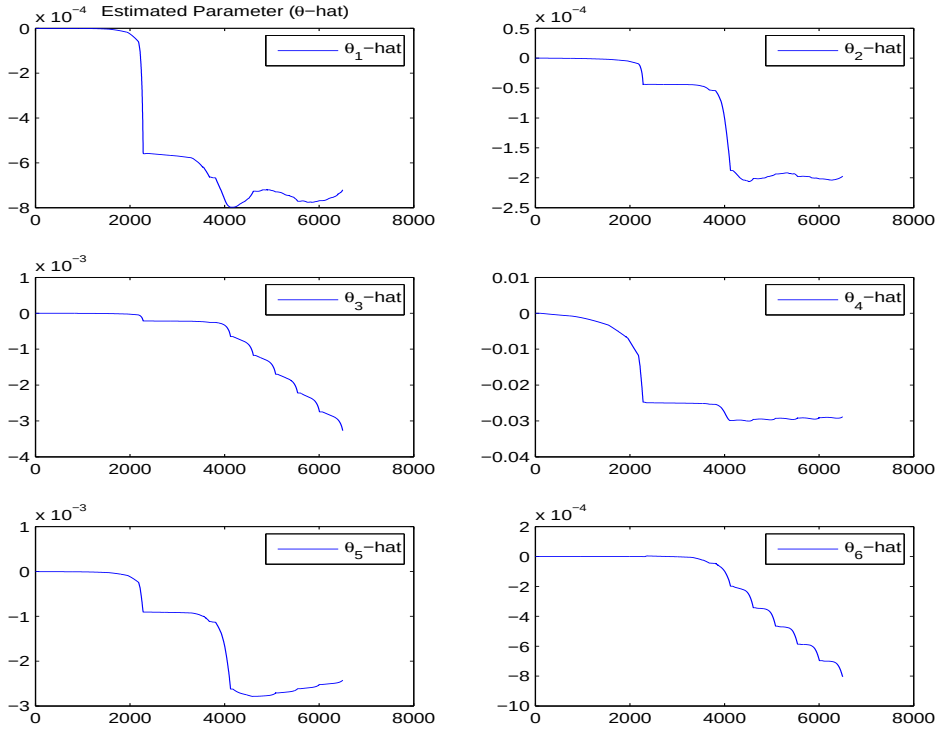

Figure 6.30: Estimated Parameter ($\hat{\theta}$) with uncertainty in parameters.

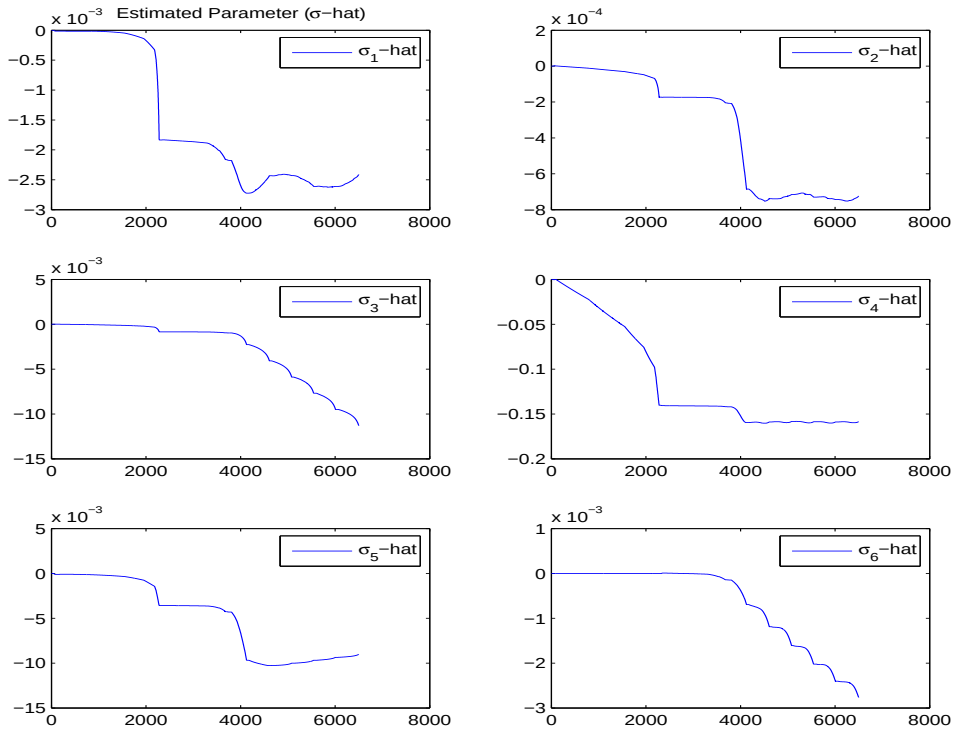

Figure 6.31: Estimated Parameter ($\hat{\sigma}$) with uncertainty in parameters.

In addition to the uncertainty in parameters as shown in the above simulations, the disturbance (with mean equal to 1, variance equal to 0.3 and frequency equal to 0.1 Hz) has been added to the input signals as well, to investigate the robustness of the proposed controller and the simulations were as in the following Figures.

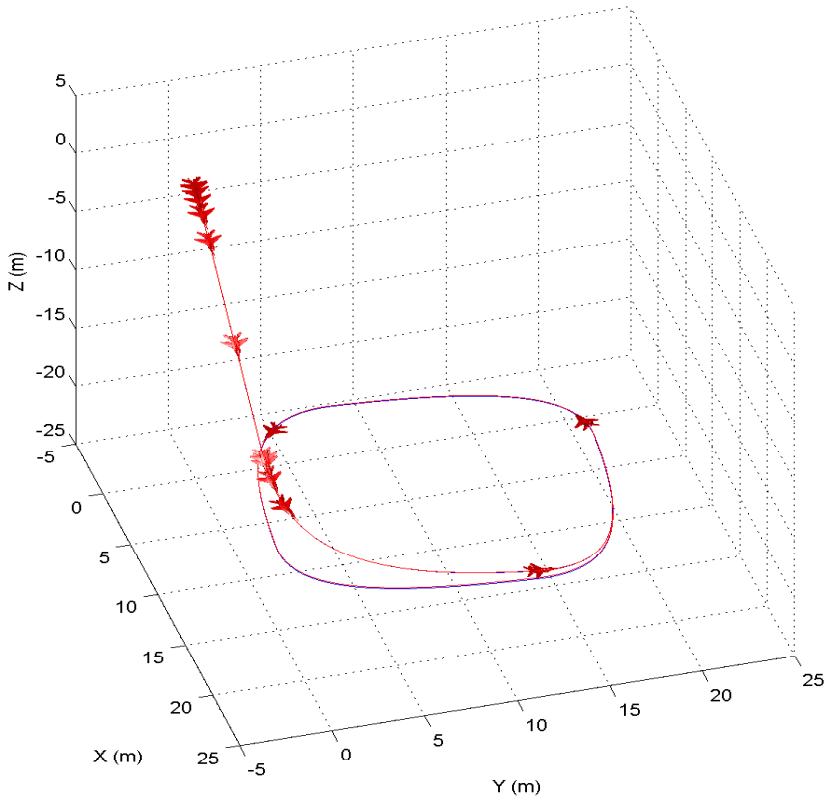

Figure 6.32: 3D trajectory tracking of the MARES AUV with uncertainty and disturbance.

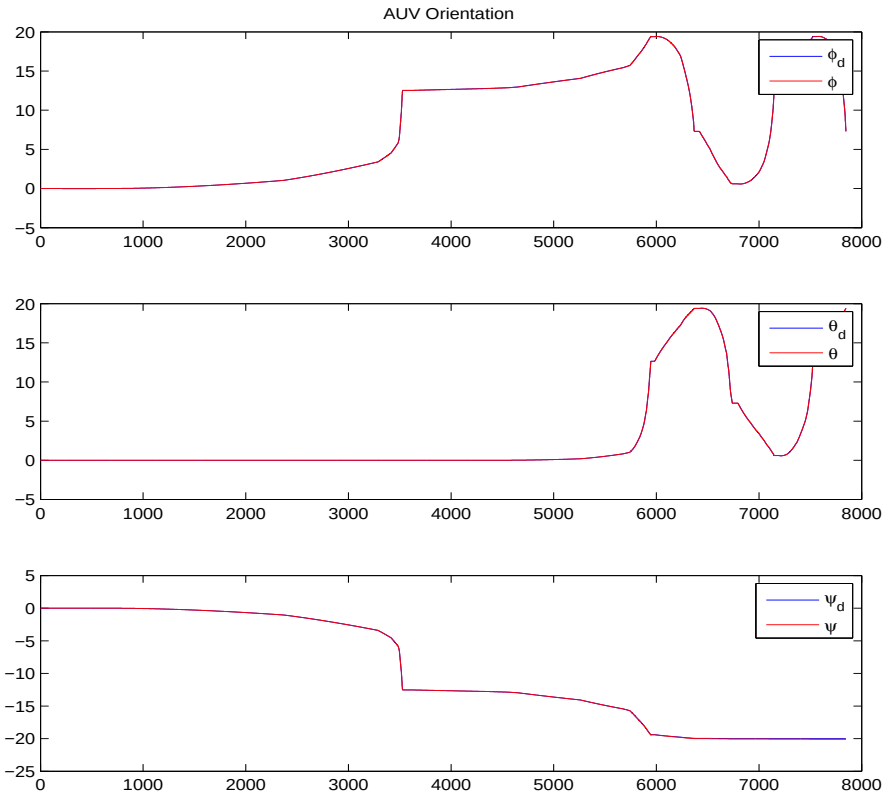

Figure 6.33: Orientation of the MARES AUV with uncertainty and disturbance.

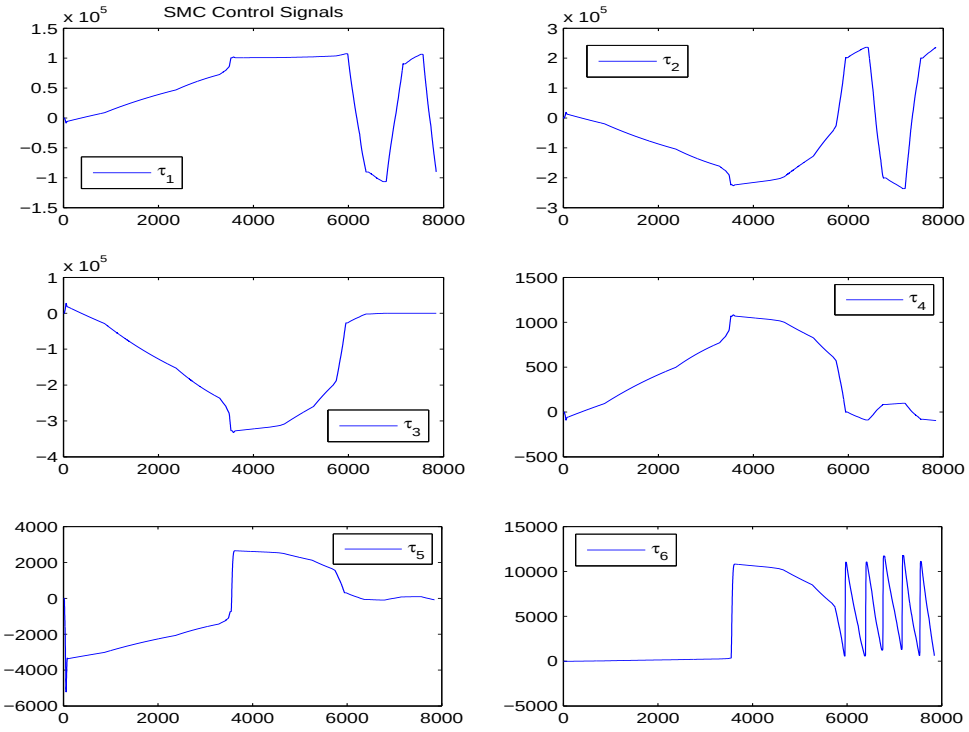

Figure 6.34: Control Signals of the MARES AUV with uncertainty and disturbance.

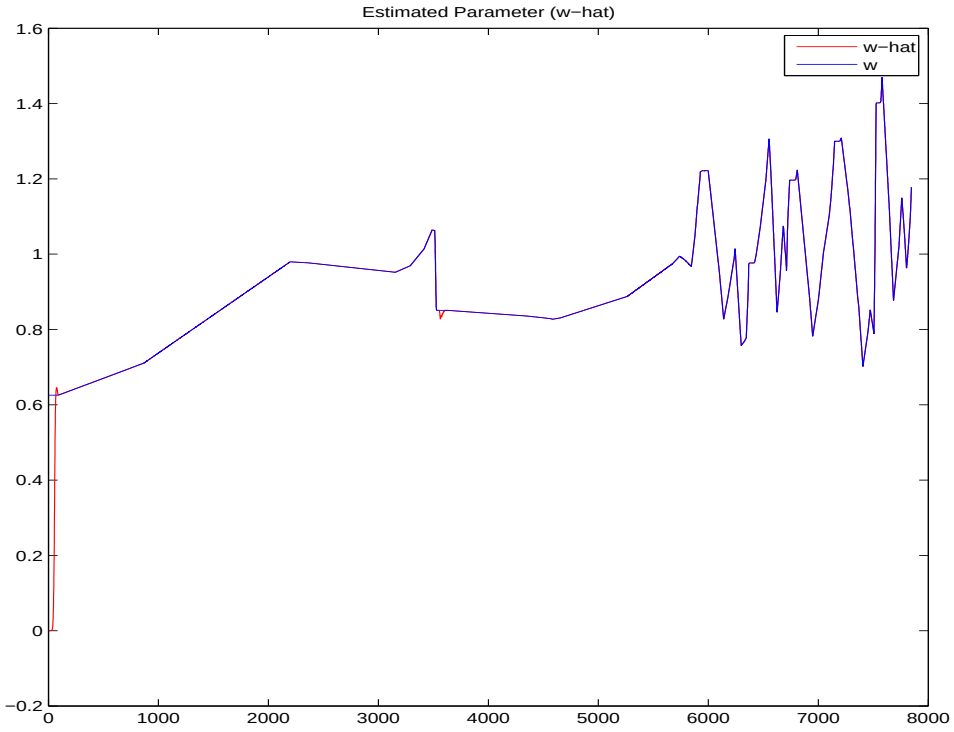

Figure 6.35: Estimated Parameter ($\hat{w}$) with uncertainty and disturbance.

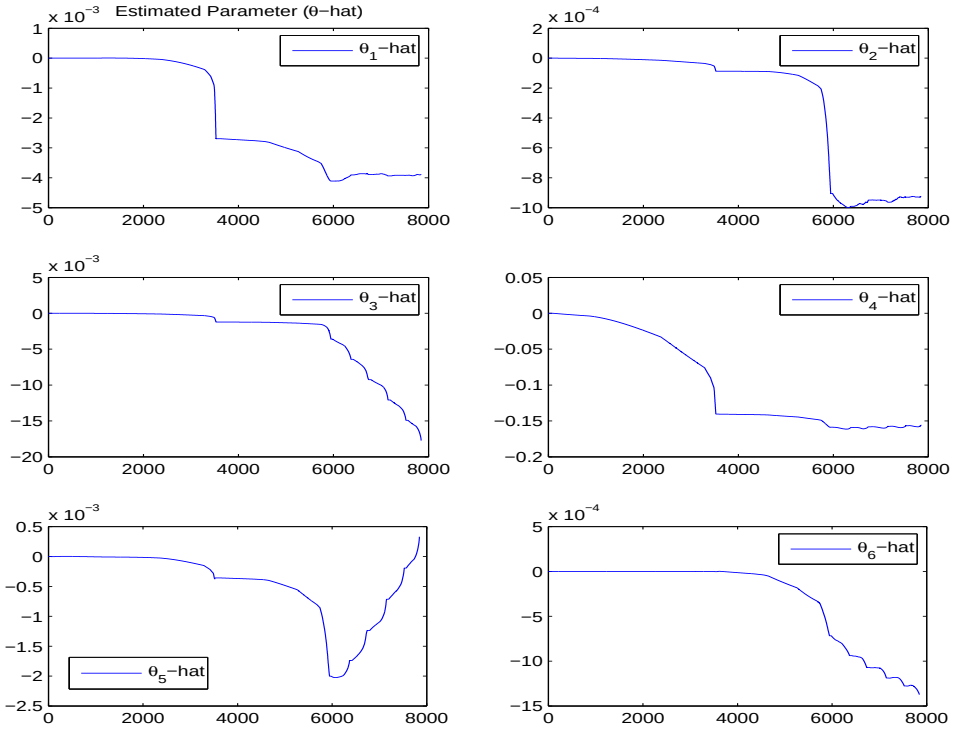

Figure 6.36: Estimated Parameter ($\hat{\theta}$) with uncertainty and disturbance.

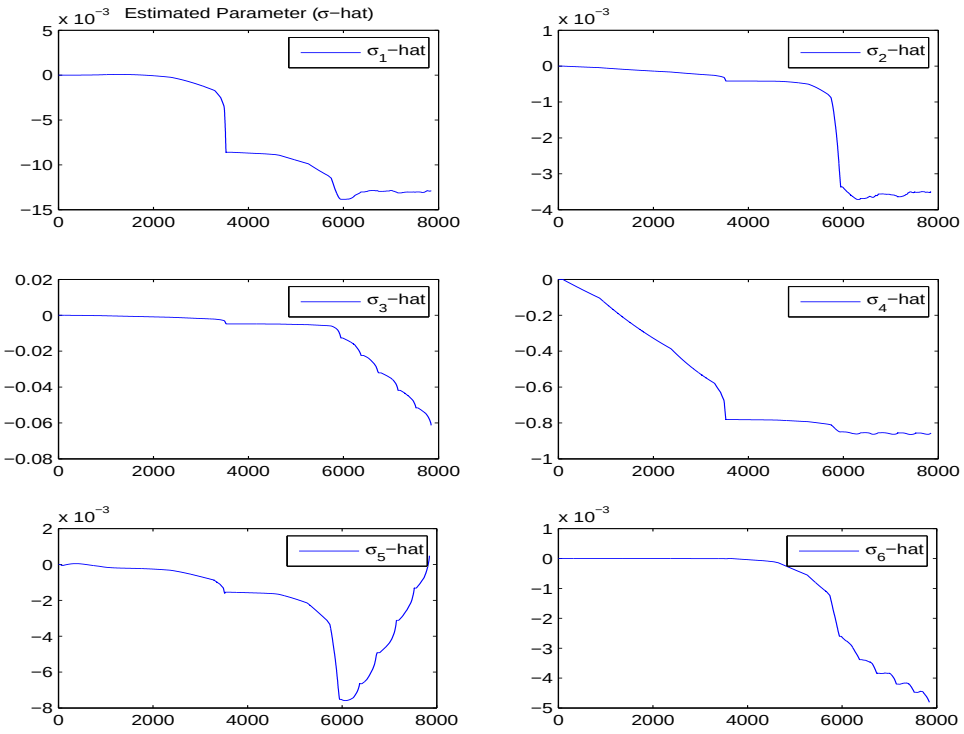

Figure 6.37: Estimated Parameter ($\hat{\sigma}$) with uncertainty and disturbance.

6.4.4 Discussion and Comparison

The performance of the designed controllers is compared in terms of the robustness against the disturbance and uncertainty in parameters and the simulations showed that the $\mathcal{L}_1$adaptive controller is better than the other controllers.

CHAPTER 7

CONTROLLER DESIGN FOR THE UVMS

Since the general dynamic equation of the AUV (4.14) and the UVMS (5.63) systems have the same structures, therefore, the derivation of the controllers (Feedback Linearization, Sliding Mode and $\mathcal{L}_1$ adaptive) will be exactly the same as in chapter 6. Thus, in this chapter the above three controllers are applied to the UVMS system by following the steps in chapter 6. For the purpose of the simulations the parameters of the UVMS model are selected to be matched with those used in Jason Underwater Vehicle [1], as well as, with the first 3 links of the Puma 560 manipulator. Therefore, the UVMS model has 9 DOFs, see tables (7.1 and 7.2).

7.1 Feedback Linearization Controller for the UVMS

7.1.1 Simulation Results

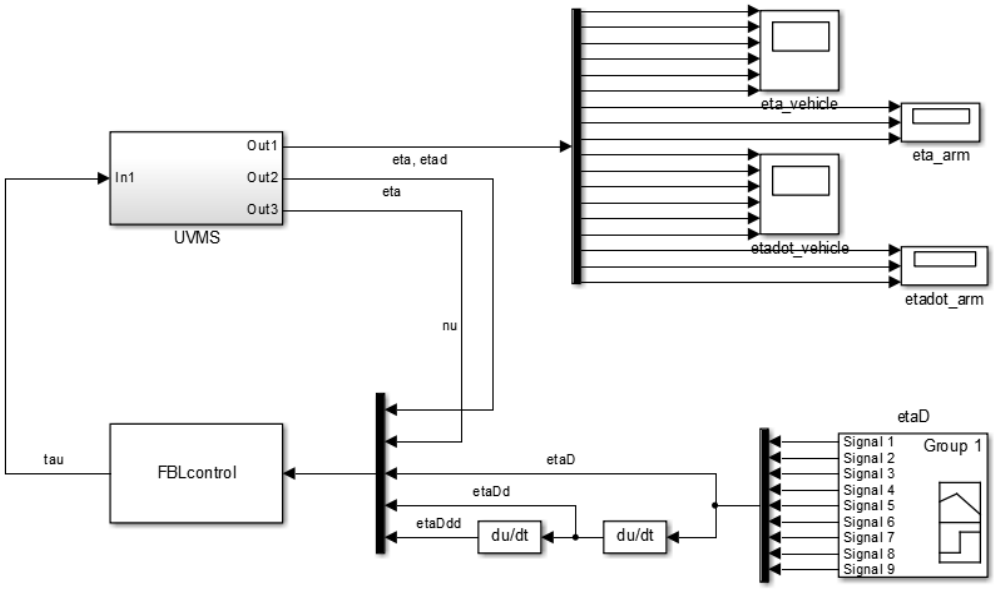

Figure 7.1: Simulink Block Diagram for the UVMS.

Length	$L = 2.2m$
Height	$H = 1.2m$
Width	$W = 1.1m$

Table 7.1: Dimension of Jason URV [1]

The first joint of the manipulator located on the vehicle at the following point;

$$\mathbf{c_0^0} = [c_{x_0} \quad c_{y_0} \quad c_{z_0}]^\top = [0.5L \quad 0 \quad 0.5H]^\top = [1.1 \quad 0 \quad 0.6]^\top \text{meters} \qquad (7.1)$$

Link	Mass kg	$I_{xx} kg.m^2$	$I_{yy} kg.m^2$	$I_{zz} kg.m^2$
Vehicle	1200	265	628	605
Link 1	12.96	1.0981	0.1774	1.1112
Link 2	22.37	0.4036	0.9684	0.9664
Link 3	5.01	0.0746	0.0755	0.0075

Table 7.2: Mass and Inertia Properties of the UVMS

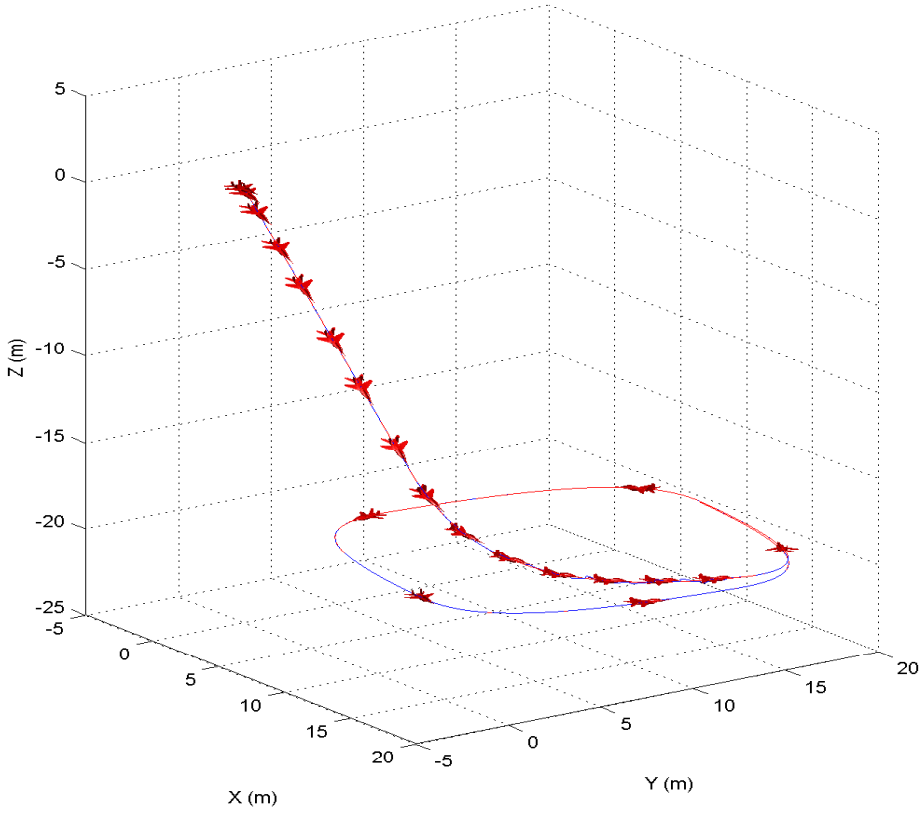

Figure 7.2: 3D trajectory tracking of the vehicle without uncertainty.

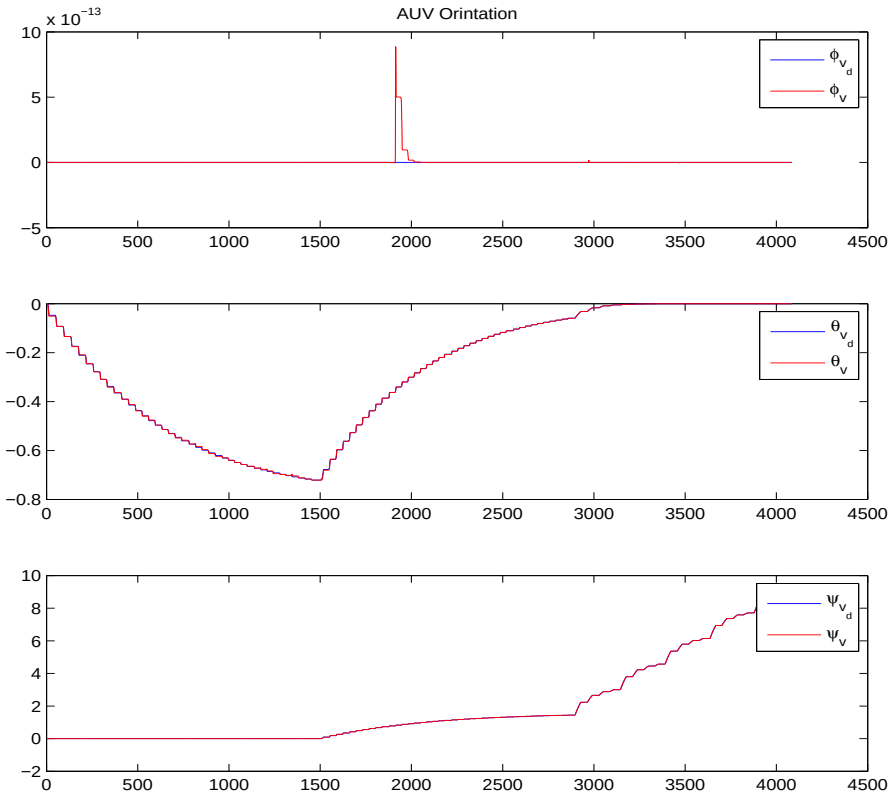

Figure 7.3: Orientation trajectory tracking of the vehicle without uncertainty.

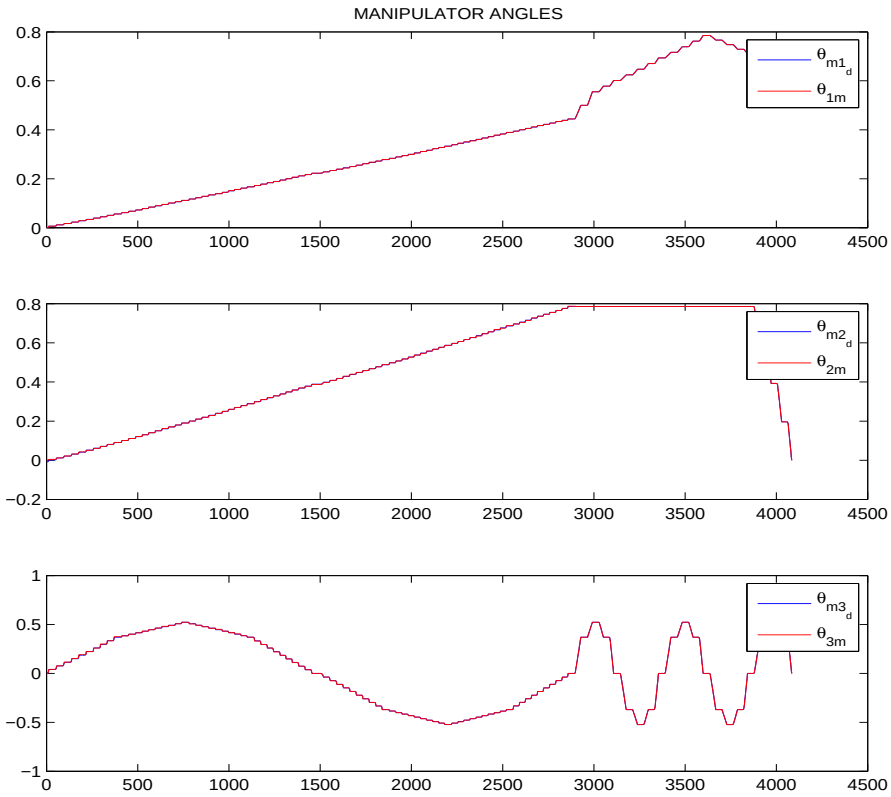

Figure 7.4: The manipulator angles trajectory tracking without uncertainty.

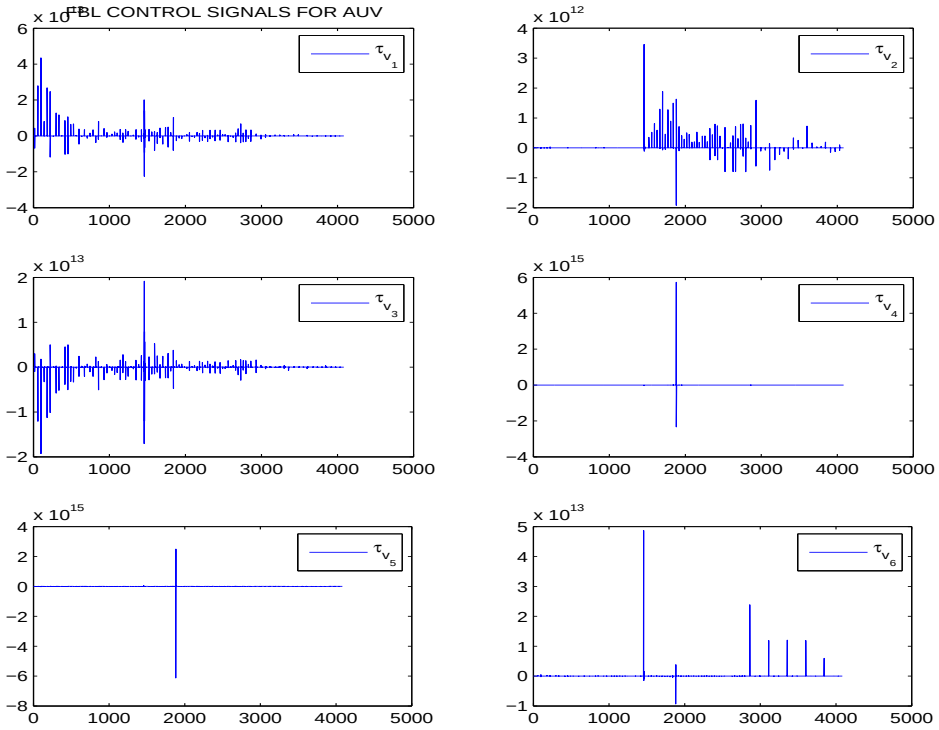

Figure 7.5: The Control Signals for the vehicle without uncertainty.

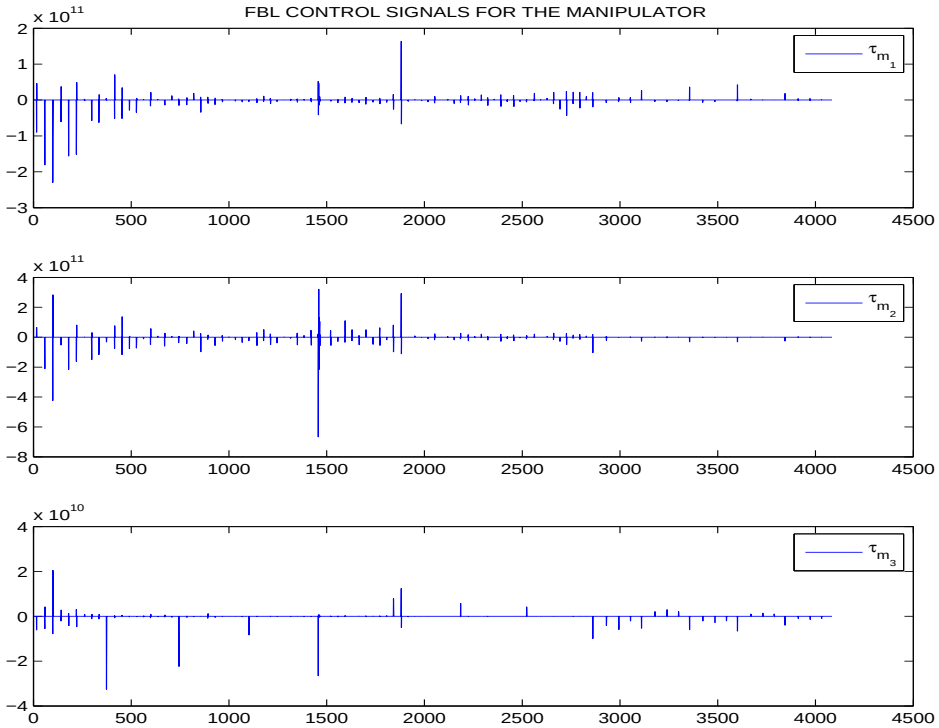

Figure 7.6: The Control Signals for the Manipulator without uncertainty.

7.2 Sliding Mode Controller for the UVMS

7.2.1 Simulation Results

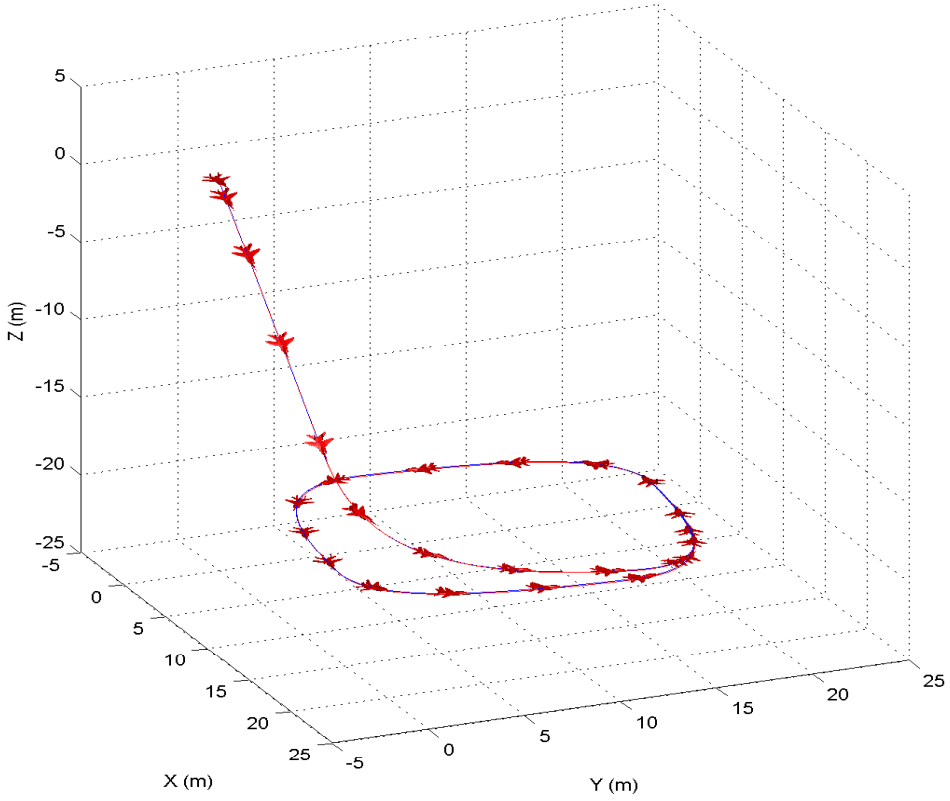

Figure 7.7: 3D trajectory tracking of the vehicle without uncertainty.

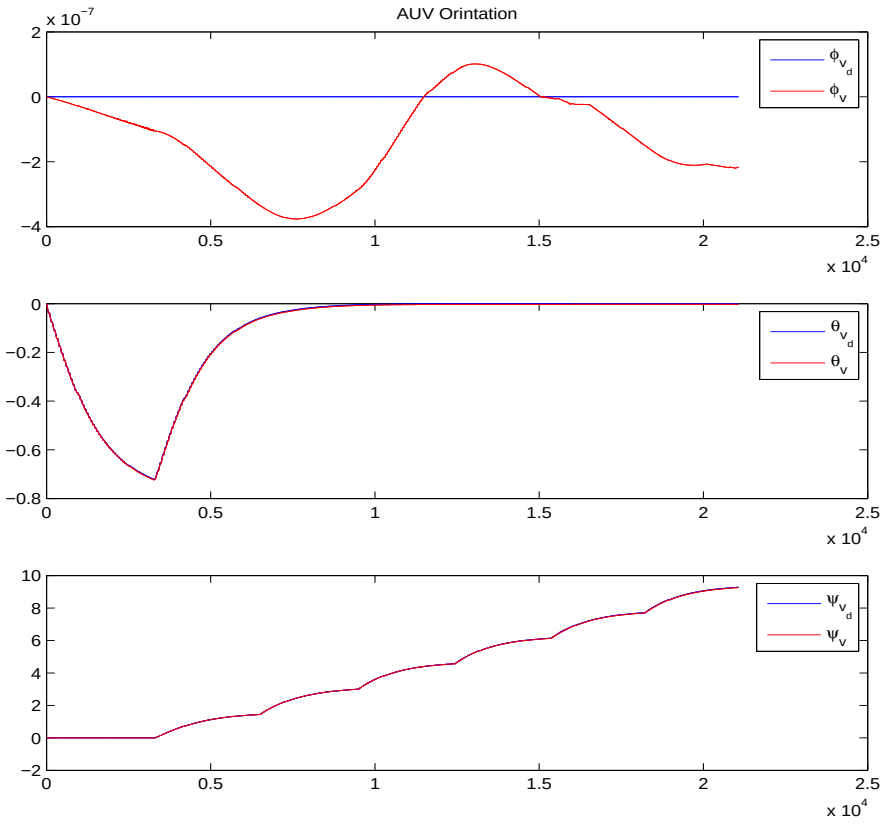

Figure 7.8: Orientation trajectory tracking of the vehicle without uncertainty.

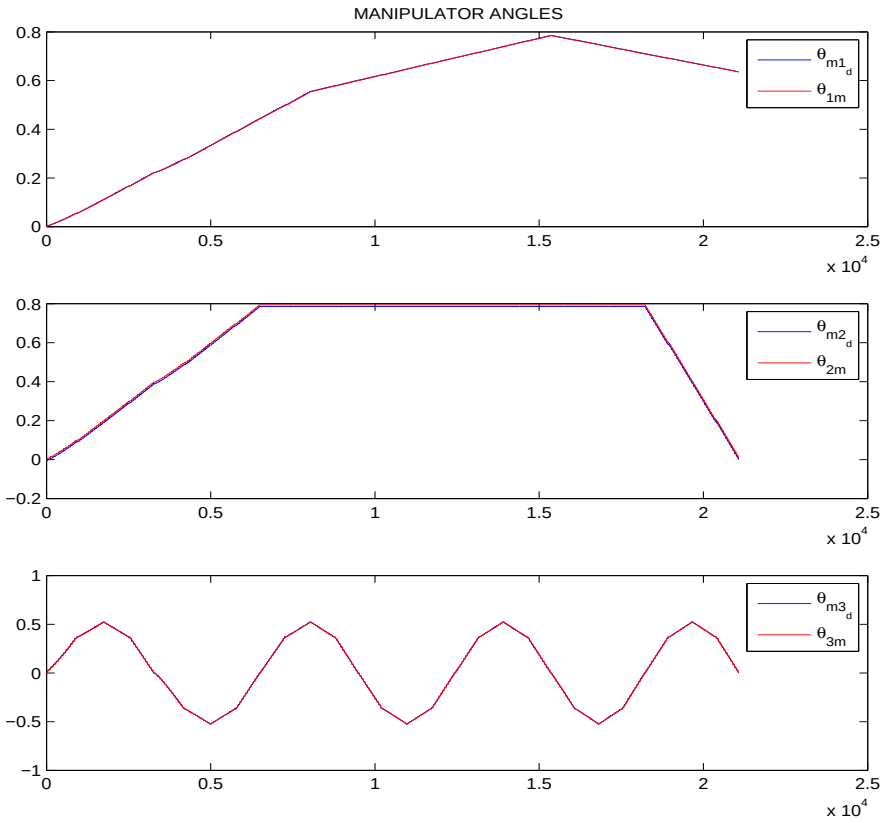

Figure 7.9: The manipulator angles trajectory tracking without uncertainty.

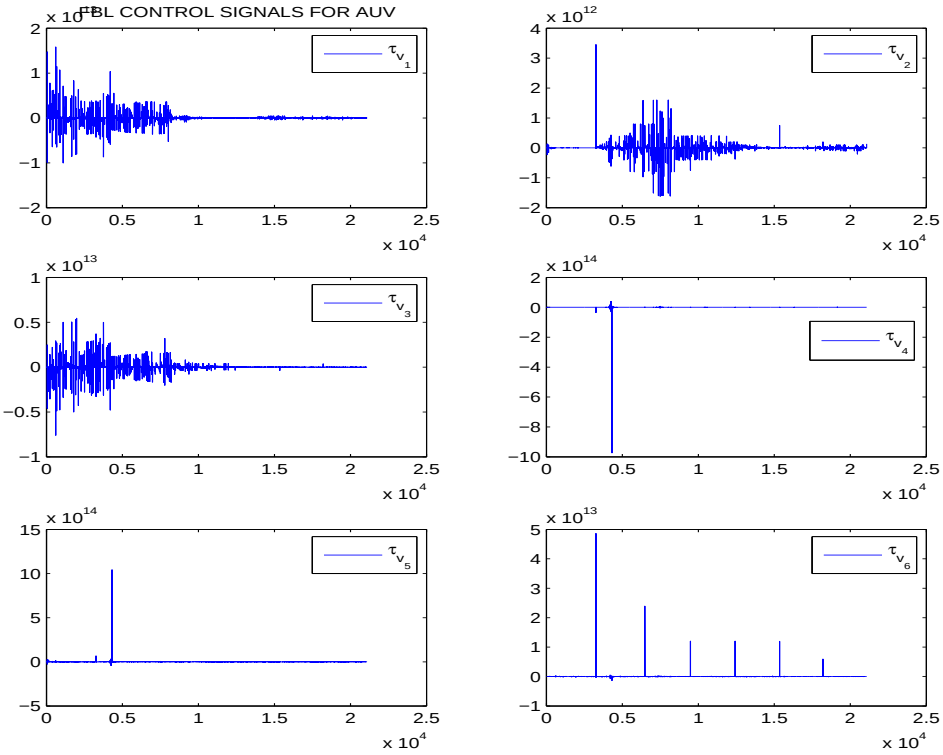

Figure 7.10: The Control Signals for the vehicle without uncertainty.

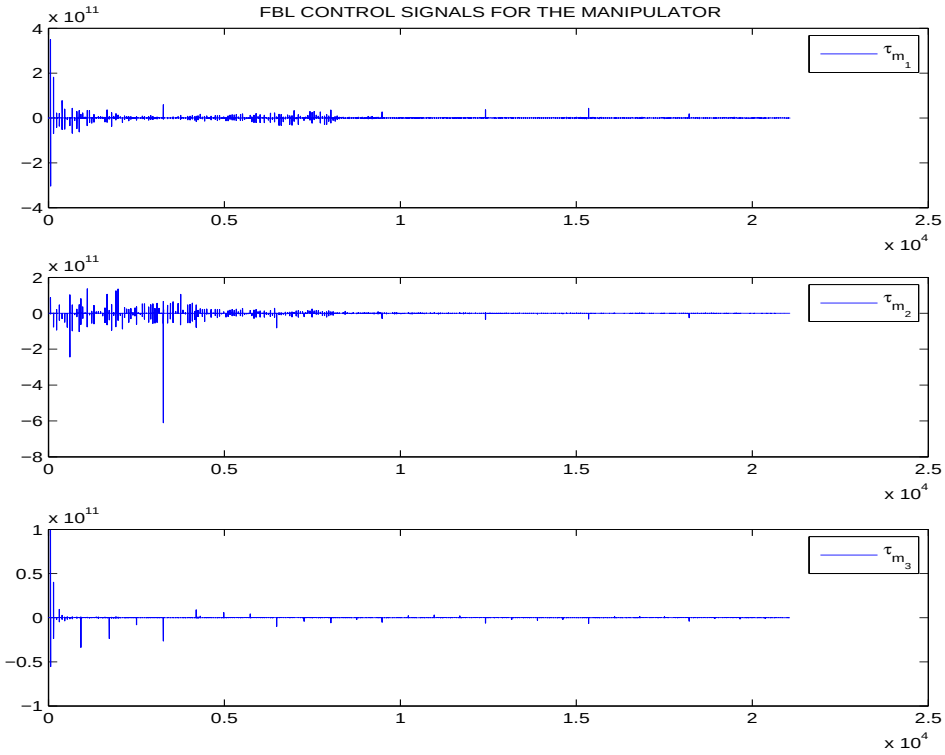

Figure 7.11: The Control Signals for the Manipulator without uncertainty.

7.3 $\mathcal{L}_1$ Adaptive controller

7.3.1 Simulation Results

In this section, the uncertainty in parameters (ρ and $\mathbf{M}$ represent water density and the inertia matrix for the UVMS, respectively) is considered as 25% error in ρ and 100% error in $\mathbf{M}$. In addition to the uncertainty in parameters the disturbance (with mean equal to 1, variance equal to 0 and frequency equal to 0 Hz) has been added to the input signals as well, to investigate the robustness of the proposed controller and the simulations were as in the following Figures.

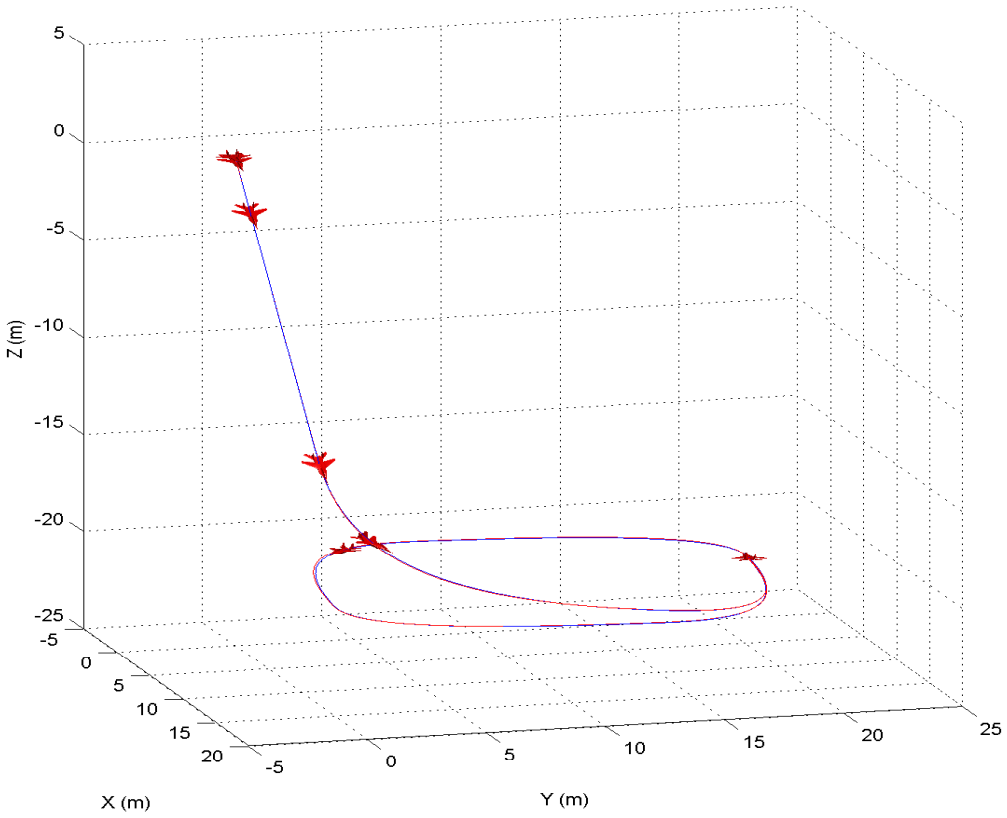

Figure 7.12: 3D trajectory tracking of the UVMS with uncertainty and disturbance.

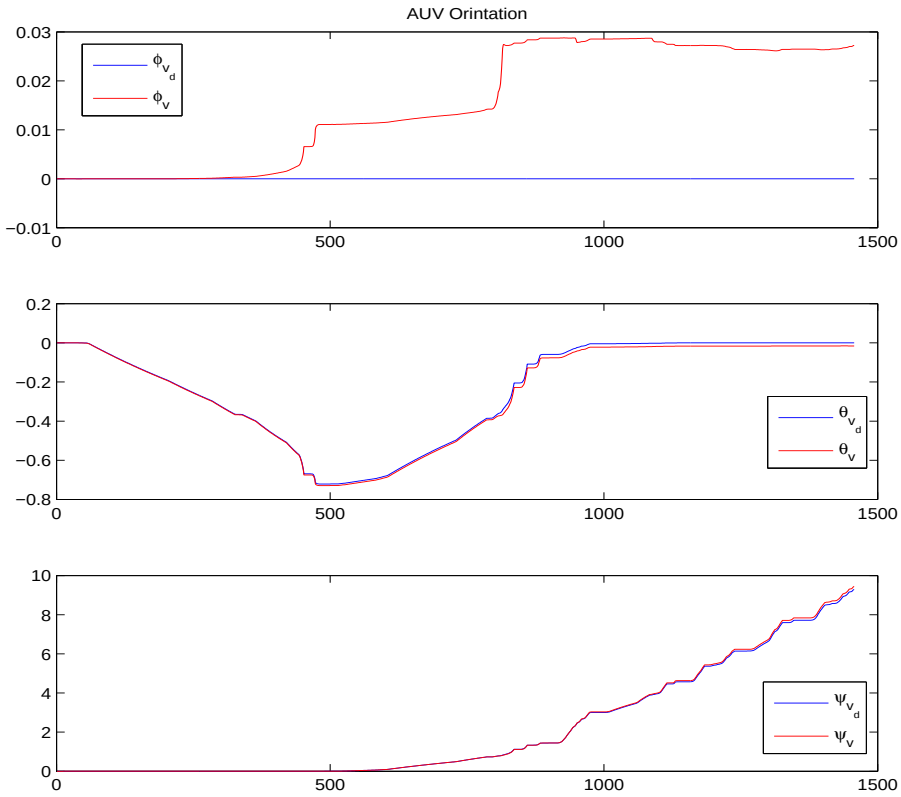

Figure 7.13: Orientation trajectory tracking of the UVMS with uncertainty and disturbance.

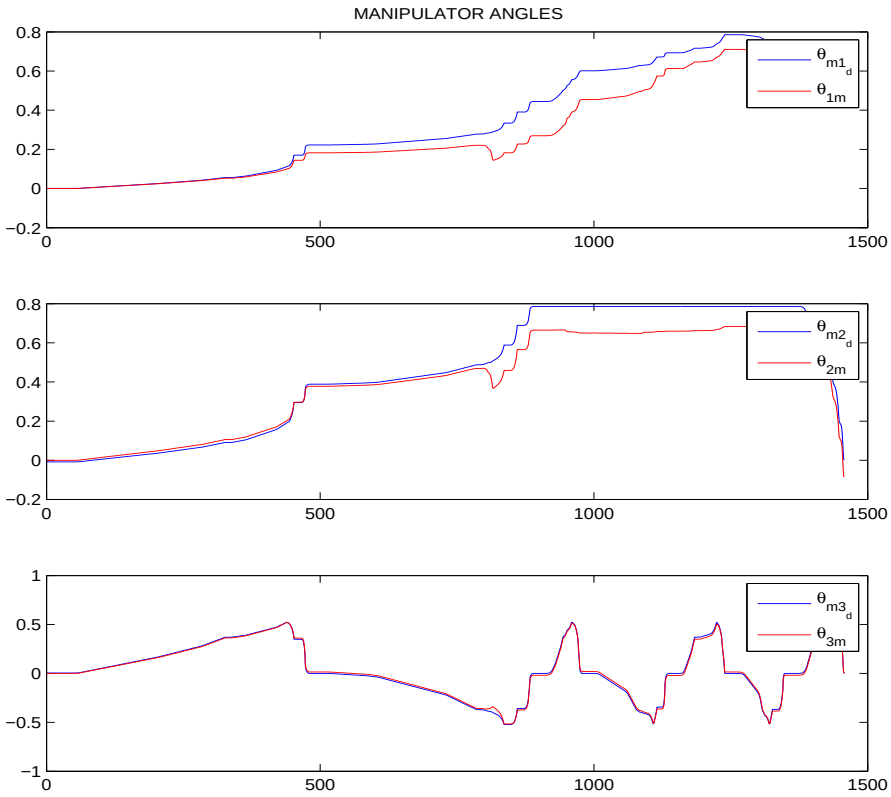

Figure 7.14: The manipulator angles trajectory tracking with uncertainty and disturbance.

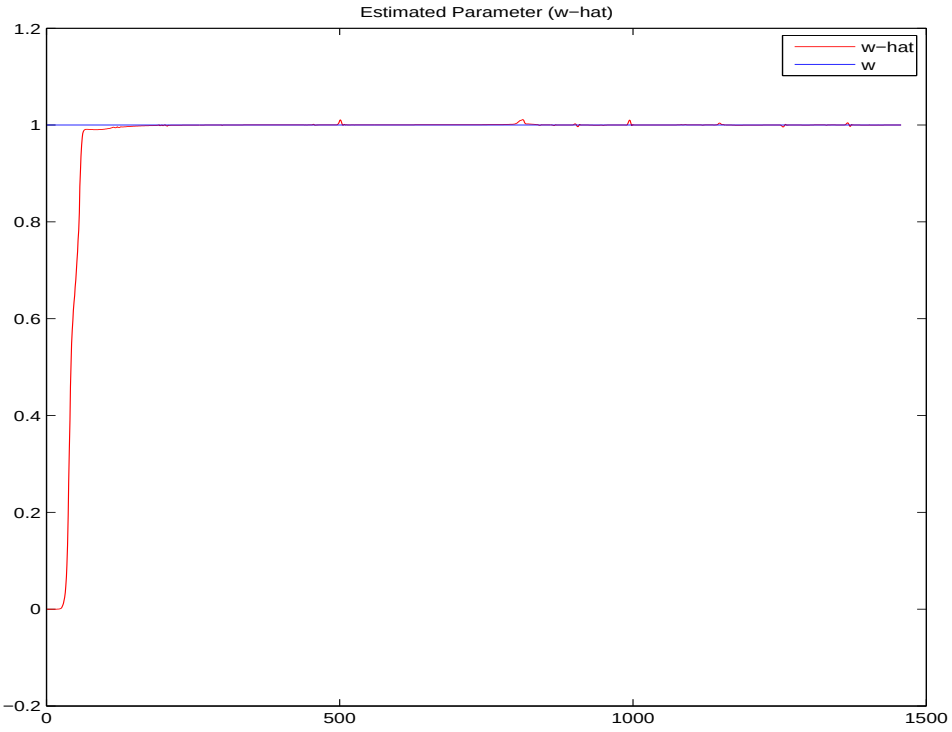

Figure 7.15: Estimated Parameter ($\hat{w}$) with uncertainty and disturbance.

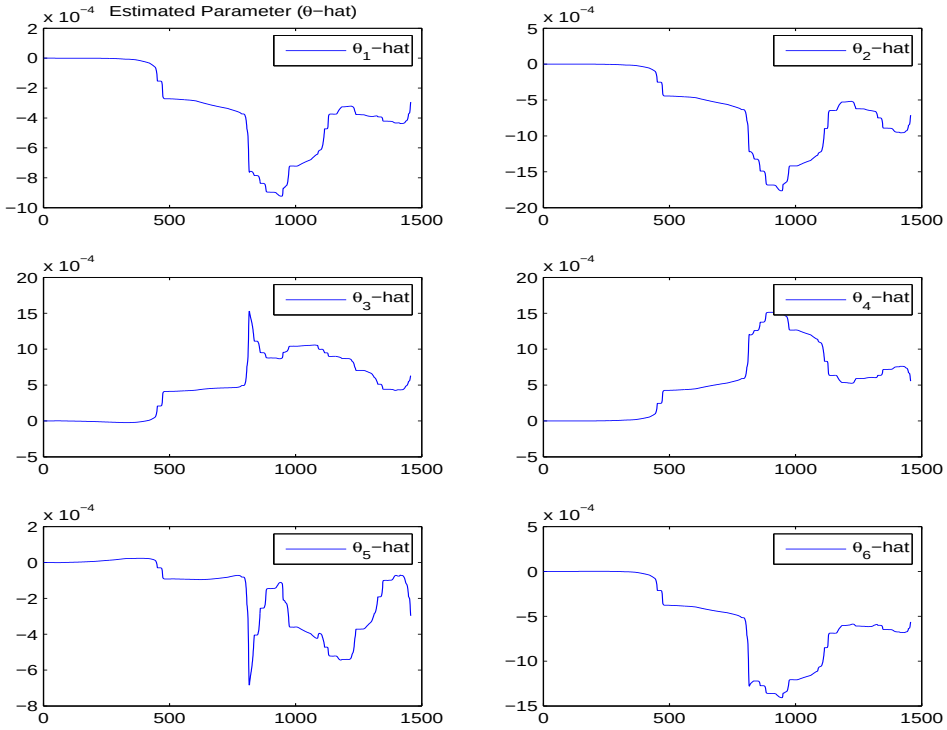

Figure 7.16: Estimated Parameter ($\hat{\theta}$) with uncertainty and disturbance.

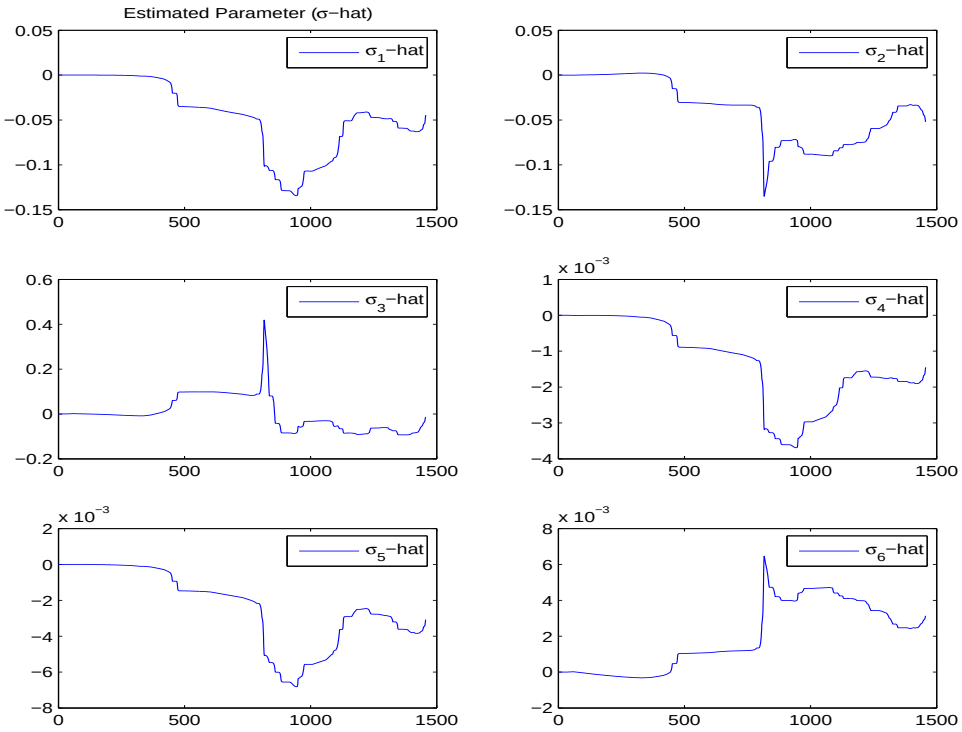

Figure 7.17: Estimated Parameter ($\hat{\sigma}$) with uncertainty and disturbance.

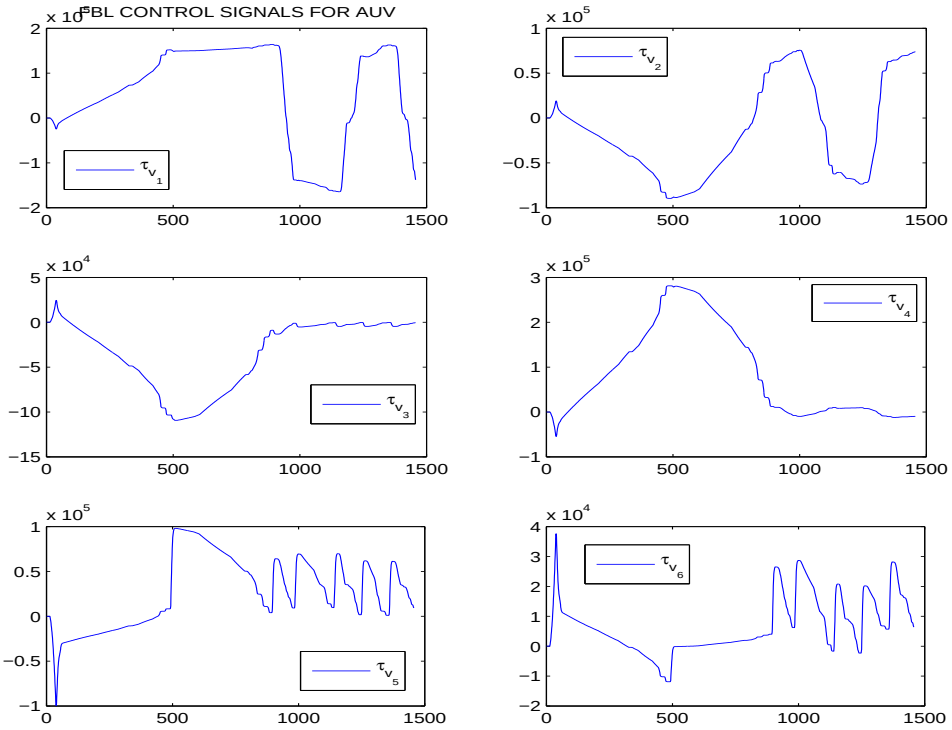

Figure 7.18: The Control Signals for the vehicle with uncertainty and disturbance.

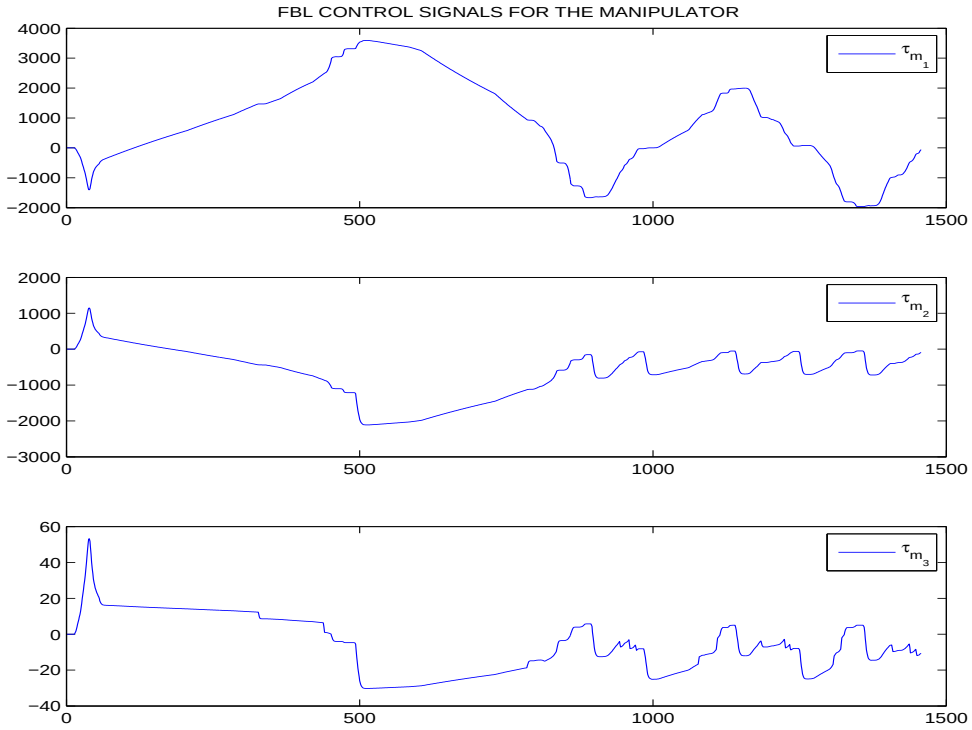

Figure 7.19: The Control Signals for the Manipulator with uncertainty and disturbance.

CHAPTER 8

CONCLUSION AND FUTURE WORK

The model of the underwater vehicle was presented briefly. The model of the UVMS was derived in detail using Kane's equations and then comparison and analysis in terms of the dynamics has been shown. Underwater vehicle with 3 link manipulator is selected as the basis model. After the model development, feedback linearization and sliding mode controllers which are selected from the literature were designed for both the underwater vehicle and UVMS to achieve tracking. A novel controller, which is $\mathcal{L}_1$ adaptive, is also designed for both the underwater vehicle and the UVMS. In case of disturbances and uncertainty in the dynamics, the $\mathcal{L}_1$ adaptive controller showed better performance than the other two controllers. Simulation results prove that the $\mathcal{L}_1$ adaptive controller delivers increased performance in terms of fast and robust adaptation.

8.1 Future work

As it can be seen, in general, Kane's equation can be used to model underwater vehicle with 2 n-link manipulators. Also, it can be used to model the unmanned aerial vehicle with slung load. In general the Kane's equation will be a good solution to model multiple unmanned or underwater vehicles working co-operatively on a task. The $\mathcal{L}_1$ adaptive controller can also be applied for the underactuated UVMS. The proposed controller can also be designed using output feedback for the UVMS.

REFERENCES

[1] A. Bowen, *The Woods Hole Oceanographic Institution's Remotely-Operated and Towed Vehicle Facilities for Deep Ocean Research: Operated for UNOLS & the US Deep Sea Science Community: Information and Technical Specifications*. Woods Hole Oceanographic Institution, 1993.

[2] Sub-atlantic rov. [Online]. Available: http://www.labicko.com

[3] A. Elahidoost and C. Cao, "Control and navigation of a three wheeled unmanned ground vehicle by $\mathcal{L}_1$ adaptive control architecture," in *Technologies for Practical Robot Applications (TePRA), 2012 IEEE International Conference on*. IEEE, 2012, pp. 13–18.

[4] T. Tarn, G. Shoults, and S. Yang, "A dynamic model of an underwater vehicle with a robotic manipulator using kane's method," *Autonomous robots*, vol. 3, no. 2, pp. 269–283, 1996.

[5] F. Fahimi, *Autonomous robots: modeling, path planning, and control*. Springer, 2008.

[6] G. A. Shoults, "Dynamics and control of an underwater robotic vehicle with an n-axis manipulator," Ph.D. dissertation, St. Louis, MO, USA, 1996, adviser-Tarn, T. J.

[7] I. Schjølberg and T. Fossen, "Modelling and control of underwater vehicle-manipulator systems," in *in Proc. rd Conf. on Marine Craft maneuvering and control*. Citeseer, 1994.

[8] T. Tarn and S. Yang, "Modeling and control for underwater robotic manipulators-an example," in *Robotics and Automation, 1997. Proceedings., 1997 IEEE International Conference on*, vol. 3. IEEE, 1997, pp. 2166–2171.

[9] B. Armstrong, O. Khatib, and J. Burdick, "The explicit dynamic model and inertial parameters of the puma 560 arm," in *Robotics and Automation. Proceedings. 1986 IEEE International Conference on*, vol. 3. IEEE, 1986, pp. 510–518.

[10] G. Antonelli, F. Caccavale, S. Chiaverini, and L. Villani, "Tracking control for underwater vehicle-manipulator systems with velocity estimation," *Oceanic Engineering, IEEE Journal of*, vol. 25, no. 3, pp. 399–413, 2000.

[11] G. Antonelli, *Underwater Robots: Motion and Force Control of Vehicle-Manipulator Systems (Springer Tracts in Advanced Robotics)*. Springer-Verlag New York, Inc., 2006.

[12] E. Xargay, N. Hovakimyan, and C. Cao, "Benchmark problems of adaptive control revisited by $\mathcal{L}_1$ adaptive control," in *Control and Automation, 2009. MED'09. 17th Mediterranean Conference on.* IEEE, 2009, pp. 31–36.

[13] B. Ferreira, M. Pinto, A. Matos, and N. Cruz, "Control of the mares autonomous underwater vehicle," in *OCEANS 2009, MTS/IEEE Biloxi-Marine Technology for Our Future: Global and Local Challenges.* IEEE, 2009, pp. 1–10.

[14] A. Matos and N. Cruz, "Mares-navigation, control and on-board software," *on Underwater vehicles, ISBN*, pp. 978–953, 2009.

[15] S. Das, D. Pal, S. Nandy, V. Kumar, S. Shome, and B. Mahanti, "Control architecture for auv-150: A systems approach," in *Trends in Intelligent Robotics.* Springer, 2010, pp. 41–48.

[16] N. Hovakimyan and C. Cao, *L1 adaptive control theory: guaranteed robustness with fast adaptation.* Siam, 2010, vol. 21.

[17] D. Maalouf, V. Creuze, A. Chemori *et al.*, "Novel application of multivariable l1 adaptive control: from design to real-time implementation on an underwater vehicle," in *2012 IEEE/RSJ International Conference on Intelligent Robots and Systems*, 2012.

[18] R. DeLuca, "A brief synopsis of kanes method."

[19] S. of Naval Architects, M. E. U. Technical, and R. Committee, *Economy and Endurance Trials Code, 1950*. Society of Naval Architects and Marine Engineers, 1950.

[20] A. Koivo, *Fundamentals for control of robotic manipulators*. John Wiley & Sons, Inc., 1989.

[21] T. I. Fossen, "Guidance and control of ocean vehicles," *New York*, 1994.

[22] S. McMillan, D. E. Orin, and R. B. McGhee, "Efficient dynamic simulation of an underwater vehicle with a robotic manipulator," *Systems, Man and Cybernetics, IEEE Transactions on*, vol. 25, no. 8, pp. 1194–1206, 1995.

[23] B. Lévesque and M. J. Richard, "Dynamic analysis of a manipulator in a fluid environment," *The International journal of robotics research*, vol. 13, no. 3, pp. 221–231, 1994.

[24] T. Tarn, A. Bejczy, G. Marth, and A. Ramadorai, "Kinematic characterization of the puma 560 manipulator," *Dept. Syst. Sci. Math., Washington Univ., Saint Louis, MO, Robotics Laboratory Rep. SSM-RL-91-15*, 1991.

[25] J.-J. E. Slotine, W. Li *et al.*, *Applied nonlinear control*. Prentice hall New Jersey, 1991, vol. 1, no. 1.

[26] C. Cao and N. Hovakimyan, "Stability margins of $\mathcal{L}_1$ adaptive controller: Part ii," in *American Control Conference, 2007. ACC'07*. IEEE, 2007, pp. 3931–3936.

[27] J.-B. Pomet and L. Praly, "Adaptive nonlinear regulation: Estimation from the lyapunov equation," *Automatic Control, IEEE Transactions on*, vol. 37, no. 6, pp. 729–740, 1992.

[28] B. Ferreira, M. Pinto, A. Matos, and N. Cruz, "Hydrodynamic modeling and motion limits of auv mares," in *Industrial Electronics, 2009. IECON'09. 35th Annual Conference of IEEE*. IEEE, 2009, pp. 2241–2246.

[29] ——, "Modeling and motion analysis of the mares autonomous underwater vehicle," in *OCEANS 2009, MTS/IEEE Biloxi - Marine Technology for Our Future: Global and Local Challenges*, 2009, pp. 1–10.

Vitae

- Name: Ahmed Eltayeb Ahmed Taha
- Nationality: Sudanese
- Date of Birth: 16/07/1981
- Email: *ahmedtayeb5@gmail.com*
- Permenant Address: Systems Engineering Dept.- KFUPM University - Dhahran - KSA

- Bsc degree from Algazira University (Sudan) in Electronics Engineering-Telecommunications and Control Systems (2008)
- Ms degree from KFUPM (KSA) in Systems Engineering-Control Systems (2013)